TRIBHUVAN UNIVERSITY
INSTITUTE OF ENGINEERING
PULCHOWK CAMPUS

Thesis No.: M-189-MSESPM-2020-2026

Assessing Climate Change Impacts on Streamflow and Power Generation in the Myagdi River Basin Using SWAT and CMIP6 Climate Projections

by
Sneha Shakya

A THESIS
SUBMITTED TO DEPARTMENT OF MECHANICAL AND AEROSPACE ENGINEERING IN PARTIAL FULFILLMENT OF THE REQUIREMENTS FOR THE DEGREE OF MSc ENGINEERING IN ENERGY SYSTEMS PLANNING AND MANAGEMENT

DEPARTMENT OF MECHANICAL AND AEROSPACE ENGINEERING
LALITPUR, NEPAL

JANUARY 2026

COPYRIGHT

TRIBHUVAN UNIVERSITY

INSTITUTE OF ENGINEERING

CENTRAL CAMPUS, PULCHOWK

DEPARTMENT OF MECHANICAL AND AEROSPACE ENGINEERING

The undersigned certify that they have read, and recommended to the Institute of Engineering for acceptance, a thesis entitled "**Assessing Climate Change Impacts on Streamflow and Power Generation in the Myagdi River Basin Using SWAT and CMIP6 Climate Projections**" submitted by Sneha Shakya in partial fulfillment of the requirements for the degree of MSc Engineering in Energy Systems Planning and Management.

Supervisor

Assoc. Prof. Dr. Shree Raj Shakya

Department of Mechanical and Aerospace Engineering

External Examiner

Dr. Ram Prasad Dhital

Chairperson, Electricity Regulatory Commission, Nepal

Tribhuvan University
Institute of Engineering
Department of Mechanical and Aerospace Engineering
Pulchowk Campus

Asst. Prof. Dr. Sudip Bhattarai

Head of Department, Department of Mechanical and Aerospace Engineering

Date: January 14, 2026

DECLARATION

I hereby declare that this study titled “Assessing Climate Change Impacts on Streamflow and Power Generation in the Myagdi River Basin Using SWAT and CMIP6 Climate Projections” is based on my original research work. Related works on the topic by other researchers have been duly acknowledged. I owe all the liabilities relating to the accuracy and authenticity of the data and any other information included hereunder.

Name of student: Sneha Shakya

Roll number of the student: PUL076MSESP017

MSc Engineering in Energy Systems Planning and Management

Date: January 2026

ACKNOWLEDGMENT

I express my deepest gratitude to my supervisor, Associate Prof. Dr. Shree Raj Shakya, Department of Mechanical and Aerospace Engineering, Pulchowk Campus, for his invaluable guidance, constructive feedback, and continuous encouragement throughout this research. His academic mentorship has been instrumental in shaping the quality and direction of this thesis.

I am sincerely thankful to Associate Prof. Dr. Nawaraj Bhattarai, Program Coordinator of the Master of Science in Energy System Planning and Management (2076-2078), for his consistent support, timely suggestions, and encouragement throughout my academic journey. My sincere thanks also to the Deputy Head of Department (Mechanical), Assistant Prof. Er. Laxman Motra, for his valuable support in addressing my queries related to the thesis work and for his guidance on meeting program timelines.

I owe special gratitude to my parents for their unwavering support throughout my academic journey. Their encouragement and belief in me have been a constant source of strength.

And finally, I thank my better half, Er. Suprim Bajra Bajracharya, for his patience, understanding, and steadfast support throughout this endeavor.

Sneha Shakya

PUL076MSESP017

ABSTRACT

The Myagdi River Basin, a rain-fed and snow-fed sub-catchment of the Kaligandaki River in western Nepal, hosts five run-of-river hydropower projects with 193 MW combined installed capacity, with an energy generation capacity of approximately 1,120 GWh annually. As climate change accelerates, high-altitude basins such as Myagdi face increasing risks from altered monsoon patterns, glacier retreat, reduced snow cover, and changing seasonal runoff. These shifts threaten dry-season water availability and hydropower reliability.

This study assesses climate change impacts on streamflow and hydropower generation by coupling the Soil and Water Assessment Tool (SWAT) with bias-corrected projections from four CMIP6 Global Climate Models (ACCESS-CM2, MIROC6, MPI-ESM1-2-HR, MRI-ESM2-0) under SSP2-4.5 (moderate emissions) and SSP5-8.5 (high emissions) scenarios. Analysis covers near-term (2026-2050), mid-century (2051-2075), and far-future (2076-2100) periods using industry-standard Q40-based hydropower assessment methodology.

SWAT calibration achieved NSE 0.59 (1995-2010) and NSE 0.73 (2011-2019) with PBIAS within ±10%, successfully capturing seasonal patterns including monsoon peaks and snowmelt-sustained baseflows. Monthly linear scaling bias correction was applied to NEX-GDDP-CMIP6 data using local observations (1992-2014), with multiplicative factors for precipitation and additive factors for temperature.

Results reveal a non-monotonic three-phase temporal response challenging linear climate impact assumptions. Phase 1 (2026-2050): Despite increased annual discharge (+8.5-9.9%), mid-range flows (Q40) decline 7.0-17.4% due to temporal flow redistribution, reducing basin-wide generation 8.45-9.81% to 1,010-1,026 GWh/yr. Phase 2 (2051-2075): Hydrological recovery stabilizes Q40 near baseline (SSP2-4.5: -3.6%) or increases modestly (SSP5-8.5: +4.7%), with generation reaching 1,190 GWh/yr (+6.25%) and 1,316 GWh/yr (+17.50%) respectively. Phase 3 (2076-2100): Emission pathways diverge dramatically – SSP2-4.5 stabilizes (+8.26%, 1,213 GWh/yr) within existing infrastructure capacity, while SSP5-8.5 produces transformative change (+46.67%, 1,643 GWh/yr) with capacity saturation suppressing ~150-180 GWh/yr of theoretical gains. The 430 GWh/yr mitigation dividend (38.4-percentage-point gap) quantifies emission reduction benefits.

Methodological contributions include quantifying systematic SWAT-DPR discrepancies (5-31% Q40 underestimation) and developing efficiency calibration factors (0.57-0.81) that reconcile model-observation differences while preserving climate signals. Key implications:

(1) near-term vulnerability requires proactive adaptation despite long-term increases, (2) infrastructure design should target mid-century conditions with expansion flexibility, (3) capacity saturation under high emissions necessitates modular designs, and (4) the quantified mitigation dividend strengthens economic arguments for emission reductions.

This comprehensive CMIP6-based assessment provides actionable insights for climate-resilient hydropower planning in Himalayan catchments, demonstrating that non-monotonic temporal response patterns – initial decline, mid-century recovery, far-future divergence – demand time-phased adaptation strategies rather than linear extrapolation approaches.

TABLE OF CONTENT

LIST OF FIGURES

LIST OF TABLES

LIST OF ABBREVIATIONS

BCSD	Bias-Correction Spatial Disaggregation
CMIP5	Coupled Model Intercomparison Project Phase 5
CMIP6	Coupled Model Intercomparison Project Phase 6
CN	SCS Curve Number
DEM	Digital Elevation Model
DHM	Department of Hydrology and Meteorology
ESM	Earth System Models
FABDEM	Forest And Buildings removed Copernicus Digital Elevation Model
GA	Green-Ampt
GCM	General Circulation Model
GDDP	Global Daily Downscaled Projections
GMFD	Global Meteorological Forcing Dataset
GWh	Giga-Watt hour
HKH	Hindu Kush Himalaya
HRU	Hydrological Response Unit
HWSD	Harmonized World Soil Database
ICIMOD	International Center for Integrated Mountain Development
IIASA	International Institute for Applied Systems Analysis
LCOE	Levelized Cost of Electricity
LULC	Land Use and Land Cover
IPCC	Intergovernmental Panel on Climate Change
m^3/s	Cubic meters per second
MRB	Myagdi River Basin
NDC	Nationally Determined Contribution

NEA	Nepal Electricity Authority
NEX	NASA Earth Exchange
NSE	Nash-Sutcliffe Efficiency
PBIAS	Percent Bias
PPA	Power Purchase Agreement
R^2	Coefficient of Determination
RCP	Representative Concentration Pathway
SSP	Shared Socioeconomic Pathway
SUFI-2	Sequential Uncertainty Fitting 2
SWAT	Soil and Water Assessment Tool
SWAT-CUP	SWAT Calibration and Uncertainty Programs
WCRP	World Climate Research Programme

1 INTRODUCTION

1.1 Background

Nepal possesses abundant water resources that originate from the Himalayas. The country's rivers form the backbone of its renewable energy sector, particularly in hydropower generation. The energy sector is a critical component of Nepal's development trajectory. Nepal has an estimated technical hydropower potential of 83,000 MW and an economically feasible potential of approximately 42,000 MW (A. B. Shrestha & Aryal, 2011); however, only a fraction of this potential has been harnessed to date. Hydropower accounts for approximately 95% of Nepal's total installed electricity capacity (*NEA,* 2025), with the country's total installed capacity exceeding 3,400 MW in 2025.

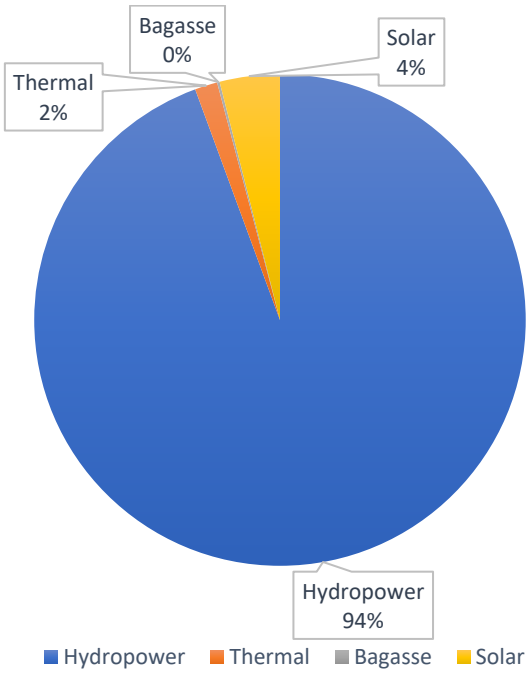

Figure 1-1 Nepal's electricity generation scenario

The rapid expansion of hydropower infrastructure in recent years demonstrates the opportunities inherent in this development. However, Nepal's significant reliance on hydropower renders it highly susceptible to variations in hydroclimatic conditions, primarily due to ongoing climate change. Climate variability directly affects the reliability of power generation, which requires accurate projections of future streamflow patterns to ensure effective and sustainable hydropower infrastructure planning in the region.

The western Himalayan region, including the Myagdi River Basin (MRB), is particularly vulnerable to climate change. Steep climatic gradients, complex topography, and monsoon-

dominated rainfall patterns create high hydrological variability across space and time. Rising temperatures, shifts in monsoon timing and intensity, altered snow accumulation and melt processes, and an increased frequency of extreme precipitation events can substantially modify the streamflow regimes. These hydrological changes can directly affect the reliability of hydropower generation, irrigation water availability, ecosystem functions, and flood-drought risk profiles. To understand these changes, modeling approaches must capture the complex interactions between climate forcing and catchment responses.

Hydrological models are essential tools for quantifying climate-driven changes in river flow. Among the available models, the Soil and Water Assessment Tool (SWAT) has emerged as one of the most widely adopted owing to its physically based representation of hydrologic processes, capability to simulate spatial heterogeneity across watersheds, and suitability for long-term scenario analysis. The SWAT's distributed modeling approach allows consideration of spatial variability in topography, land use, soil properties, and climate inputs, which are particularly relevant for mountainous catchments such as the MRB. When properly calibrated and validated against observed data, SWAT provides a powerful basis for assessing future hydrologic responses to climate change scenarios.

Recent advances in climate modeling have significantly enhanced the quality of future projections available for impact assessments. The Coupled Model Intercomparison Project Phase 6 (CMIP6) represents a major improvement over CMIP5. This is due to several factors, including improved spatial resolution, better representation of clouds and aerosols, and enhanced modeling of climate processes (*Hausfather, Z., 2019*). CMIP6 models generally show improved representations of temperature and precipitation in mountainous areas compared to CMIP5 simulations (*ClimateData.Ca*, n.d.), making them particularly useful for studies in the Himalayan Basin. CMIP6 introduces Shared Socioeconomic Pathways (SSPs) that complement the previous Representative Concentration Pathways (RCPs) by exploring the socioeconomic conditions behind various emission levels in a standardized way.

Bias-corrected, downscaled CMIP6 datasets, such as the NASA Earth Exchange Global Daily Downscaled Projections (NEX-GDDP-CMIP6), provide high-resolution daily climate data at 0.25-degree spatial resolution (approximately 25 km) for the period 1950-2100 (*NASA Center for Climate Simulation*, n.d.; Thrasher et al., 2022). These datasets apply statistical downscaling techniques to address the coarse resolution and systematic biases inherent in General Circulation Model (GCM) outputs, making them suitable for driving hydrological models at the basin scale. The NEX-GDDP-CMIP6 dataset includes projections from 35 GCMs

across multiple SSP scenarios, providing a comprehensive basis for quantifying the uncertainty.

Despite these advances, basin-specific studies applying CMIP6 projections to Himalayan catchments are limited. Recent comparative studies have shown that CMIP6 generally projects stronger climate change impacts on streamflow than CMIP5, with larger inter-model variability (Ma et al., 2024). However, such comprehensive assessments have not yet been conducted in the MRB. With increasing interest in developing hydropower in the region and the demonstrated sensitivity of the region to climate variability, it is crucial to evaluate how streamflow may change in the MRB over the next several decades to support informed decision-making and planning regarding investments in hydropower infrastructure in the region.

This study developed a calibrated SWAT hydrological model of the MRB and integrated climate projections from multiple CMIP6 GCMs under two contrasting socioeconomic scenarios, namely, SSP2-4.5 (middle-of-the-road development) and SSP5-8.5 (fossil-fueled development), to comprehensively assess future streamflow changes across three time horizons extending to 2100.

1.2 Problem Statement

The hydrology of the MRB is strongly influenced by monsoon rainfall patterns and high mountain hydrological processes, including snowmelt and glacial contributions. The observed trends globally and in the Himalayan region indicate increasing temperatures, shifts in rainfall patterns, changes in the frequency of extreme events, and modifications to snow and ice dynamics, ultimately altering streamflow characteristics.

These hydrological changes have significant implications for various sectors. Hydropower plants depend on predictable flow regimes for optimal generation scheduling and long-term viability assessments. Agricultural systems rely on seasonal water availability for irrigation purposes. Downstream communities face altered flood-risk profiles. Ecosystems adapted to historical flow patterns may experience stress under modified regimes due to anthropogenic activity. Although there are numerous concerns related to hydrological changes associated with climate change, only a few SWAT-based assessments of climate impact using advanced CMIP6 scenarios have been conducted in the MRB to date.

Several key challenges motivated this study.

1. Limited prior hydrological modeling: The basin lacks comprehensive, calibrated hydrological models that can serve as reliable tools for climate impact assessment and water resource planning.
2. Absence of basin-specific climate change projections: No quantitative estimates exist for how future climate change may affect flow magnitude, timing, and variability, specifically for the MRB under the latest CMIP6 scenarios. This knowledge gap leaves infrastructure planners and policymakers without the crucial information required for long-term decision-making.
3. Projection uncertainty quantification: Owing to differences in model structure, parameterization, and climate sensitivity, different GCMs produce different projections of future climate conditions. Understanding the range and uncertainty in future projections requires a multi-model ensemble analysis, which has not yet been conducted for this basin.
4. Seasonal impact characterization: Nepal's hydropower sector and water management strategies depend critically on understanding seasonal flow patterns, particularly the contribution of the monsoon season and dry-season low flows. Detailed seasonal impact assessments are not available for the MRB.
5. Knowledge gaps in infrastructure planning: Current approaches to hydropower feasibility studies, design flow estimation, and water allocation planning primarily rely on historical hydrological records. Without climate-informed projections, long-term infrastructure designs and management strategies are at risk of being inaccurate, potentially overestimating or underestimating future water availability.

1.3 Research Questions

- How effectively does the SWAT model, when integrated with CMIP6 climate data, simulate future streamflow patterns in the snow-fed MRB?
- What will be the impact of projected climate change on streamflow in the MRB under different climate scenarios?
- How will hydropower generation in the MRB change under different climate scenarios?

1.4 Objectives

1.4.1 Main Objective

To assess the impacts of climate change on streamflow patterns and hydropower generation potential in the MRB under different SSPs (SSP2-4.5 and SSP5-8.5) for the periods 2026-2050, 2051-2075 and 2076-2100.

1.4.2 Specific Objectives

1. To assess the performance of the SWAT model in simulating streamflow in the MRB when driven by CMIP6-based climate inputs.
2. To evaluate the impacts of future climate conditions on streamflow dynamics in the MRB using bias-corrected CMIP6 climate data.
3. To analyze the changes in hydropower generation in the MRB under different climate scenarios.

1.5 Need of the Study

The MRB, a glacier-fed and snow-fed sub-catchment of the Kaligandaki River in western Nepal, plays a vital role in hydropower generation and regional water supply. The basin hosts eight run-of-river hydropower projects, of which five projects are under-construction and three projects are in the study phase. The five under-construction hydropower projects have a combined capacity of 193 MW and are projected to generate approximately 1,120 GWh annually (*DoED*, 2025). As climate change accelerates, high-altitude basins such as Myagdi face increasing risks from altered monsoon patterns, glacier retreat, reduced snow cover, and changing seasonal runoff. These shifts threaten dry-season water availability and hydropower reliability.

Basin-specific climate change assessments remain limited, particularly using CMIP6 projections and addressing hydropower implications. Bajracharya et al., 2018 applied SWAT to the entire Kaligandaki Basin using CMIP5 ensemble GCMs under RCP 4.5 and RCP 8.5 scenarios. They projected increases in discharge (50%), snowmelt (90%), and water yield (41-51%) by 2090 but focused on water balance components rather than hydropower generation. Aryal et al., 2023 successfully applied SWAT to simulate historical streamflow in the Myagdi basin (NSE 0.57-0.63) but evaluated satellite precipitation products for 2009-2019 without addressing future scenarios. The Myagdi Khola watershed has significant elevation variability (835-8136 m) with land cover dominated by glaciers, snow, forests, and grasslands (Aryal et al., 2023). Rain gauge stations are sparse at high elevations, posing difficulty for hydro-meteorological studies (Aryal et al., 2023). No studies have quantified climate impacts on hydropower using design discharge metrics (Q40) consistent with Nepal's industry practice, nor have they used CMIP6 projections for this sub-basin.

SWAT modeling with downscaled CMIP6 projections under SSP2-4.5 and SSP5-8.5 scenarios provides an opportunity to generate improved streamflow forecasts. The proven applicability of SWAT in the Kaligandaki basin (Bajracharya et al., 2018: NSE 0.78-0.80) and Myagdi sub-

basin (Aryal et al., 2023: NSE 0.57-0.63) provides confidence for extending to CMIP6-based projections and hydropower analysis. This is important for climate-resilient infrastructure planning, hydropower optimization, capacity expansion decisions, and adaptive water governance. This study provides localized, scenario-based insights into future water availability and hydropower generation potential under changing climate conditions using the latest generation of climate models.

1.6 Limitations of the Study

Several important limitations constrain the scope and interpretation of this study.

1. Calibration data constraints: Single-site discharge calibration was used due to limited observed streamflow data availability within the basin. Multi-site calibration would provide stronger constraints on internal basin processes but cannot be implemented given the current data availability. The spatial transferability of the calibrated parameters within the basin assumes reasonable homogeneity in hydrological processes.
2. Glacier dynamics: Glacier mass balance processes are not explicitly modeled. While the glacierized area in MRB is smaller than in higher-elevation basins (Bajracharya et al., 2018 reported >2000 km² glacier coverage across the broader Kaligandaki Basin), glacier and snowmelt contributions remain important for dry-season flows. The temperature-index snowmelt routine in SWAT provides a simplified representation that may not fully capture complex glacier dynamics, mass balance feedbacks, or elevation-dependent melt patterns under substantial warming.
3. GCM projection uncertainty: CMIP6 model projections contain inherent uncertainties arising from an incomplete understanding of climate processes, parameterization choices, initial conditions, and natural climate variability. The four selected model ensemble samples do not fully span the complete uncertainty space represented by all available CMIP6 models.
4. Climate variables: Only precipitation and temperature were considered as climate-forcing variables. Other potentially relevant factors, such as changes in relative humidity, wind speed, solar radiation, and atmospheric CO_2 fertilization effects on vegetation, were not explicitly modified in future scenarios, representing a limitation for processes sensitive to these variables.
5. Downscaling methodology: Statistical downscaling (Bias-Correction Spatial Disaggregation (BCSD) method in NEX-GDDP-CMIP6) may not fully capture

changes in local extremes, orographic effects, or convective processes in the region. While providing valuable basin-scale climate inputs, downscaled products carry assumptions about the stationarity of climate-topography relationships that may not hold under substantial climate change.

6. Land use and water management: Future simulations assume static land use, land cover, and water management practices. Changes in agricultural practices, reservoir operations, irrigation development, or land use conversion were not considered, although these could significantly modify future water availability and flow regimes of the river.
7. Hydropower infrastructure assumptions: Future hydropower projections assume static installed capacity and design parameters based on current DPR specifications. Turbine degradation, maintenance schedules, sediment-related efficiency losses, and potential infrastructure upgrades or retrofits are not considered. Capacity constraint analyses assume no expansion to capture excess flows under high-discharge scenarios.
8. Temporal resolution: Analysis focuses on annual and seasonal aggregates. Sub-daily or daily extreme events (peak floods, drought duration) are not explicitly analyzed, though these may be important for infrastructure design and operational planning. The Q40 metric (flow exceeded 40% of time) by definition focuses on mid-range flows rather than extremes.

1.7 Structure of the Thesis

This thesis comprises five chapters, structured to provide a coherent progression from contextual background and methodological framework through results to conclusions and recommendations.

Chapter 1 (Introduction) establishes the research foundation by presenting the background on Nepal's hydropower dependence and vulnerability to climate change. It articulates the specific research problem for the MRB, defines the research objectives, and outlines the scope and limitations of the study.

Chapter 2 (Literature Review) reviews relevant scientific literature across multiple domains, including hydrological modeling approaches with emphasis on SWAT applications; climate change impacts on Himalayan hydrology; the evolution and advancements of CMIP6 relative to earlier generations of climate models; bias correction methodologies for GCM outputs; and prior studies conducted in Nepal and comparable Himalayan catchments. This chapter situates

the present research within the broader scientific discourse and identifies key knowledge gaps addressed by the study.

Chapter 3 (Data and Methodology) integrates the description of the study area with the research methodology. It first characterizes the MRB, detailing its physiography, elevation distribution, drainage network, climatic characteristics with particular emphasis on monsoon dynamics and temperature gradients, land use and land cover patterns, soil properties, and the availability of hydrological and meteorological observations. The chapter then describes the data sources and preprocessing procedures; the SWAT model setup, including watershed delineation, Hydrological Response Unit (HRU) definition, and input database preparation; the calibration and validation framework using the Sequential Uncertainty Fitting Procedure 2 (SUFI-2) algorithm; the selection and extraction of CMIP6 GCM datasets; the implementation of bias correction techniques; and the analytical methods employed to assess projected changes in streamflow characteristics across multiple temporal scales and statistical indicators.

Chapter 4 (Results and Discussion) presents the research findings, beginning with the evaluation of SWAT calibration and validation performance to demonstrate model reliability. It then provides a detailed analysis of projected streamflow changes and changes in hydropower generation under different emission scenarios and future periods, examining annual trends, seasonal and monthly shifts, and changes in extreme flow characteristics. Uncertainty associated with climate projections is explicitly addressed through ensemble-based analysis.

Chapter 5 (Conclusion and Recommendation) synthesizes the key results and discusses their implications for hydropower development and water resources management in the MRB. It also acknowledges the study's limitations and discusses prospects for future research that could further refine climate impact assessments and support sustainable hydropower planning in Himalayan river basins.

2 LITERATURE REVIEW

2.1 Climate Change and Himalayan Hydrological Systems

Climate change has emerged as a critical driver of hydrological transformation in mountain regions globally. The Hindu Kush Himalaya (HKH) region is warming faster than the global average, with temperatures increasing at rates of 0.2-0.5°C per decade since the 1970s (U. B. Shrestha et al., 2012). This accelerated warming has triggered profound alterations in snow cover extent, glacier mass balance, and seasonal streamflow patterns (Immerzeel et al., 2010). Glacier mass loss across the Himalayas has doubled in recent decades, with ice loss rates increasing from −0.22 m w.e. year^{-1} during 1975-2000 to −0.43 m w.e. year^{-1} during 2000-2016 (Maurer et al., 2019).

The intensification of precipitation variability and shifting monsoon patterns compound these cryospheric changes, creating substantial uncertainty for water resource management in the region (Lutz et al., 2014). Snow-dominated basins are experiencing reduced snowpack accumulation, earlier onset of snowmelt, and modified seasonal runoff regimes (Singh & Bengtsson, 2005). These hydrological shifts directly threaten downstream communities that depend on consistent water supplies for agriculture, drinking water, and energy generation (Viviroli et al., 2007).

2.2 Climate Change Impacts on Himalayan Hydropower

The Himalayan region possesses immense hydropower potential, with Nepal alone harboring a theoretical capacity exceeding 83,000 MW (A. B. Shrestha & Aryal, 2011). However, climate-induced hydrological variability poses significant challenges for existing and planned hydropower infrastructure. Studies using SWAT hydrological modeling in Himalayan basins have projected substantial increases in annual discharge under future climate scenarios, with projections ranging from 32% to 88% by the end of the century depending on emission pathways (Bajracharya et al., 2018; Immerzeel et al., 2013).

Despite projected increases in total annual flow, seasonal distribution patterns reveal concerning trends. Several studies report potential declines in dry-season discharge during mid-century periods before eventual recovery, with significant implications for run-of-river hydropower plants that depend on consistent baseflow (Nepal, 2016; S. Shrestha et al., 2016). For the Kaligandaki Basin, which encompasses the Myagdi River system, climate projections suggest a 50% increase in discharge at the basin outlet by 2090 under high-emission scenarios,

driven primarily by increased precipitation and accelerated snowmelt (Bajracharya et al., 2018).

However, basin-specific assessments remain limited. While Bajracharya et al., 2018 evaluated water balance components for the entire Kaligandaki Basin using CMIP5 projections, and Aryal et al., 2023 validated SWAT for historical streamflow simulation in Myagdi River, no studies have quantified climate impacts on hydropower energy generation using industry-standard design discharge metrics. Furthermore, the transition from CMIP5 to CMIP6 climate projections, which incorporate updated emission scenarios (SSP2-4.5 and SSP5-8.5) and improved model physics, necessitates updated assessments for informed infrastructure planning and climate adaptation strategies.

2.3 Global Circulation Models (GCMs) and CMIP6

GCMs, also known as Earth System Models (ESMs), are the primary tools for projecting future climate change under different greenhouse gas emission scenarios. These complex numerical models simulate interactions among the atmosphere, oceans, land surface, and cryosphere by solving fundamental equations of physics (conservation of mass, momentum, and energy) on three-dimensional grids covering the globe (Taylor et al., 2012).

The CMIP6, coordinated by the World Climate Research Programme (WCRP), represents the latest generation of internationally coordinated climate model experiments. CMIP6 includes contributions from over 100 climate modeling groups worldwide, providing standardized simulations that enable systematic comparison of model outputs and quantification of projection uncertainty (Eyring et al., 2016). Compared to the previous CMIP5 generation, CMIP6 models generally feature higher spatial resolution (many at 50-100 km horizontal grid spacing), improved representation of physical processes including aerosol-cloud interactions and ocean mixing, and enhanced Earth system components such as interactive carbon cycle and dynamic vegetation (Eyring et al., 2016).

A key innovation in CMIP6 is the adoption of SSPs as the scenario framework, replacing the RCPs used in CMIP5 (Tebaldi et al., 2021). SSPs describe alternative futures of socioeconomic development (e.g., population growth, economic development, energy systems, land use) that lead to different greenhouse gas emission trajectories and radiative forcing levels by 2100 (O'Neill et al., 2016). The SSP2-4.5 scenario represents a "middle-of-the-road" future with moderate climate mitigation, reaching 4.5 W/m² radiative forcing and approximately 2.5-3.0°C global warming by 2100 relative to pre-industrial levels. SSP5-8.5 represents a fossil-fuel

intensive pathway with limited mitigation, reaching 8.5 W/m² forcing and >4°C warming, though this scenario is increasingly regarded as an upper-bound "stress test" given recent shifts toward renewable energy and stated national climate commitments (Meinshausen et al., 2020).

Projection uncertainty in climate models arises from three main sources: internal climate variability (natural fluctuations), model uncertainty (differences among GCMs in representing climate processes), and scenario uncertainty (differences in future emissions). For near-term projections (2020-2040), internal variability and model uncertainty dominate, while scenario uncertainty becomes increasingly important for mid- and late-century projections (Hawkins & Sutton, 2009).

2.4 Downscaling and Bias Correction: The NEX-GDDP-CMIP6 Dataset

While GCMs provide valuable information about large-scale climate trends, their coarse spatial resolution (typically 100-250 km grid spacing) inadequately captures local-scale climate features critical for watershed-scale hydrological modeling, particularly in topographically complex regions like the Himalayas. Statistical downscaling techniques address this scale mismatch by establishing empirical relationships between large-scale climate variables from GCMs and local-scale observations, then applying these relationships to future climate projections (Maraun et al., 2010).

The NEX-GDDP-CMIP6 dataset provides bias-corrected, spatially disaggregated daily climate data derived from CMIP6 models, making global climate projections accessible for regional impact assessments (Thrasher et al., 2022). NEX-GDDP-CMIP6 applies the BCSD methodology to outputs from 35 CMIP6 models across four SSP scenarios, producing a global archive of downscaled daily climate data at 0.25° × 0.25° resolution (~25 km at the equator) spanning 1950-2100 (Thrasher et al., 2022).

The dataset includes nine essential climate variables: daily maximum temperature (tasmax), minimum temperature (tasmin), average temperature (tas), precipitation (pr), near-surface specific humidity (huss), relative humidity (hurs), downwelling shortwave radiation (rsds), downwelling longwave radiation (rlds), and near-surface wind speed (sfcWind) (*NASA Center for Climate Simulation*, n.d.). This comprehensive variable set supports applications ranging from agricultural impact modeling requiring humidity and radiation for evapotranspiration calculations to hydrological modeling demanding temperature and precipitation for snowmelt and runoff generation.

The BCSD algorithm combines quantile mapping for bias correction with spatial interpolation techniques for disaggregation (Wood et al., 2004). Quantile mapping adjusts the entire probability distribution of GCM-simulated variables to match observed distributions by establishing transfer functions between GCM and observed quantiles at multiple probability thresholds, thereby correcting biases not only in the mean but also in variance and the frequency distribution of extremes (Cannon et al., 2015). Spatial disaggregation interpolates bias-corrected fields from the coarse GCM resolution to the finer 0.25° grid by preserving fine-scale spatial patterns from observations, under the assumption that relative spatial patterns of climate (e.g., the ratio of precipitation on a windward slope vs. adjacent valley) remain constant under climate change (Wood et al., 2002).

Despite these methodological advances, users must recognize inherent limitations. The stationarity assumption – that historical relationships between large-scale and local climate remain valid under future climate change – may be violated if climate change alters atmospheric circulation patterns or precipitation mechanisms. For basins with steep topography like the Myagdi River, additional local-scale bias correction or elevation-based adjustments may improve representation of climate gradients (M. Shrestha et al., 2017).

2.5 The SWAT Hydrological Model Framework

SWAT is a physically-based, semi-distributed watershed model developed to predict the impact of land management practices on water, sediment, and agricultural chemical yields in complex watersheds with varying soils, land use, and management conditions over extended time periods (Arnold et al.,1998). Originally developed in the early 1990s by the USDA Agricultural Research Service, SWAT has evolved into one of the most widely applied watershed-scale models globally, with applications spanning agricultural water quality assessment, climate change impact studies, and water resource management (*Gassman et al.*, 2007).

SWAT operates on a daily time step and subdivides watersheds into sub-basins based on topography, which are further discretized into HRUs – unique combinations of land use, soil type, and slope within each sub-basin. This spatial discretization allows SWAT to reflect differences in evapotranspiration, surface runoff, infiltration, and other hydrological processes for different land covers and soil types while maintaining computational efficiency (Neitsch et al., 2011). The model simulates the hydrologic cycle through major components including precipitation, canopy interception, surface runoff (using the SCS Curve Number (CN) method or Green-Ampt (GA) infiltration), lateral subsurface flow, groundwater flow (represented by

shallow and deep aquifers), evapotranspiration (using methods such as Hargreaves, Priestley-Taylor, or Penman-Monteith), and channel routing using the variable storage coefficient method or Muskingum routing (Tan et al., 2020).

SWAT has demonstrated particular utility in mountainous regions with significant elevation gradients, including applications in the Himalayas where snowmelt processes, glacier contributions, and orographic precipitation patterns add complexity to hydrological modeling (Marahatta et al., 2021). For snow-dominated catchments, SWAT incorporates a temperature-index snowmelt routine that simulates snow accumulation and melt as a function of air temperature, with parameters including snowfall temperature threshold (SFTMP), snowmelt base temperature (SMTMP), and snowmelt rate factors (SMFMX, SMFMN). Studies in the Nepal Himalayas have successfully applied SWAT to simulate streamflow in basins with significant snow and glacier contributions, though challenges remain in accurately representing high-elevation processes with limited observational data for calibration (Bajracharya et al., 2018).

Model performance is evaluated using statistical metrics including the Nash-Sutcliffe Efficiency (NSE), coefficient of determination (R^2), and percent bias (PBIAS), with widely accepted criteria for satisfactory model performance being NSE > 0.5, |PBIAS| < ±25%, and R^2 > 0.5 for streamflow simulation at daily time steps (Moriasi et al., 2007; Moriasi et al., 2015).

2.6 SWAT Calibration and Validation Using SUFI-2

Calibration and validation are critical steps in establishing the credibility of hydrological models for predictive applications. SWAT calibration involves adjusting model parameters within physically realistic ranges to minimize discrepancies between simulated and observed streamflow, while validation tests model performance on an independent time period not used during calibration, thereby assessing the model's predictive capability and transferability (K. Abbaspour et al., 2017).

The SUFI-2 algorithm, implemented in the SWAT Calibration and Uncertainty Programs (SWAT-CUP) software, has become a standard approach for SWAT calibration due to its computational efficiency and ability to quantify predictive uncertainty (K. C. Abbaspour et al., 2015). SUFI-2 employs a semi-automated inverse modeling procedure that combines Latin Hypercube Sampling for parameter space exploration with iterative refinement of parameter ranges based on objective function performance. The algorithm generates a 95% prediction

uncertainty (95PPU) band that ideally brackets most observed data, with two key metrics – p-factor (percentage of observed data bracketed by the 95PPU) and r-factor (thickness of the 95PPU band divided by standard deviation of observations) – used to assess the balance between goodness-of-fit and uncertainty. Target values of p-factor > 0.7 and r-factor < 1.5 are generally recommended for acceptable calibration (Arnold et al., 2012).

2.7 SWAT Applications in Nepal and the Himalayas

SWAT has been extensively applied for hydrological simulation and climate change impact assessment across Nepal and the broader Himalayan region, with varying degrees of success depending on data availability, basin characteristics, and calibration strategies (Bajracharya et al., 2018).

In the Bagmati River Basin of central Nepal, SWAT successfully simulated streamflow with NSE values exceeding 0.7 during both calibration and validation periods, demonstrating the model's capability in monsoonal climates with strong seasonal precipitation variability (S. Shrestha et al., 2023). The Koshi Basin, one of Nepal's largest river systems draining from the high Himalayas to the Ganges Plain, has been modeled using SWAT to assess historical and future hydrological variability, revealing high sensitivity of streamflow to both precipitation changes and temperature-driven shifts in snowmelt timing (Bharati et al., 2016).

A critical challenge in applying SWAT to data-scarce Himalayan catchments is parameter uncertainty and the question of spatial transferability – whether parameters calibrated in one basin can be applied to ungauged basins with similar physiographic characteristics. Research on SWAT parameter transferability in the Nepal Himalayas indicates that while some parameters (particularly those related to surface runoff generation and channel routing) exhibit reasonable transferability, others (especially groundwater parameters and snowmelt factors) show high spatial variability and require basin-specific calibration (Nepal et al., 2017).

Snowmelt modeling remains a persistent challenge in high-elevation Himalayan applications. While SWAT's temperature-index snowmelt routine provides reasonable first-order approximations of seasonal snowmelt patterns, the limited availability of high-elevation meteorological stations and snow cover observations constrains parameter calibration and validation (Ragettli et al., 2015). Comparative studies evaluating satellite-derived precipitation products (e.g., TRMM, CHIRPS, IMERG) against ground observations in western Nepal basins like the Myagdi Khola indicate substantial biases in satellite estimates, particularly for high-intensity monsoon events and winter precipitation at high elevations, underscoring the

importance of bias correction for both observational and model-projected climate data (Aryal et al., 2023).

2.8 Research Gap and Study Justification

Despite the extensive body of research on Himalayan hydrology and climate change impacts, significant knowledge gaps remain, particularly for medium-sized river basins in western Nepal that exhibit transitional characteristics between heavily glacierized and purely monsoon-dominated systems (Hasson, 2016).

First, while global datasets like NEX-GDDP-CMIP6 provide valuable downscaled climate projections, the effectiveness of these products for hydrological applications in specific Himalayan sub-regions requires basin-specific evaluation. The 0.25° resolution, though finer than raw GCM outputs, still represents ~625 km² per grid cell – potentially averaging over substantial elevation gradients and topographic precipitation variations in mountainous terrain (O'Neill et al., 2016). Additional basin-scale bias correction using local observations can improve the representation of climate forcing for hydrological models.

Second, uncertainty quantification in climate change impact projections remains incomplete in many Himalayan studies. While multi-model ensembles address GCM uncertainty and scenario comparisons address emission uncertainty, the cascade of uncertainties through the downscaling, bias correction, and hydrological modeling chain is rarely comprehensively assessed (Meinshausen et al., 2020). Studies that isolate different sources of uncertainty (e.g., GCM selection vs. bias correction methodology vs. hydrological model parameterization) provide more robust guidance for water resource planning and adaptation decisions.

Third, the relative importance of glacier retreat vs. precipitation changes vs. temperature-driven evapotranspiration shifts for future water availability in glacierized basins remains poorly quantified (Lutz et al., 2014). The MRB, with approximately 18.52% glacier coverage, represents a moderately glacierized system where both cryospheric processes and monsoonal precipitation influence hydrology, yet their relative contributions remain uncertain.

Finally, linking hydrological projections to sectoral water demands and policy frameworks enhances the relevance of climate impact research. Nepal's Nationally Determined Contribution (NDC) under the Paris Agreement identifies hydropower development and water resource management as priority adaptation sectors, yet robust scientific assessments integrating climate projections, hydrological modeling, and sectoral vulnerability remain

limited for many river basins with planned or existing hydropower infrastructure (*MoFE,* 2025).

This study addresses these gaps by applying bias-corrected CMIP6 climate projections to a calibrated SWAT model of the MRB, quantifying projection uncertainty across multiple GCMs and SSP scenarios, and providing insights relevant to hydropower planning and water resource management in a climatically sensitive Himalayan watershed.

3 DATA AND METHODOLOGY

3.1 Overall Workflow and Methodological Framework

This chapter describes the integrated methodological approach employed to assess climate change impacts on streamflow in the MRB. The research design comprises five major components executed sequentially: (1) data acquisition and preparation, (2) bias correction of climate model projections, (3) SWAT hydrological model setup and parameterization, (4) model calibration and validation, and (5) future scenario simulations and ensemble analysis. Projected climate trends were analyzed using ensemble outputs from four CMIP6 Global Climate Models under SSP2-4.5 and SSP5-8.5 scenarios. The SWAT model was calibrated and validated using observed streamflow data to evaluate its performance in simulating basin hydrology. Bias-corrected climate projections were then used to drive the calibrated model for simulating future streamflow patterns through 2100. The overall methodological framework is illustrated in Figure 3-1, and a coordination schema linking the research problem, objectives, methods, and outputs is presented in Table 3-1.

3.1.1 Workflow Overview

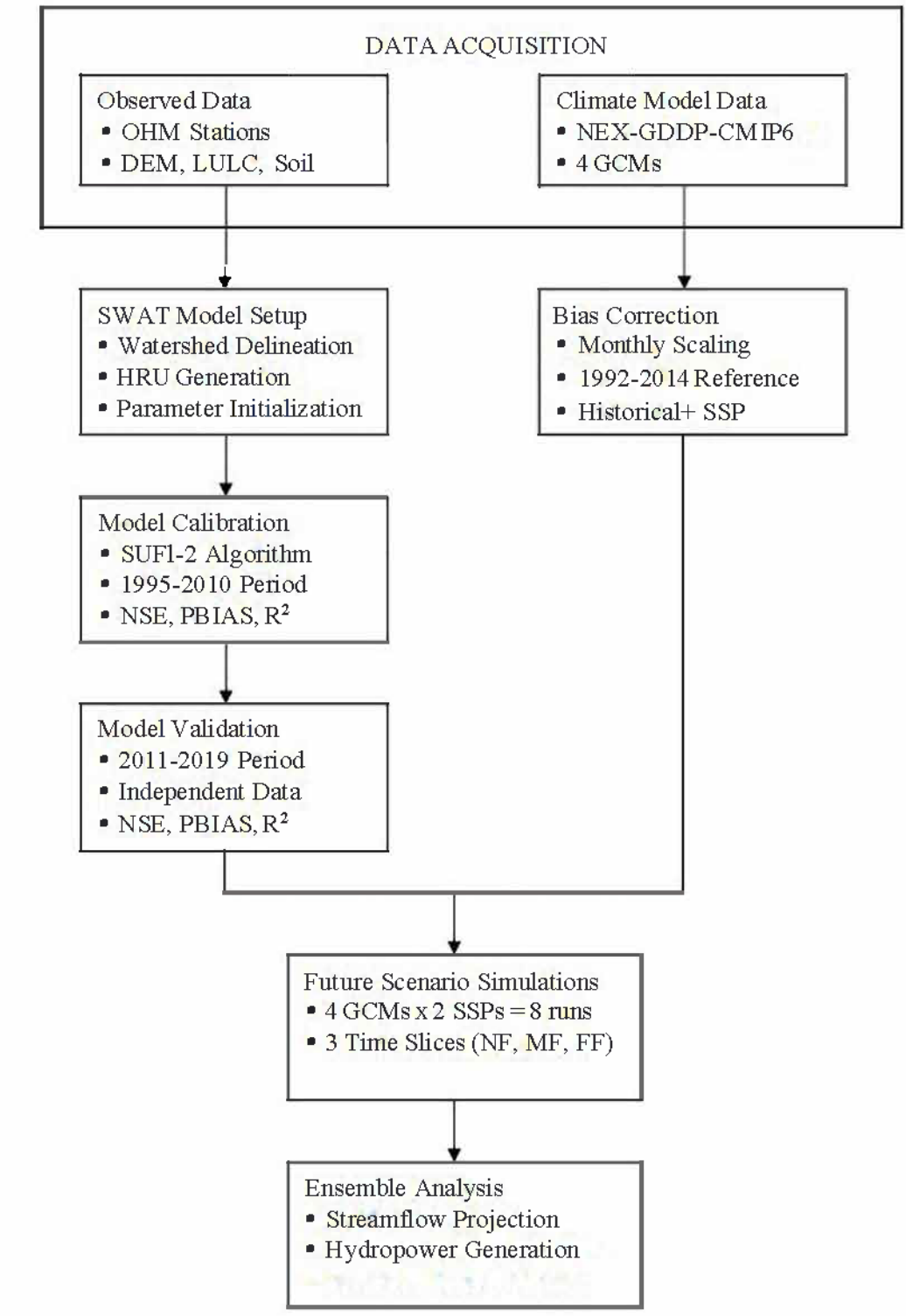

Figure 3-1 Methodological framework for analysing the impact of climate change on streamflow and hydropower generation

Table 3-1 Coordination schema table

Problem Statement Component	Specific Objective	Method Applied	Data/Tools Used	Expected Output
Need to validate streamflow simulation for Himalayan sub-basins	**Objective 1:** Evaluate SWAT model performance	SWAT calibration and validation using SUFI-2	SWAT, SWAT-CUP, Myagdi streamflow data	Calibrated hydrological model with NSE, R^2, PBIAS
Uncertainty in future streamflow under SSP scenarios	**Objective 2:** Simulate streamflow using CMIP6 scenarios	Climate forcing in SWAT and ensemble analysis	Bias-corrected climate data, SWAT, Python, Excel	Future streamflow trends under SSP2-4.5 and SSP5-8.5
Uncertainty in future hydropower generation under SSP scenarios	**Objective 3:** Analyze hydropower generation using CMIP6 scenarios	Ensemble analysis	Hydropower generation data, SWAT streamflow outputs, Python, Excel	Future hydropower generation trends under SSP2-4.5 and SSP5-8.5

3.2 Study Area

3.2.1 Spatial Characteristics

The MRB is located in the western region of Nepal, forming part of the larger Gandaki (Narayani) river system. The basin lies between longitudes 83° 08′ 22.20″ E and 83° 33′ 50.40″ E, and latitudes 28° 18′ 47.16″ N and 28° 47′ 37.68″ N, encompassing a catchment area of approximately 1,093.15 km² at the Mangalghat gauging station. The Myagdi River originates from the Chhonbarban-Dhaulagiri Himalayan massif, with its headwaters near Dhaulagiri I (8,167 m above sea level, masl), one of the world's highest peaks. The river flows southward through deeply incised V-shaped valleys before converging with the Kaligandaki River at Beni (~850 masl).

3.2.2 Elevation Profile

The MRB exhibits one of the most dramatic elevation gradients in Nepal, spanning from 835.75 masl at the Kaligandaki confluence to 8,135.43 masl at Dhaulagiri I – a vertical relief exceeding

7,300 meters over a horizontal distance of less than 40 kilometers. This steep altitudinal gradient generates pronounced hydro-climatic zonation and controls fundamental hydrological processes including precipitation distribution, snowmelt timing, and runoff generation.

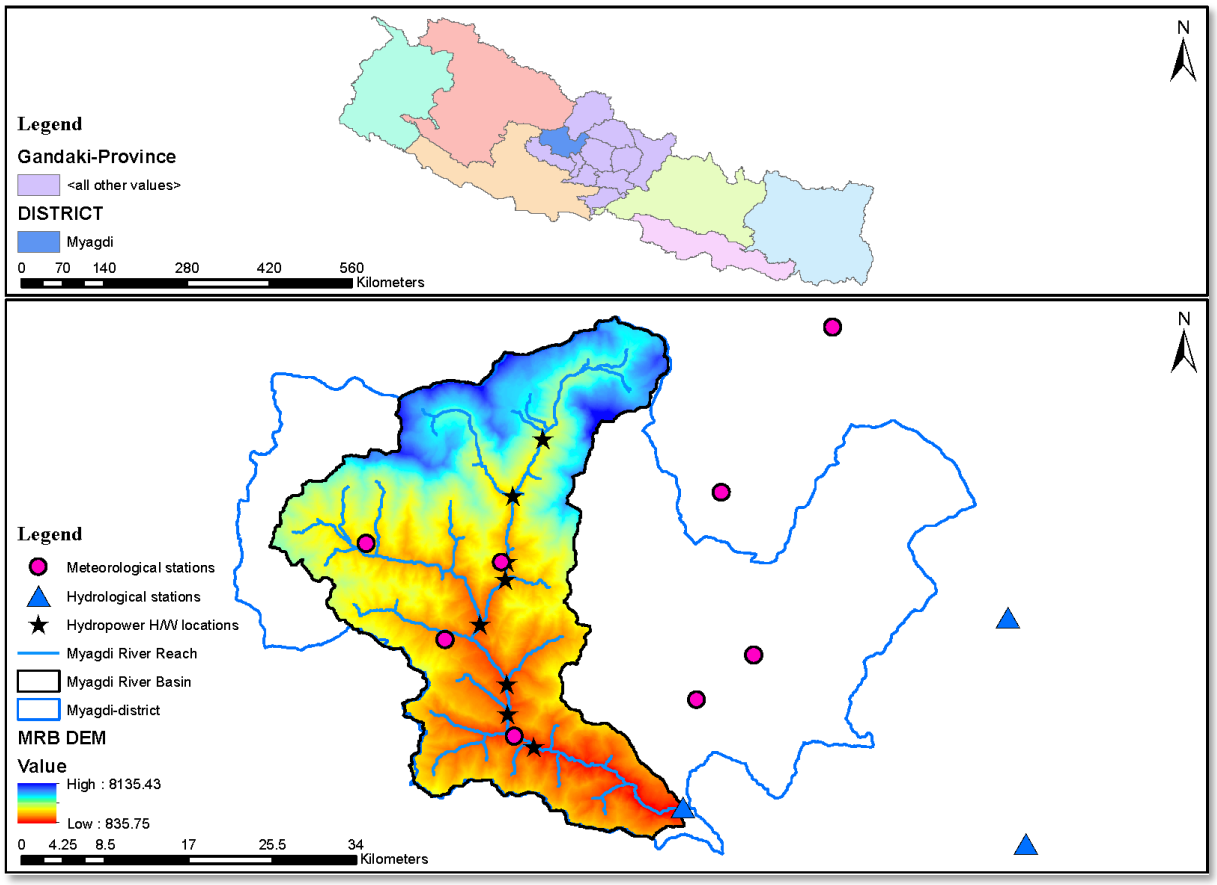

Figure 3-2 Myagdi River Basin with river network, hydrometeorological stations, and hydropower projects

More than 76% of the basin area lies above 3,000 masl, providing extensive zones for snow accumulation and sustained melt contributions during pre-monsoon and early monsoon periods. This high-elevation dominance distinguishes the Myagdi from lower-elevation monsoon-fed catchments and requires explicit treatment of cryospheric processes in hydrological modeling.

3.2.3 Slope Characteristics

The basin exhibits extremely steep terrain throughout its extent. Average river gradients approach 3% in the main channel, with tributary channels often exceeding 5-10% in upper reaches. Slope steepness directly influences:

- Runoff response time: Concentrated flow arrival during intense precipitation events.
- Erosion potential: High sediment loads and frequent mass wasting.

- Infiltration capacity: Limited soil development on steep slopes reduces groundwater recharge.
- Channel morphology: Steep, boulder-dominated channels with limited floodplain development.

3.2.4 Physiographic Zones

The MRB spans three major physiographic divisions of the Himalaya:

- Higher Himalaya (>5,000 masl): Characterized by glaciated peaks and permanent snowfields, periglacial landforms including cirques, U-shaped valleys, and moraines, minimal vegetation, barren rock and ice-dominated landscapes, source zones for tributary headwaters.
- Lesser Himalaya (3,000-5,000 masl): Characterized by sub-alpine meadows and shrublands, steep V-shaped valleys with narrow valley floors, mixed rainfall-snowfall regimes during monsoon, important transition zone for hydrological processes.
- Mid-Hills and Foothills (<3,000 masl): Characterized by forested slopes with agricultural terraces in accessible areas, deeply weathered bedrock and colluvial deposits, rainfall-dominated hydrology during monsoon, settlement concentration along valley bottoms.

The north-south valley alignment enhances orographic uplift of monsoon air masses, producing precipitation maxima on southern-facing slopes. This topographic configuration, combined with the steep relief, makes the basin hydrologically "flashy" – exhibiting rapid response to precipitation inputs during monsoon while maintaining sustained baseflows from snowmelt and groundwater during dry seasons.

3.2.5 Climate Characteristics

3.2.5.1 General Climate Regime

The Myagdi River Basin experiences a monsoon-dominated climate characteristic of the central Himalayan region. The South Asian summer monsoon, driven by differential heating between the Indian subcontinent and the Tibetan Plateau, dominates the annual hydrological cycle. Approximately 80% of annual precipitation occurs during the four-month monsoon season (June-September), with relatively dry conditions prevailing from October through May.

This pronounced seasonality controls streamflow patterns, agricultural water availability, and hydropower generation potential – all sensitive to projected climate change impacts on monsoon intensity and timing.

3.2.5.2 Precipitation Patterns

Mean annual precipitation is approximately 2,372 mm, though this basin-wide average masks substantial spatial variability driven by elevation and orographic effects.

Seasonal Distribution:

- Pre-monsoon (March-May): ~10-15% of annual total; increasing frequency of convective afternoon storms.
- Monsoon (June-September): ~80% of annual total; persistent heavy rainfall with embedded extreme events.
- Post-monsoon (October-November): ~5-10% of annual total; occasional westerly disturbances.
- Winter (December-February): <5% of annual total; light precipitation, predominantly as snow at high elevations.

Spatial Variability:

Precipitation exhibits strong gradients controlled by elevation and aspect:

- Southern mid-hills (1,000-3,000 masl): 2,500-3,500 mm/year due to orographic enhancement of monsoon moisture.
- Sub-alpine zone (3,000-5,000 masl): 1,500-2,500 mm/year; mixed rain-snow transitions.
- High Himalaya (>5,000 masl): <1,000 mm/year water equivalent; predominantly solid precipitation in rainshadow.

These patterns require careful consideration of precipitation lapse rates and orographic correction factors in hydrological modeling, particularly for accurate representation of snow accumulation zones.

3.2.5.3 Temperature Regime

- Winter minimum temperatures approach freezing even at mid-elevation stations such as Gurjakhani (~2,513 masl), with sub-zero conditions persistent above 3,500 masl.
- Summer maximum temperatures exceed 20-25°C in mid-hill regions, creating strong diurnal temperature ranges (15-20°C) during clear-sky pre-monsoon periods.
- Temperature lapse rates average 0.6°C per 100m elevation gain, though this varies seasonally and with atmospheric stability.
- Freezing level elevation fluctuates seasonally from ~4,500-5,000 masl in summer to ~2,500-3,000 masl in winter, controlling the rain-snow transition zone.

These temperature patterns are critical to climate change impact assessment because they:

1. Govern snowmelt timing and magnitude through energy balance at high elevations.
2. Control the elevation of rain-snow transition, which determines the proportion of precipitation contributing to snowpack versus immediate runoff.
3. Influence evapotranspiration rates through atmospheric demand, particularly during pre-monsoon dry season.
4. Modulate glacier mass balance in the headwater regions.

3.2.5.4 Snow and Glacier Influence

The high-elevation character of the basin results in significant cryospheric influences on hydrology:

- Seasonal snowpack develops above ~3,500 masl during winter, providing frozen water storage that contributes to pre-monsoon flows.
- Permanent snow and ice exist above ~5,500 masl, though glacier coverage is limited compared to extensively glacierized basins.
- Snowmelt contributions are particularly important during the pre-monsoon dry season (March-May), sustaining baseflows when precipitation is minimal and water demand peaks for irrigation.

Climate warming is expected to elevate the freezing level, reduce seasonal snow accumulation, and accelerate snowmelt timing – altering seasonal streamflow distribution with implications for water resource management and hydropower operations.

3.3 Data Sources and Collection

3.3.1 Temporal Scope

To assess hydrological changes across varying climate futures, three projection windows are considered: the near future (2026-2050), the mid future (2051-2075) and the far future (2076-2100). These time slices are commonly adopted in climate impact assessments and broadly align with the near-term, mid-century, and end-century horizons assessed by the Intergovernmental Panel on Climate Change (IPCC), enabling comparative analysis under moderate and high greenhouse gas emission pathways.

Table 3-2 Collected data and sources

SN	Data Type	Specific Parameter	Time Period	Source
1	Climate Data (Observed)	Precipitation, Temperature (max, min)	1992-2019 (historical)	Department of Hydrology and Meteorology (DHM), Government of Nepal
2	Climate Data (Projected)	Precipitation, Temperature (max, min)	2026-2050, 2051-2075, 2076-2100	4 CMIP6 GCMs (ACCESS-CM2, MIROC6, MPI-ESM1-2-HR, and MRI-ESM2-0) (NASA-GDDP-CMIP6)
3	Hydrological Data	Streamflow (daily)	1992-2019	Myagdi River (Mangalghat Station – STN 404.7) from DHM
4	Topographical Data	Digital Elevation Model (DEM)	Static	SRTM 30m DEM from FABDEM; Processed in ArcGIS for delineation
5	Land Use and Land Cover (LULC) Data	Land cover classification, vegetation types	2022	ICIMOD LULC data; Processed using lookup table
6	Soil Data	Soil texture, type, infiltration capacity	Static	HWSD v2.0 data; Processed using lookup table
7	Snow Consideration	Modeled using SWAT built-in snowmelt module	1992-2019 (implicit)	No direct input; Derived from temperature-based melt within SWAT

3.3.2 Observed Meteorological Data

Observed climate data were obtained from the Department of Hydrology and Meteorology (DHM), Government of Nepal. These data served dual purposes: (1) forcing the SWAT model during calibration and validation, and (2) providing reference climatology for bias correction of climate model outputs.

Table 3-3 Stations for precipitation data

Station Code	Station Name	Latitude	Longitude	Elevation	Station Description
1	601	28.78	83.73	2741	Jomsom
2	606	28.48	83.64	1161	Tatopani
3	607	28.63	83.61	2490	Lete
4	616	28.59	83.24	2627	Gurja Khani
5	621	28.41	83.39	1160	Darbang
6	626	28.44	83.58	1682	Bega
7	628	28.5	83.32	1970	Muna
8	629	28.57	83.38	1884	Baghara

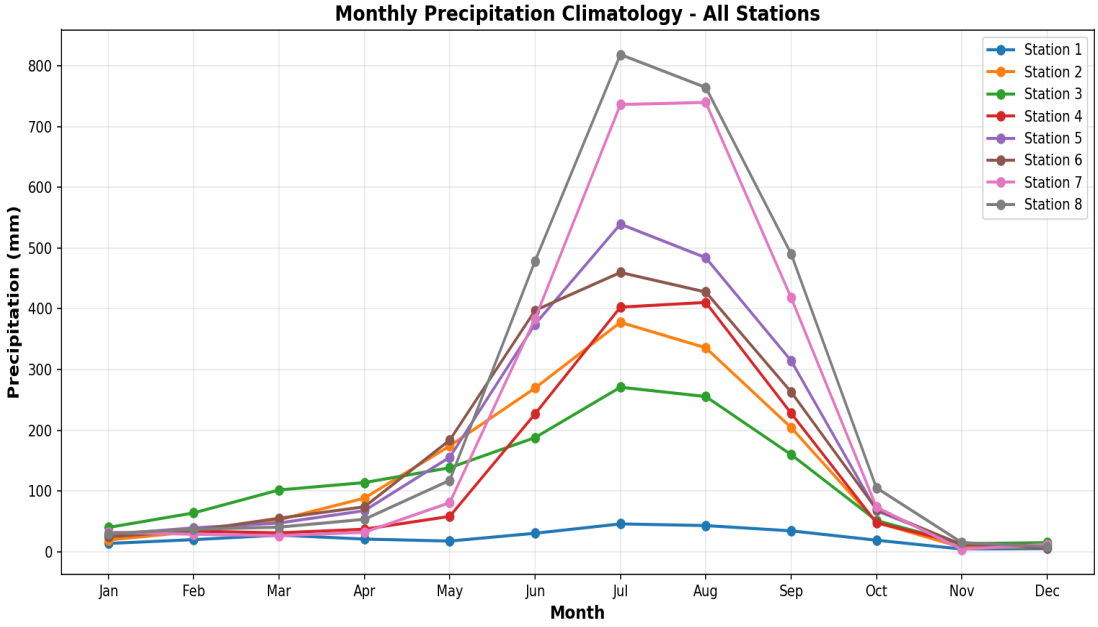

Figure 3-3 Monthly precipitation climatology for 8 stations, DHM (1992-2019)

Table 3-4 Stations for temperature data

Station Code	Station Name	Latitude	Longitude	Elevation	Station Description
1	601	28.78	83.73	2741	Jomsom
3	607	28.63	83.61	2490	Lete
4	616	28.59	83.24	2627	Gurja Khani

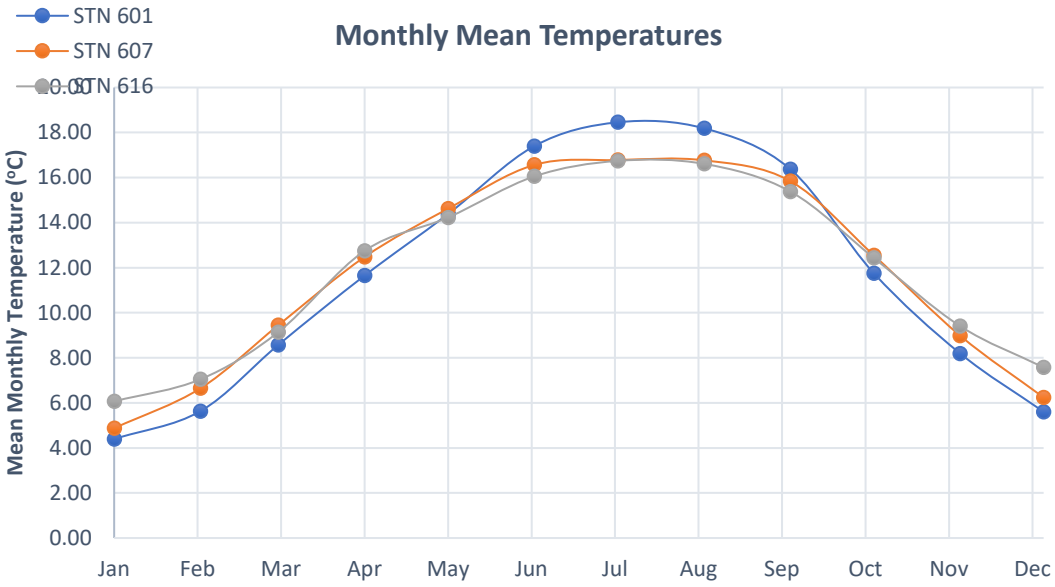

Figure 3-4 Monthly mean temperatures for 3 stations, DHM (1992-2019)

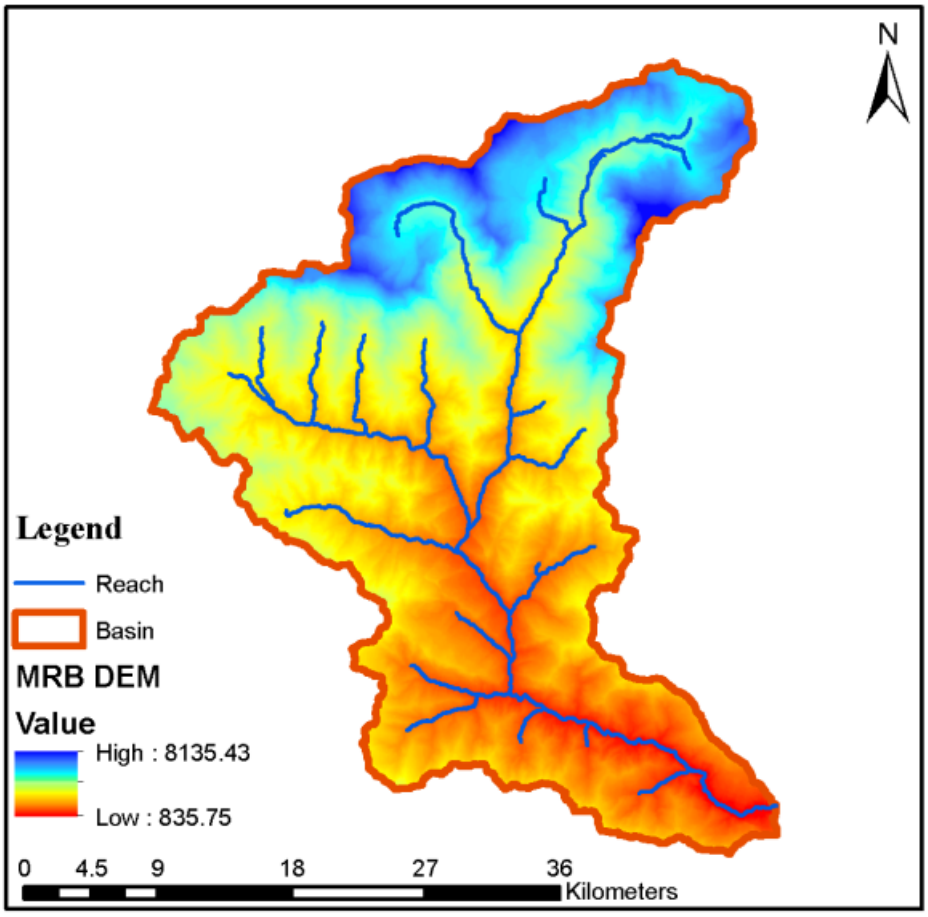

Figure 3-5 Digital Elevation Model of Myagdi River Basin

3.3.3 Observed Hydrological Data

The primary hydrological reference for the MRB is the DHM gauging station located at Mangalghat (Station 404.7). This gauge provides the primary validation target for SWAT model calibration. Observed daily discharge data were used to:

- Calibrate hydrological parameters through SWAT-CUP SUFI-2 algorithm.
- Validate model performance for independent time periods.
- Assess model skill in reproducing seasonal flow patterns, peak flows, and low-flow recession.

Table 3-5 Station for streamflow data

Station Code	Station Location	Outlet ID	Latitude	Longitude	Elevation
404.7	Mangalghat	35	28° 21′ 10″ N	83° 31′ 16″ E	914

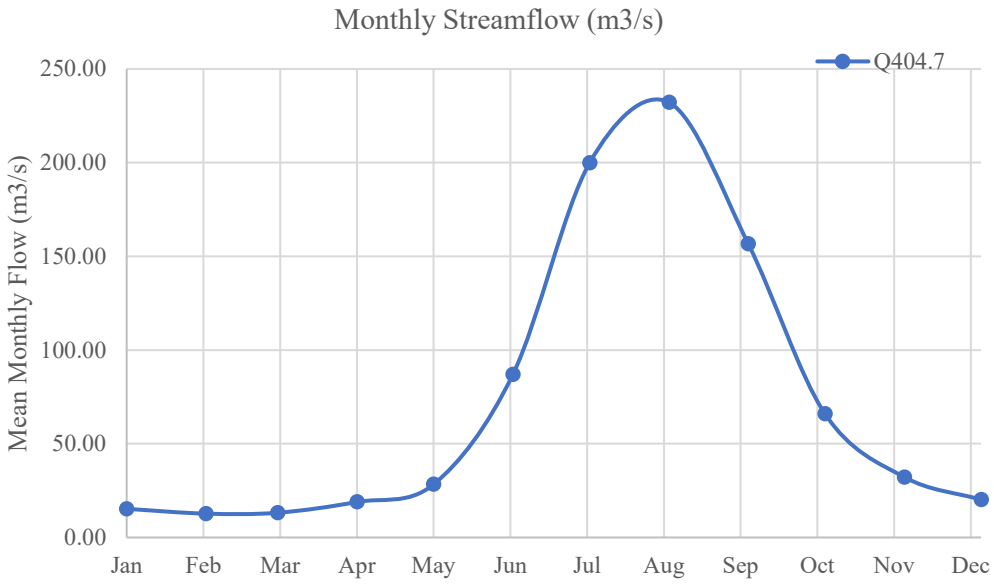

Figure 3-6 Monthly streamflow in m^3/s

3.3.4 Land Use and Land Cover

Land use and land cover patterns in the MRB reflect the strong elevational zonation and limited human modification of high-elevation areas. Land cover data for SWAT modeling were derived from International Center for Integrated Mountain Development (ICIMOD), which provides high-resolution, regionally validated LULC classifications suitable for Himalayan basins. These data capture the spatial distribution of forest types, agricultural terraces, shrubland, barren land, and snow/glacier cover – critical for representing vegetation growth, evapotranspiration, and land-surface processes in SWAT.

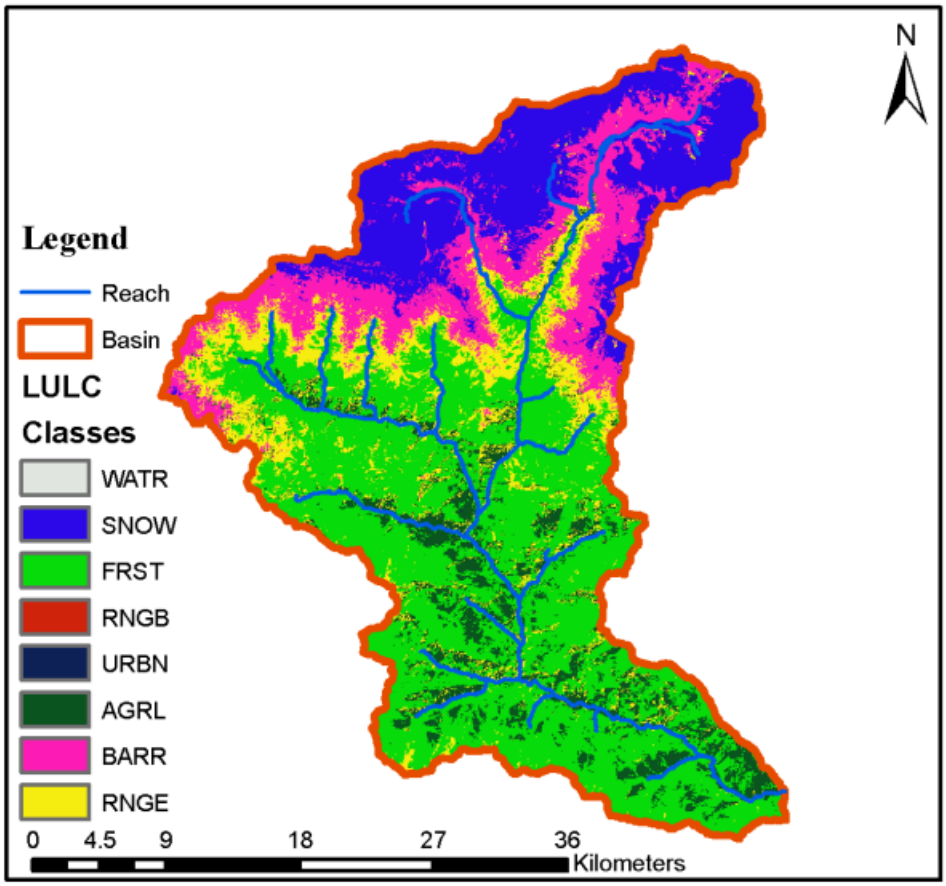

Figure 3-7 Land use land cover map of Myagdi River Basin

3.3.5 Soil Characteristics

Soil development in the MRB is strongly controlled by parent material (lithology), slope gradient, elevation, and climate. Soils are generally shallow and poorly developed on steep slopes, with deeper alluvial deposits limited to narrow valley floors.

The Harmonized World Soil Database version 2.0 (HWSD v2.0) was used to characterize the basin's soil properties, including texture, depth, hydraulic conductivity, and water-holding capacity. HWSD v2.0 is a unique global soil inventory providing information on the morphological, chemical and physical properties of soils at approximately 1 km resolution. Its main objective is to serve as a basis for prospective studies on agro-ecological zoning, food security and climate change. Incorporating HWSD v2.0 ensures that each HRU reflects realistic soil-land interactions across the steep environmental gradients of the Myagdi Basin.

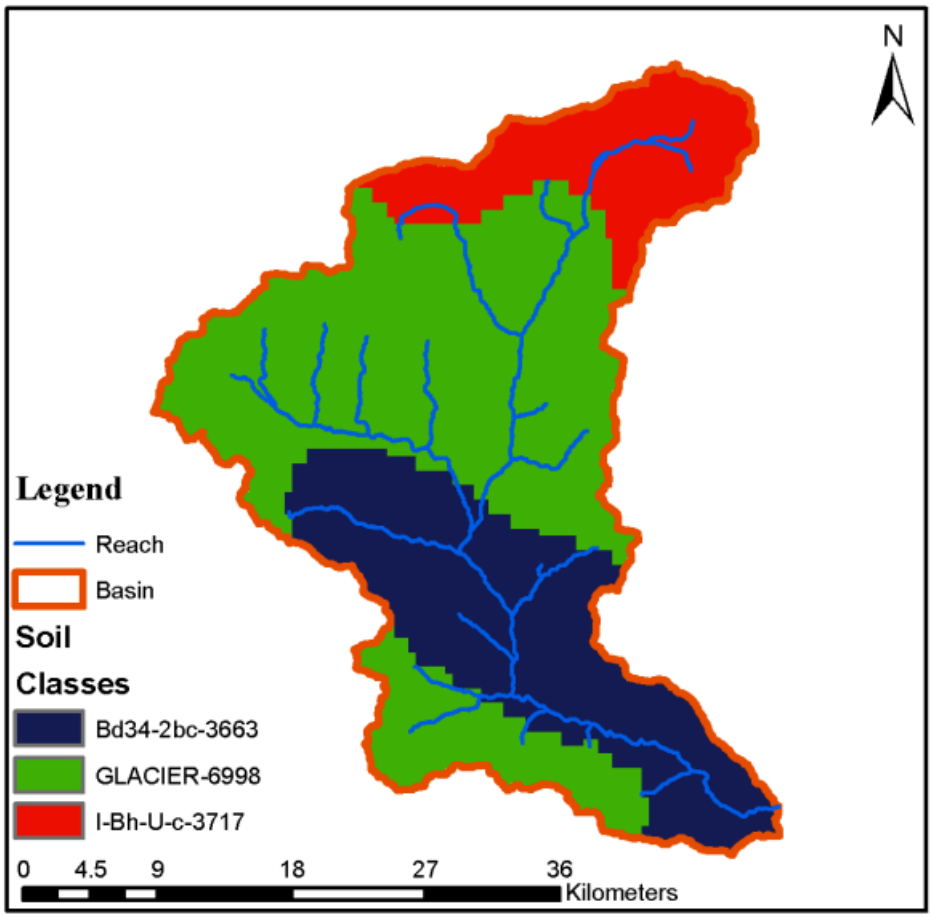

Figure 3-8 Soil map of Myagdi River Basin

3.3.6 Climate Model Data

3.3.6.1 NASA NEX-GDDP-CMIP6 Dataset

Climate projections were obtained from the NEX-GDDP-CMIP6 dataset (Thrasher et al., 2022), which provides:

- Spatial resolution: 0.25° × 0.25° (~25 km at the equator)
- Temporal coverage: 1950-2100 (daily)
- Temporal resolution: Daily
- Downscaling method: Bias-Corrected Spatial Disaggregation (BCSD)
- Reference dataset: Global Meteorological Forcing Dataset (GMFD)

Variables extracted:

- pr: Precipitation (kg m^{-2} s^{-1})
- tasmax: Daily maximum near-surface air temperature (K)
- tasmin: Daily minimum near-surface air temperature (K)

3.3.6.2 Selected Global Circulation Models (GCMs)

Four CMIP6 models were selected to represent diverse climate sensitivities and institutional origins while ensuring data availability in NEX-GDDP-CMIP6 archive:

Table 3-6 Selected Global Circulation Models (GCMs)

Model	Institution	Country	Horizontal Resolution	Equilibrium Climate Sensitivity (°C)	Selection Rationale
ACCESS-CM2	CSIRO-ARCCSS	Australia	250 km (N96)	4.7	High sensitivity; strong monsoon representation
MIROC6	MIROC	Japan	250 km (T85)	2.6	Low sensitivity; good Asian monsoon skill
MPI-ESM1-2-HR	MPI-M	Germany	100 km (T127)	3	High resolution; moderate sensitivity
MRI-ESM2-0	MRI	Japan	100 km (TL159)	3.1	Moderate sensitivity; monsoon emphasis

3.3.6.3 Shared Socioeconomic Pathways (SSPs)

Two emission scenarios representing intermediate and high forcing pathways were selected:

Table 3-7 Shared Socioeconomic Pathways (SSPs)

Scenario	Description	Radiative Forcing by 2100	Global Warming by 2100 (relative to 1850-1900)	Policy Context
SSP2-4.5	Middle-of-the-road	4.5 W m^{-2}	~2.0-3.0°C	Intermediate mitigation; aligns with NDCs
SSP5-8.5	Fossil-fueled development	8.5 W m^{-2}	>4.5°C	Limited mitigation; high-emission trajectory

Rationale for SSP Selection

- SSP2-4.5: Represents a plausible future consistent with current national climate commitments and moderate mitigation efforts; provides "business-as-usual with some climate policy" baseline.
- SSP5-8.5: Serves as upper-bound "stress test" scenario; illustrates potential impacts under continued fossil fuel dependence; increasingly regarded as low-probability but high-impact scenario useful for infrastructure planning.

Table 3-8 Data period coverage

Dataset Type	Period	Use in Study
Historical simulation	1950-2014	Bias correction reference (1992-2014); baseline period (1992-2019)
SSP2-4.5	2015-2100	Future projections (three time slices; Near Future (NF): 2026-2050, Mid Future (MF): 2051-2075, Far Future (FF): 2076-2100)
SSP5-8.5	2015-2100	

3.3.7 Climate Scenario Bias Correction

3.3.7.1 Rationale for Additional Bias Correction

Although NEX-GDDP-CMIP6 data are already bias-corrected at the global scale using BCSD methodology, additional basin-specific bias correction was implemented for two reasons:

- **Local terrain complexity**: The MRB's steep topographic gradients (835-8136 masl over <40 km horizontal distance) create precipitation and temperature patterns that global gridded products may not fully capture.
- **Reference dataset differences**: NEX-GDDP uses Global Meteorological Forcing Dataset (GMFD) as reference (1960-2014), which may differ from local DHM observations in mountainous Nepal.
- **Standard practice**: Basin-specific bias correction using local observations is recommended practice for regional hydrological impact studies (Teutschbein & Seibert, 2012).

3.3.7.2 Bias Correction Method: Monthly Linear Scaling

Climate model data covering the basin were extracted using Python scripting with *xarray* and *netCDF4* libraries.

The monthly linear scaling bias correction method (also termed "delta change" or "multiplicative/additive adjustment") was applied. This approach corrects systematic biases in

monthly mean values while preserving GCM-simulated temporal sequencing and variance structure.

Precipitation Correction (Multiplicative)

Precipitation was corrected using a multiplicative monthly correction factor to preserve zero-precipitation days and avoid negative values:

$$P_{\text{corrected}}(d,m) = P_{\text{raw}}(d,m) \times CF_m$$

where: $P_{\text{corrected}}(d,m)$ = bias-corrected precipitation on day d in month m (mm day^{-1}) - $P_{\text{raw}}(d,m)$ = raw GCM precipitation (mm day^{-1}) - CF_m = monthly correction factor for month m

The monthly correction factor is calculated as:

$$CF_m = \frac{\overline{P}_{\text{obs},m}}{\overline{P}_{\text{GCM},m}}$$

where: - $\overline{P}_{\text{obs},m}$ = observed mean precipitation for month m averaged over 1988-2003 - $\overline{P}_{\text{GCM},m}$ = GCM-simulated mean precipitation for month m averaged over 1988-2003

Separate correction factors were computed for each month (12 values per GCM).

Temperature Correction (Additive)

Temperature (both Tmax and Tmin) was corrected using an additive monthly adjustment to preserve GCM-simulated temperature trends and variability:

$$T_{\text{corrected}}(d,m) = T_{\text{raw}}(d,m) + \Delta T_m$$

where:

$T_{\text{corrected}}(d,m)$ = bias-corrected temperature on day d in month m (°C)

$T_{\text{raw}}(d,m)$ = raw GCM temperature (°C, after conversion from Kelvin)

ΔT_m = monthly temperature adjustment for month m

The monthly adjustment is calculated as:

$$\Delta T_m = \overline{T}_{\text{obs},m} - \overline{T}_{\text{GCM},m}$$

where:

$\overline{T}_{\text{obs},m}$= observed mean temperature for month m averaged over 1988-2003

$\overline{T}_{\text{obs},m}\overline{T}_{\text{GCM},m}$ = GCM-simulated mean temperature for month m averaged over 1988-2003

Assumptions and Limitations

This bias correction approach assumes:

- Stationarity: The bias structure (ratio for precipitation, difference for temperature) remains constant over time.
- Preserved climate change signal: The adjustment corrects baseline climatology but does not alter GCM-projected trends or changes in variability.
- Monthly resolution: Sub-monthly variations (e.g., diurnal cycles, storm characteristics) are not explicitly corrected beyond what NEX-GDDP BCSD already provides.

These limitations are acceptable for water resource planning applications focused on seasonal and annual streamflow patterns, though they may underestimate changes in extreme precipitation intensity.

3.4 SWAT Model Setup and Configuration

SWAT model was employed to simulate hydrological processes in the MRB. SWAT simulates watershed hydrology through physically-based representations of surface runoff, infiltration, evapotranspiration, lateral flow, groundwater recharge, and channel routing (Arnold et al., 2012). SWAT has been widely applied across Himalayan river basins for a range of hydrological studies, particularly in assessing climate change impacts and supporting water resources management (Subedi et al., 2024; Khatri et al., 2024; Marahatta et al., 2021; Nepal et al., 2017). SWAT is a physically based, semi-distributed model capable of simulating hydrological processes, vegetation growth, sediment transport, and nutrient dynamics under varying environmental conditions, including changes in land use, soil characteristics, and climate (Neitsch et al., 2011).

SWAT represents the watershed as a set of interconnected sub-basins, each subdivided into HRUs, and simulates hydrological processes at the HRU scale using the following water balance equation:

$$SWt = SW_0 + \Sigma_{i=1}^{t}\left(R_{day} - Q_{surf} - E_a - w_{seep} - Q_{gw}\right)$$

where,

SWt and SW_0 are the final and initial stages of soil water content (mm H_2O) respectively

R_{day} is the daily precipitation (mm H_2O)

Q_{surf} is the daily surface runoff (mm H_2O)

E_a is the daily evapotranspiration (mm H_2O)

w_{seep} is the daily percolation (mm H_2O)

Q_{gw} is the daily return flow (mm H_2O), and t is the time (days)

Watershed delineation was carried out using a 30-meter resolution Digital Elevation Model (DEM) obtained from FABDEM. The model setup incorporated spatial inputs such as land use, soil type, slope, and climate variables specific to the region.

3.4.1 Spatial Data Preparation

- DEM: FABDEM 30m
- LULC: ICIMOD 2022
- Soil Data: HWSD v2.0

All spatial datasets were projected to WGS84 UTM Zone 44N for consistency and clipped to the MRB boundary extended by a 2-km buffer to ensure watershed delineation stability.

3.4.2 Watershed Delineation

Watershed delineation was performed using ArcSWAT 2012 interface for ArcGIS 10.x.

3.4.3 Hydrologic Response Unit (HRU) Definition

663 HRUs were generated based on unique combinations of land use, soil type, and slope class within each sub-basin.

Table 3-9 SWAT configuration parameters for Myagdi River Basin

Watershed Area	HRUs	Sub-basins
1093.15 km^2	663	49

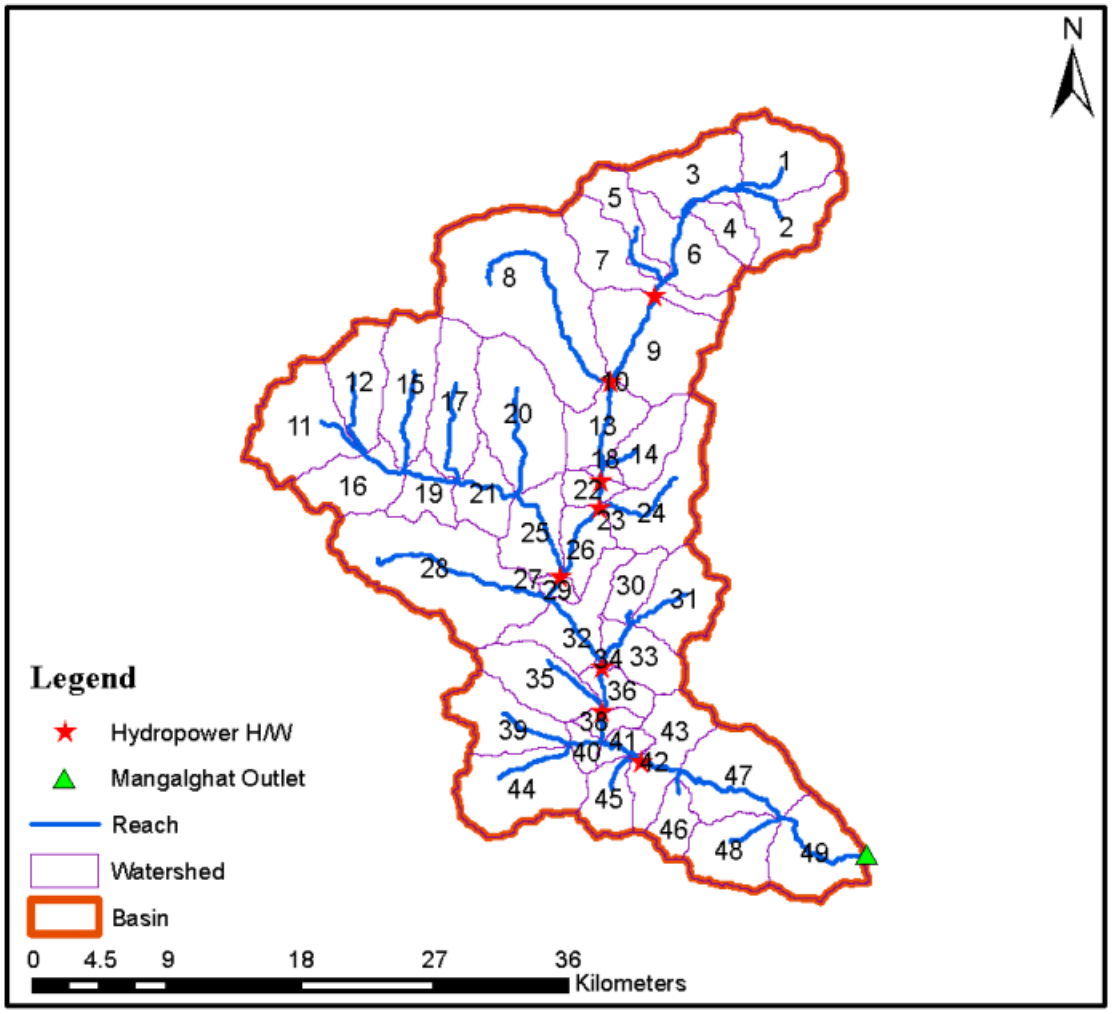

Figure 3-9 Watershed delineation in the Myagdi River Basin

3.4.4 Snowmelt Representation

The MRB is a high-elevation catchment where snow accumulation and melt significantly influence seasonal streamflow, particularly during the pre-monsoon (March-May) and early monsoon periods when baseflows are sustained by snowmelt contributions. Although direct remote sensing-based snow modeling was not implemented in this study, snow dynamics were accounted for through elevation bands and SWAT's built-in temperature-index snowmelt routine.

The model uses key snow-related parameters including:

- SMFMX: Maximum snowmelt rate on 21 June (mm H_2O/°C/day)
- SMFMN: Minimum snowmelt rate on 21 December (mm H_2O/°C/day)
- SFTMP: Snowfall temperature threshold (°C)
- SMTMP: Snowmelt base temperature threshold (°C)
- TIMP: Snowpack temperature lag factor

These parameters were calibrated within physically reasonable ranges informed by literature values for similar Himalayan catchments. Although no external snow cover datasets (e.g., MODIS) were assimilated for validation, the model's ability to reproduce observed seasonal flow patterns – particularly the pre-monsoon baseflow sustained by snowmelt – provided confidence in the snowmelt parameterization for this snow-influenced basin.

3.5 SWAT Model Calibration and Validation

The SWAT model was calibrated and validated to simulate streamflow dynamics in the Myagdi River Basin. The basin outlet was fixed at Mangalghat Station (STN 404.7) on the Myagdi River.

3.5.1 Model Initialization and Configuration

The calibration and validation periods were selected to capture interannual variability, including both monsoon peaks and dry-season baseflow in order to ensure the model's robustness across seasonal regimes.

Table 3-10 Simulation period settings

Parameter	Setting
Total simulation period	1992-2019 (28 years)
Warm-up period	1992-1994 (3 years)
Calibration period	1995-2010 (16 years)
Validation period	2011-2019 (9 years)

Warm-up Period:

A 3-year warm-up period (1992-1994) was implemented to initialize soil moisture states to realistic values (SWAT default starts with 50% saturation), stabilize groundwater levels and baseflow contributions, allow seasonal snowpack to develop realistic patterns in high-elevation zones, eliminate unrealistic "spin-up" effects in early simulation years.

Outputs from the warm-up period were excluded from calibration and performance evaluation.

3.5.2 Calibration Framework: SUFI-2 in SWAT-CUP

Model calibration was performed using the SUFI-2 algorithm implemented in SWAT-CUP 2019 (Abbaspour, 2015). SUFI-2 is a semi-automated inverse modeling procedure that uses Latin Hypercube Sampling to explore parameter space efficiently, quantifies predictive uncertainty through the 95% prediction uncertainty (95PPU) band, and optimizes parameters toward maximum objective function values. SUFI-2 balances goodness-of-fit with uncertainty metrics.

A total of 25 parameters were chosen based on their influence on surface runoff, baseflow, evapotranspiration, and snowmelt processes shown in Appendix II. Parameter ranges were defined using literature review and trial-based refinement.

3.5.3 Objective Functions and Performance Metrics

Multiple statistical metrics were computed to assess model performance and to compare observed and simulated streamflow and evaluate model efficiency across both calibration and validation periods.

Primary Objective Function:

Maximize: Nash-Sutcliffe Efficiency (NSE) - Calibration target metric:

$$NSE = 1 - \frac{\sum_{i=1}^{n} \left(Q_{obs,i} - Q_{sim,i}\right)^2}{\sum_{i=1}^{n} \left(Q_{obs,i} - \overline{Q}_{obs}\right)^2}$$

where:

$Q_{obs,i}$ = observed streamflow on day i

$Q_{sim,i}$ = simulated streamflow on day i

$\overline{Q}_{obs}$ = mean observed streamflow over evaluation period

n = number of observations

Supplementary Metrics:

Maximize: Coefficient of Determination (R^2)

$$R^2 = \left(\frac{\sum_{i=1}^{n} \left(Q_{obs,i} - \overline{Q}_{obs}\right)\left(Q_{sim,i} - \overline{Q}_{sim}\right)}{\sqrt{\sum_{i=1}^{n} \left(Q_{obs,i} - \overline{Q}_{obs}\right)^2} \sqrt{\sum_{i=1}^{n} \left(Q_{sim,i} - \overline{Q}_{sim}\right)^2}} \right)^2$$

Minimize: Percent Bias (PBIAS)

$$PBIAS = \frac{\sum_{i=1}^{n} \left(Q_{obs,i} - Q_{sim,i}\right)}{\sum_{i=1}^{n} Q_{obs,i}} \times 100\%$$

3.6 Future Scenario Simulations

The calibrated and validated SWAT model was used to simulate future streamflow in the Myagdi River Basin under bias-corrected climate projections from four CMIP6 Global Climate Models (GCMs): ACCESS-CM2, MIROC6, MPI-ESM1-2-HR, and MRI-ESM2-0. These models were selected for their representation of South Asian monsoon dynamics and availability of daily temperature and precipitation variables across the full projection period. Two emission scenarios were applied:

- SSP2-4.5: A moderate emission pathway representing stabilization through mid-century policy interventions.
- SSP5-8.5: A high-emission trajectory reflecting fossil fuel-intensive development.

All GCM outputs were bias-corrected using monthly correction factors – multiplicative for precipitation and additive for temperature – derived from the historical overlap period (1992-2014) as described in Section 3.3.7.2.

3.6.1 Ensemble Simulation Strategy

To preserve inter-model variability and capture non-linear hydrological responses, bias-corrected climate data from each GCM were used to drive individual SWAT simulations rather than creating ensemble-averaged climate inputs. This approach generated eight distinct streamflow projections (4 GCMs × 2 SSPs), each representing a physically consistent realization of future hydrology under a specific climate model and emission scenario.

This methodology offers several advantages over approaches that ensemble-average climate inputs prior to hydrological modeling:

- Non-linear preservation: SWAT's non-linear process representations (e.g., threshold-based snowmelt, saturation-excess runoff) mean that hydrological response to averaged climate inputs differs from the average of individual responses.
- Uncertainty quantification: The spread among individual projections enables calculation of uncertainty bounds (p10–p90 percentiles) around the ensemble mean.
- Extreme scenario identification: Individual model runs reveal the range of plausible futures, including worst-case and best-case outcomes critical for risk assessment.
- Model-specific diagnostics: Retention of individual projections allows evaluation of inter-model agreement and identification of outlier behaviors.

Following individual simulations, streamflow outputs were ensemble-averaged to produce robust central estimates while preserving uncertainty information through percentile analysis.

3.6.2 Projection Periods

Future simulations were conducted for three 25-year periods to assess climate impacts across multiple time horizons:

- Near-term (2026–2050): Early adaptation planning horizon
- Mid-term (2051–2075): Medium-range infrastructure design horizon
- Long-term (2076–2100): End-of-century assessment for long-lived infrastructure

All future periods were compared against the historical baseline period (1992-2014).

3.6.3 Analysis Framework

Streamflow outputs were analyzed at multiple temporal scales to characterize changes in flow regime and assess implications for hydropower generation.

3.6.3.1 Streamflow Analysis

- Monthly and seasonal patterns: Identification of shifts in intra-annual distribution, with particular focus on pre-monsoon (March–May) baseflows sustained by snowmelt.
- Flow Duration Curves (FDCs): Assessment of changes across the full flow spectrum, from low flows to high flows.
- Q40 exceedance flows: Evaluation of mid-range flows critical for run-of-river hydropower generation, representing flow exceeded 40% of the time.
- Percent change metrics: Quantification of absolute and relative changes between historical baseline and future periods.

3.6.3.2 Hydropower Impact Assessment

Using the ensemble-mean streamflow projections, annual energy generation was estimated for the five-existing run-of-river hydropower projects in the basin (193 MW total installed capacity) across all three future periods (near-term, mid-term, long-term) and both emission scenarios (SSP2-4.5, SSP5-8.5).

The calculation for hydropower potential and hydro-energy generation was done using the following equations (Shrestha et al., 2016; Khare et al., 2017):

$P = \eta \,.\gamma \,.Q \,.H$ and $E = P \,.T$

where,

P is the power generated

η is the overall efficiency

γ is the specific weight of water

Q is the flow rate

H is the hydraulic head or height of water above the turbine

E is the hydroelectric energy generated

T is time in hours

The assessment employed Q40-based methodology consistent with industry design practice, allowing direct comparison with industry Detailed Project Report (DPR) practices. The Q40 flow exceedance level (flow exceeded 40% of time) serves as design discharge for most Nepalese run-of-river projects. Changes in energy generation were calculated relative to the approved annual energy generation to quantify climate change impacts on existing hydropower infrastructure performance.

The following chapter presents the results of these simulations, including projected changes in annual and seasonal streamflow, extreme flow indicators, and projected changes in hydropower development.

4 RESULTS AND DISCUSSION

This chapter presents and discusses results from climate projection analysis, SWAT model calibration, and future streamflow simulation in the MRB. The findings directly address the three research objectives: (1) SWAT model performance assessment, (2) projected streamflow changes under climate scenarios, and (3) climate change impacts on hydropower generation. Results are presented sequentially, with interpretation of observed patterns and discussion of their implications for water resources management and hydropower operations in high-elevation Himalayan basins.

4.1 SWAT Model Performance Assessment

The SWAT model was calibrated and validated to simulate streamflow dynamics in the MRB. The basin outlet was fixed at Mangalghat Station on the Myagdi River.

The model was run for a historical simulation period from 1992 to 2019, with the following split:

- Calibration period: 1992-2010
- Validation period: 2011-2019

Calibration and validation were performed using SWAT-CUP SUFI-2 algorithm. SWAT-CUP has integrated tools for sensitivity analysis, parameter adjustment, and performance evaluation. After iterative simulations and parameter tuning, the model produced reliable outputs consistent with observed trends.

4.1.1 Calibration Results

The calibration achieved acceptable to good performance based on established criteria (Moriasi et al., 2015; Moriasi et al., 2007), with all key metrics exceeding the recommended thresholds for data-scarce, snow-fed Himalayan catchments:

- NSE = 0.59 indicates the model explains 59% of variance in observed streamflow, which is borderline satisfactory for daily time step in a data-limited mountainous catchment.
- PBIAS = -8.20% shows slight underestimation of total flow volume, well within the ±15% threshold for good performance.
- R^2 = 0.60 confirms reasonable correlation between observed and simulated flows.

Table 4-1 Calibration performance (1995-2010)

Metric	**Value**	**Rating** (Moriasi et al., 2015)
NSE (daily)	0.59	Acceptable
R^2	0.60	Good
PBIAS (%)	-8.20	Very Good
p-factor	0.53	
r-factor	0.32	

4.1.2 Validation Results

Model validation was performed by running SWAT over the independent validation period (2011-2019) using the final calibrated parameter values without any further adjustment in order to test the model's predictive capability on data not used during calibration.

Table 4-2 Validation performance (2011-2019)

Metric	**Value**	**Rating**	**Change from Calibration**
NSE (daily)	0.73	Very Good	+0.14 (improved)
R^2	0.73	Very Good	+0.13 (improved)
PBIAS (%)	-4.80	Very Good	-3.4% (improved)
p-factor	0.63		
r-factor	0.34		

The model demonstrated very good performance during the independent validation period, with NSE = 0.73 exceeding the calibration NSE. This improvement suggests that model parameters are robust and transferable to independent time periods. There is no apparent overfitting during calibration, and hydrological processes are adequately represented.

PBIAS and R^2 also improved and remained within acceptable thresholds. Overall, the validation confirms the model's reliability for climate scenario simulations.

The model effectively captured seasonal discharge patterns, particularly monsoon peak flows and winter low flows. The low bias (±10%), NSE > 0.5, and $R^2 \geq 0.60$ indicate a strong match between simulated and observed streamflow. These values are considered satisfactory for high-altitude regions, where sparse monitoring and snowmelt processes introduce additional modeling complexity.

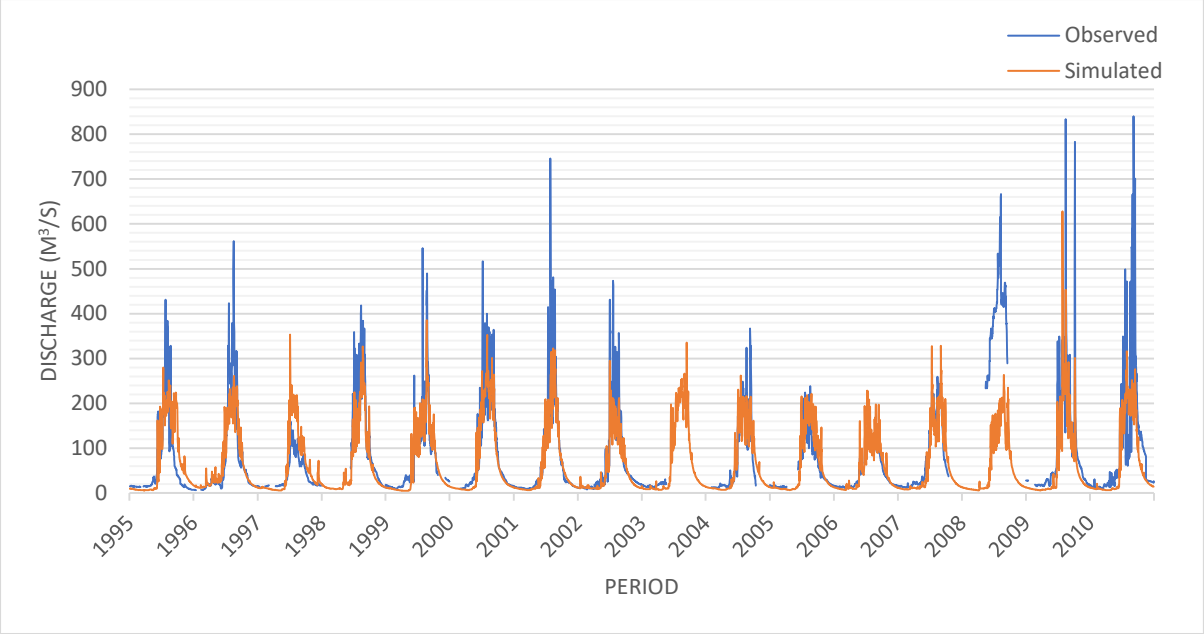

Figure 4-1 Observed vs. simulated streamflow during calibration (1995-2010)

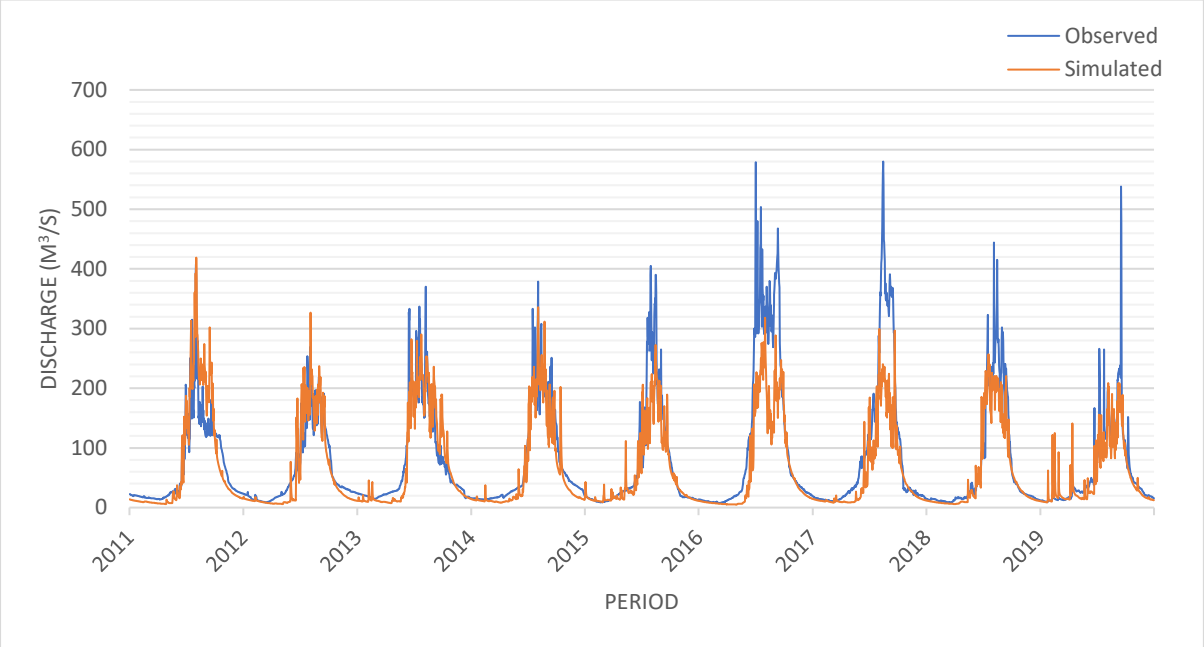

Figure 4-2 Observed vs. simulated streamflow during validation (2011-2019)

4.1.3 Interpretation and Applicability

Despite the limited availability of high-elevation meteorological stations and the inherent challenges of modeling snow-influenced hydrology in steep Himalayan terrain, the SWAT model demonstrated strong performance in simulating streamflow in the MRB. The calibration achieved an NSE of 0.59 and R^2 of 0.60 during the calibration period (1995-2010), with improved performance during validation (NSE = 0.73, R^2 = 0.73; 2010-2019). The PBIAS of -8.2% to -4.8% indicates slight model overestimation, well within acceptable limits for daily

streamflow simulation. Importantly, the model successfully captured seasonal flow patterns, including pre-monsoon baseflows sustained by snowmelt and monsoon peak flows, as evidenced by visual agreement between observed and simulated hydrographs. The satisfactory statistical performance across multiple metrics confirms the model's capability to represent the basin's hydrological processes and its suitability for projecting future streamflow responses under climate change scenarios. The calibrated model provides a reliable foundation for assessing climate impacts on the five run-of-river hydropower projects operating within the basin.

4.2 Projected Streamflow Changes under Climate Change Scenarios

4.2.1 Baseline Streamflow Characteristics

The historical baseline period (1995–2019) establishes reference conditions against which future climate impacts are assessed. Mean annual discharge at the basin outlet, Mangalghat Station (Reach 49), is 62.45 m³/s, with inter-annual variability ranging from 51.47 to 74.96 m³/s (Figure 4-3).

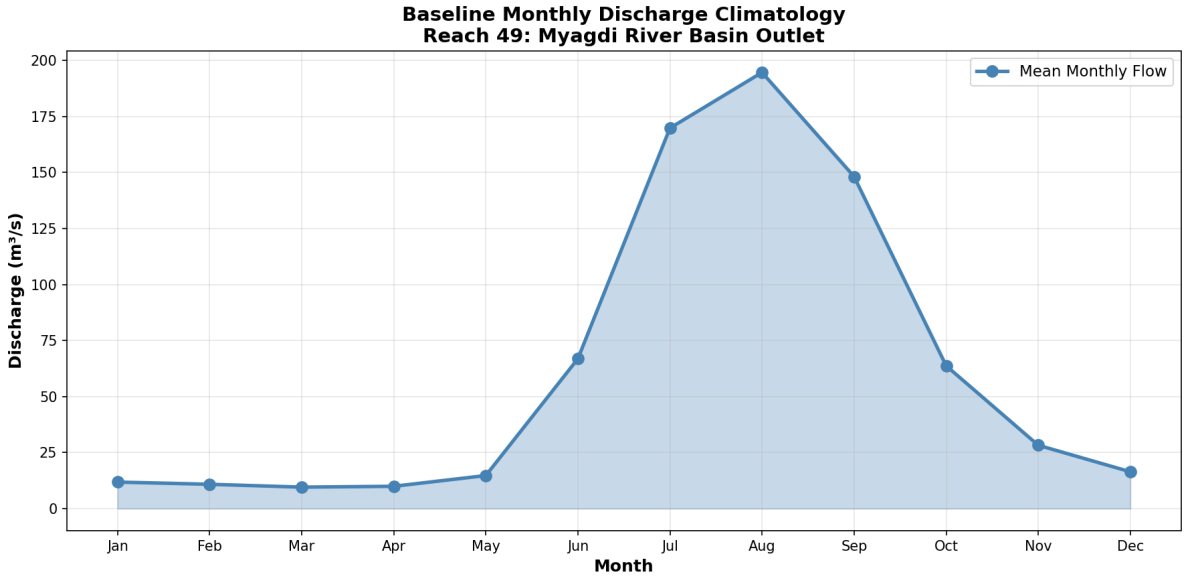

Figure 4-3 Baseline monthly discharge climatology at Mangalghat Station

Streamflow exhibits pronounced seasonal patterns characteristic of monsoon-influenced Himalayan basins. The monsoon season (June-August) dominates hydrological inputs, with peak flows occurring in August (~195 m³/s) and July (~170 m³/s). Monsoon season discharge averages 144.62 m³/s. Post-monsoon (September-November) maintains elevated flows (~80 m³/s) due to sustained groundwater contributions and delayed recession. Winter (December–February) and pre-monsoon (March–May) periods exhibit low flows averaging 13.08 m³/s and

11.45 m³/s respectively, sustained primarily by groundwater discharge and limited snowmelt contributions before the monsoon onset.

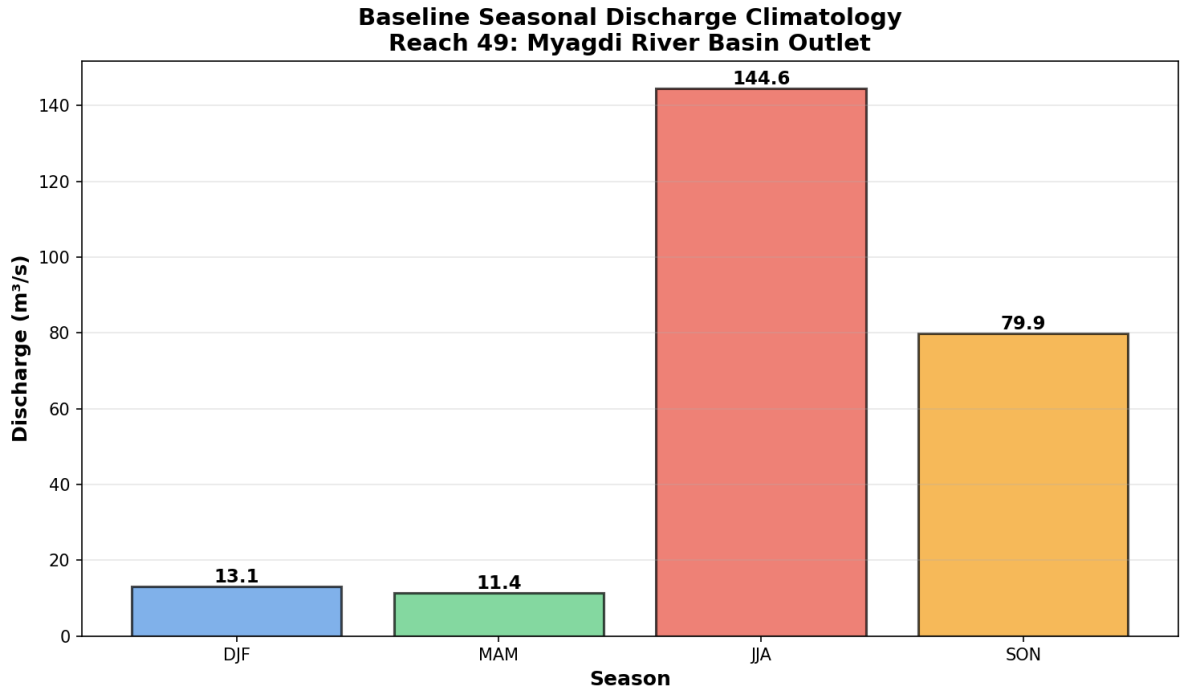

Figure 4-4 Baseline seasonal discharge climatology at Mangalghat Station

This seasonal distribution reflects the basin's dual hydrological regime: monsoon rainfall dominates annual water balance while high-elevation snowmelt sustains critical dry-season baseflows. The steep decline from post-monsoon to winter-spring flows highlights the basin's limited groundwater storage capacity and strong dependence on seasonal precipitation timing.

4.2.2 Projected Changes in Annual Mean Discharge

Annual mean discharge increases across all future periods under both emission scenarios, though trajectories diverge substantially by century-end. Under SSP2-4.5, discharge increases progressively from baseline (62.45 m³/s) to 68.65 m³/s in the near-term period (2026-2050, +9.9%), reaching 74.25 m³/s by mid-century (2051-2075, +18.9%). The stabilization scenario shows minimal additional change in the far-future period (2076-2100, 74.56 m³/s, +19.4%), suggesting near-equilibrium response by late century under moderate emissions.

SSP5-8.5 exhibits similar near-term increases (67.74 m³/s, +8.5%) but accelerates dramatically through the projection period. Mid-century discharge reaches 78.66 m³/s (+26.0%), with the far-future period showing a 56.7% increase to 97.86 m³/s. This non-linear acceleration reflects intensifying hydrological cycle amplification under high radiative forcing. Far-future discharge

increases (35.4 m³/s) exceed mid-century increases (16.2 m³/s) by a factor of 2.2 under SSP5-8.5.

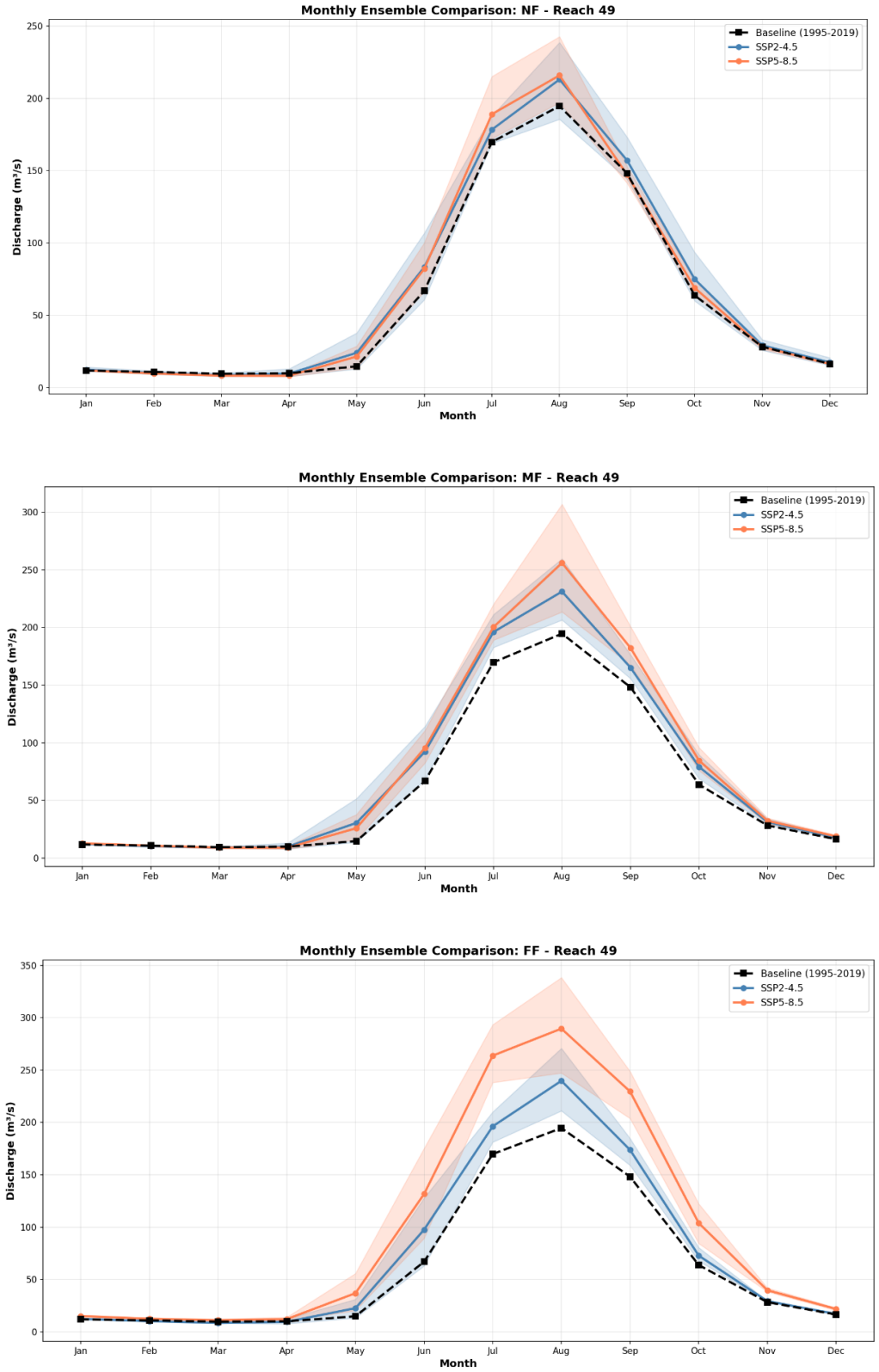

Figure 4-5 Monthly discharge comparison for NF, MF and FF at the outlet of the Myagdi River Basin (Mangalghat Station)

The convergence of scenarios in the near-term period (difference <2%) reflects committed climate change from historical emissions. Divergence emerges clearly by mid-century (~6% higher discharge under SSP5-8.5) and becomes pronounced by 2076-2100 (+31% higher under SSP5-8.5), demonstrating the critical role of emissions mitigation in controlling long-term hydrological response.

4.2.3 Seasonal Pattern Evolution

Seasonal discharge patterns show differential responses to climate forcing across emission scenarios and time periods. Monsoon season flows exhibit the largest absolute increases, ranging from +10% in near-term to +60% under SSP5-8.5 far-future (144 → 231 m³/s), consistent with expected intensification of the South Asian summer monsoon under warming. The monsoon response drives the majority of annual discharge increases.

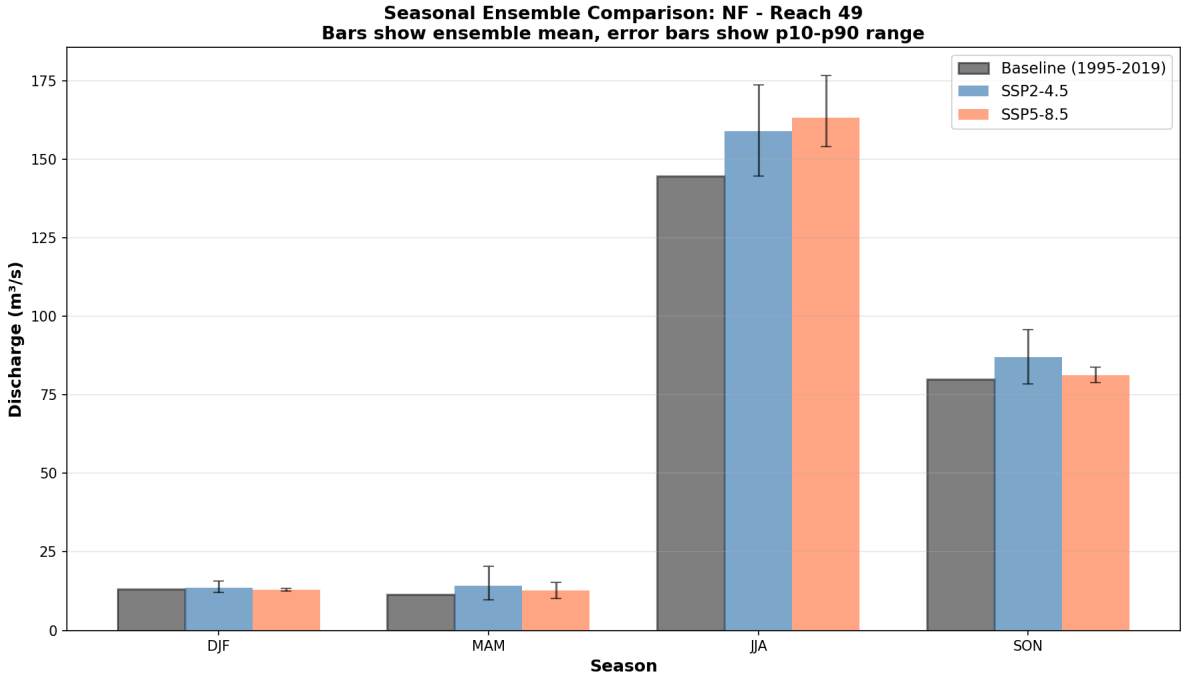

Figure 4-6 Seasonal discharge comparison for NF at Mangalghat Station

Pre-monsoon flows show the largest relative changes, particularly under high-emission scenarios. Far-future SSP5-8.5 projections reach 22 m³/s (+100% from baseline 11 m³/s), indicating fundamental shifts in snowmelt timing. Earlier snowmelt onset and accelerated melt rates under warming deplete seasonal snow storage, transferring water from summer to spring months. This temporal redistribution has significant implications for dry-season water availability: enhanced spring flows may benefit early-season irrigation demands but reduce sustained summer contributions from snowpack when demand peaks.

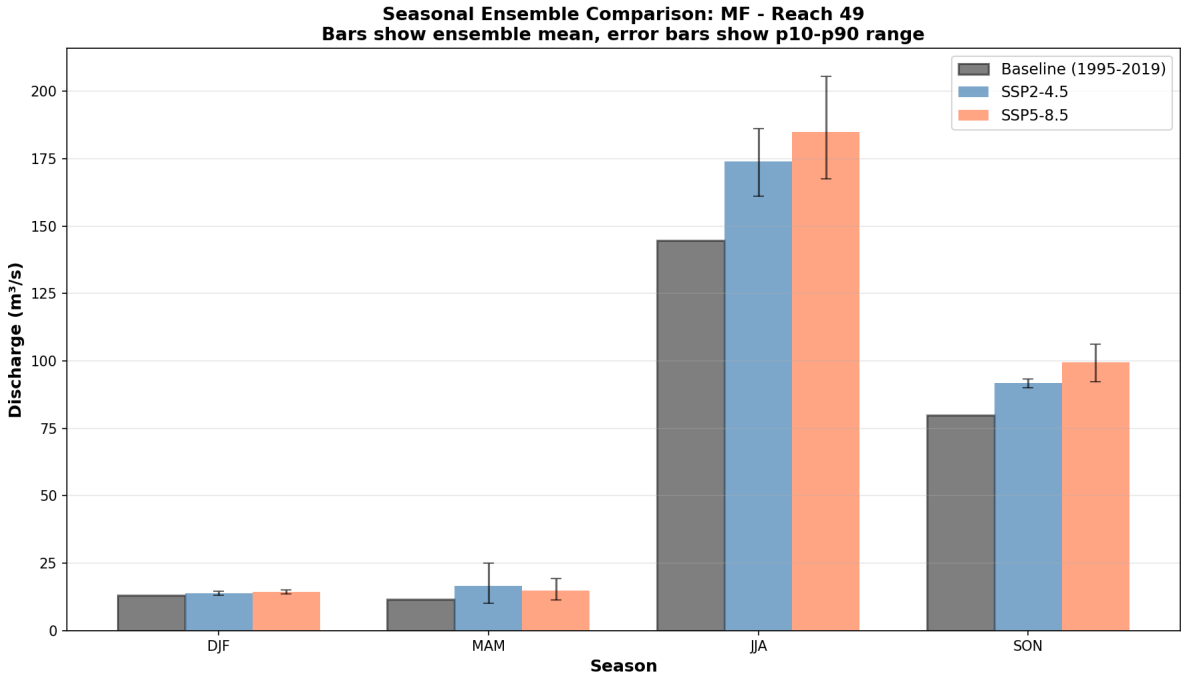

Figure 4-7 Seasonal discharge comparison for MF at Mangalghat Station

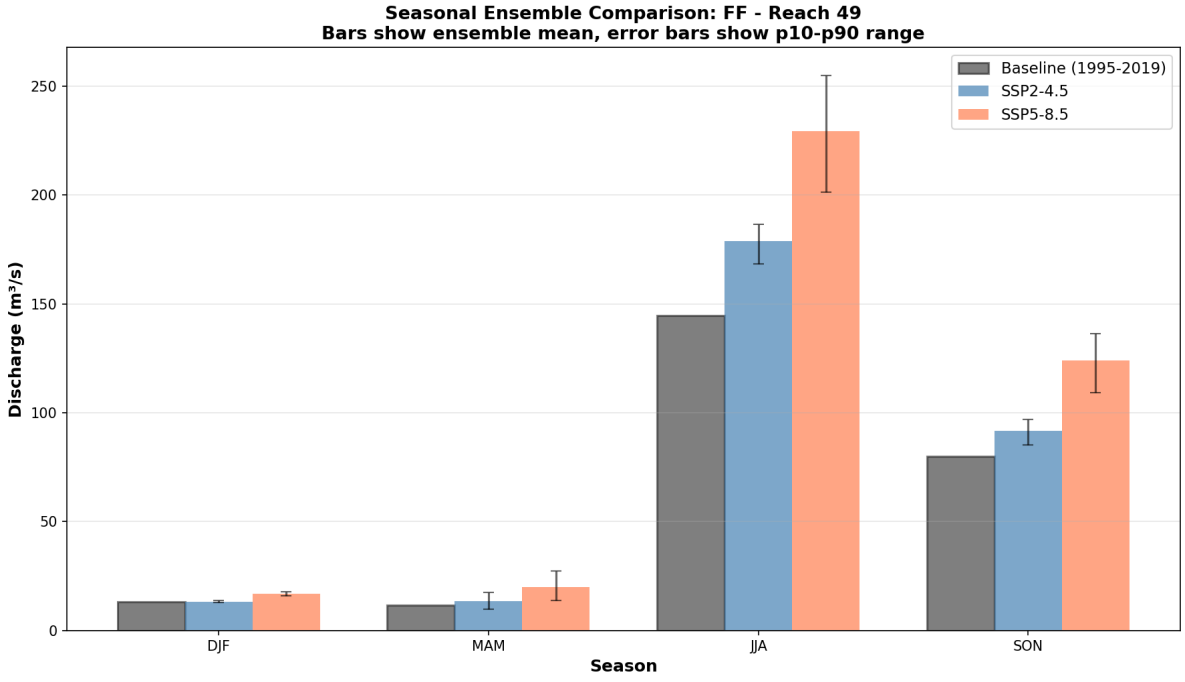

Figure 4-8 Seasonal discharge comparison for FF at Mangalghat Station

Winter flows remain relatively stable across near- and mid-century projections, with modest increases emerging only in far-future SSP5-8.5 (38% increase to 18 m³/s). This delayed response reflects limited winter warming compared to other seasons and the basin's low glacial coverage (~18%), which constrains winter melt contributions.

Post-monsoon flows demonstrate progressive increases from near-term (+2-9%) to far-future (+14% SSP2-4.5, +55% SSP5-8.5), reflecting both extended monsoon duration and enhanced groundwater recharge from intensified precipitation events. The post-monsoon period serves as a critical transition between monsoon-dominated and baseflow-sustained regimes, with future increases supporting extended hydropower generation into the dry season.

Projection uncertainty, represented by p10-p90 ensemble ranges, increases substantially in far-future periods, particularly for high-emission monsoon flows (±22% of ensemble mean), indicating divergent GCM responses to strong radiative forcing.

4.2.4 Flow Duration Curve Analysis

Flow Duration Curves reveal a critical non-monotonic three-phase temporal response pattern that challenges linear assumptions about climate change impacts on streamflow. Rather than exhibiting monotonic increases or decreases, the basin demonstrates: (1) near-term vulnerability (2026-2050) with mid-range flow reductions despite increased total discharge; (2) mid-century recovery (2051-2075) as competing hydrological processes equilibrate; and (3) far-future scenario divergence (2076-2100) where emission pathways produce fundamentally different outcomes. This non-monotonic trajectory, consistent across all GCM ensemble members, has profound implications for infrastructure design and water resources planning, as it demonstrates that endpoint analyses alone are insufficient to capture the full complexity of hydrological response to climate forcing.

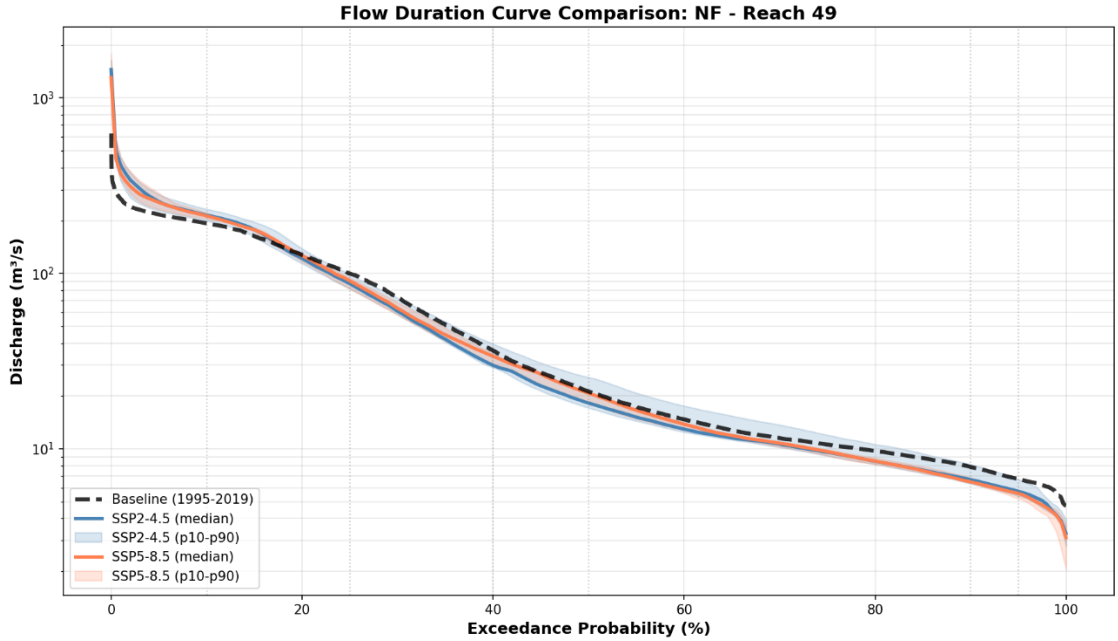

Figure 4-9 Flow Duration Curve comparison for NF at Mangalghat Station

4.2.4.1 Near-term Period (2026–2050): Transition-Phase Vulnerability

The near-term period exhibits a bifurcated response pattern with critical implications for water resources management. High flows (Q10, exceeded 10% of time) increase by approximately 10-11% under both scenarios (SSP2-4.5: +11.2%, SSP5-8.5: +10.2%), indicating enhanced peak flow magnitudes consistent with monsoon intensification. However, mid-range and low flows show consistent and substantial declines across the flow spectrum.

Under SSP2-4.5, Q40 decreases by 17.4% (from 36.23 to 29.92 m^3/s), Q50 decreases by 14.1% (from 21.20 to 18.21 m^3/s), and Q90 decreases by 15.5% (from 7.88 to 6.66 m^3/s). SSP5-8.5 shows similar patterns with slightly attenuated mid-range declines: Q40 reduces by 7.0% (to 33.70 m^3/s), Q50 by 2.1%, and Q90 by 17.9%. This near-term reduction in Q40-Q90 flows represents a critical finding, as these mid-range flows are fundamental to sustained water availability and run-of-river hydropower generation.

The bifurcation between increased high flows and decreased mid-to-low flows suggests competing hydrological processes operating on different timescales. Enhanced monsoon peak intensification raises extreme flows, while disruption of snowmelt regimes, altered recession dynamics, or changes in evapotranspiration patterns reduce sustained baseflows. The near-term period thus represents a transition phase where traditional flow regime structure undergoes reorganization before stabilizing under new climate forcing.

The steepness of FDC slopes shows modest changes, suggesting that while absolute discharge magnitudes shift substantially, the relative variability structure of the flow regime remains broadly similar. This persistence of regime characteristics simplifies adaptation planning compared to scenarios involving fundamental regime reorganization.

4.2.4.2 Mid-century Period (2051–2075): Recovery and Stabilization

Mid-century projections show partial to complete recovery of mid-range and low flows from near-term deficits. High flows continue increasing under both scenarios (SSP2-4.5: +16.5%, SSP5-8.5: +21.0%), while mid-range flows stabilize near or above baseline levels. Under SSP2-4.5, Q40 recovers to 34.91 m^3/s (-3.6% from baseline), Q50 reaches 21.27 m^3/s (+0.3%), indicating near-complete recovery to historical conditions. SSP5-8.5 demonstrates stronger recovery with Q40 shifting to positive change territory at 37.95 m^3/s (+4.7%) and Q50 increasing to 22.54 m^3/s (+6.3%).

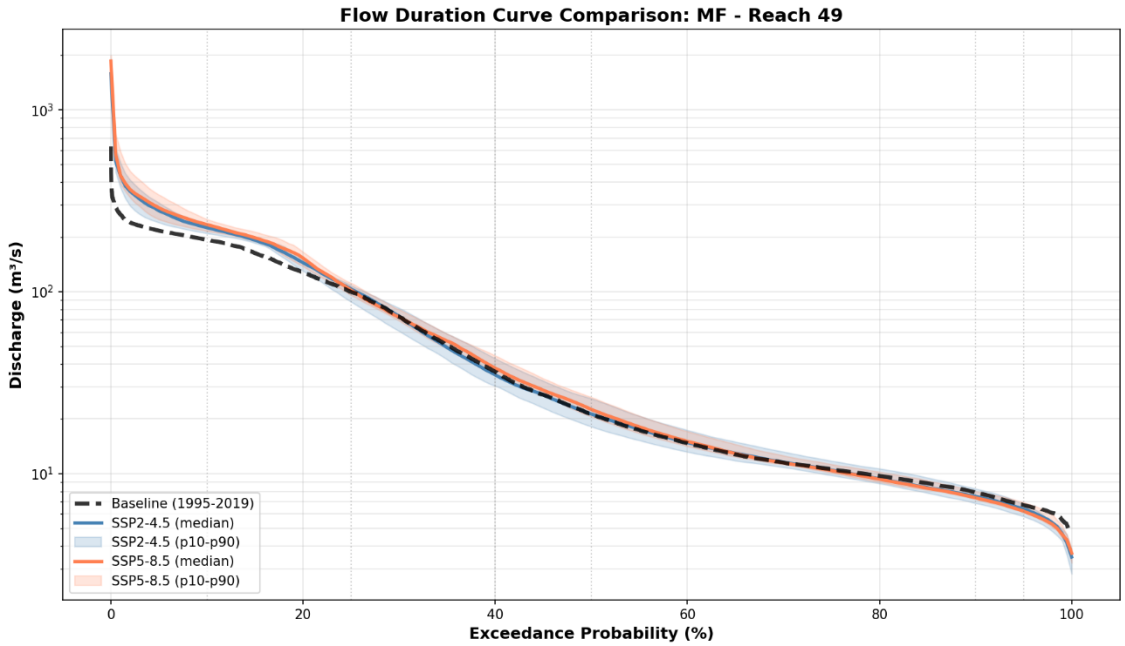

Figure 4-10 Flow Duration Curve comparison for MF at Mangalghat Station

Low flows (Q90, Q95) remain modestly depressed under both scenarios (-5% to -7%), suggesting that baseflow processes respond more slowly to climate forcing than peak flow mechanisms or that sustained low-flow deficits represent persistent features of the transformed regime. The slower recovery of extreme low flows may reflect groundwater storage depletion, reduced dry-season recharge, or threshold-dependent responses in subsurface hydrology requiring longer adjustment periods.

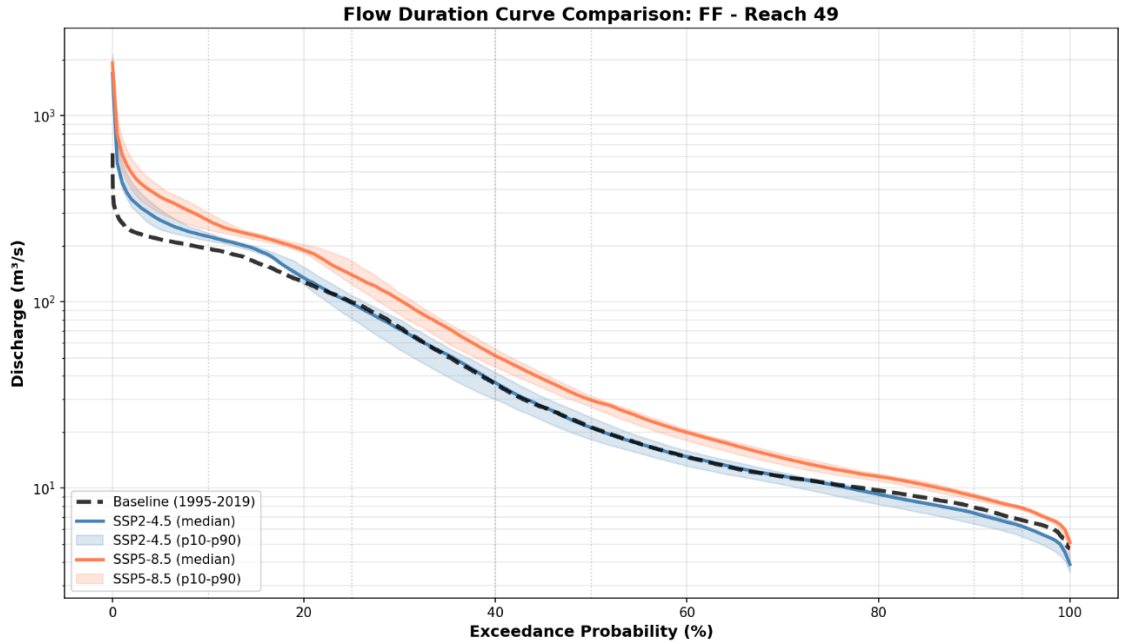

Figure 4-11 Flow Duration Curve comparison for FF at Mangalghat Station

4.2.4.3 Far-future Period (2076–2100): Dramatic Scenario Divergence

Far-future projections exhibit the most pronounced divergence between emission scenarios, with fundamentally different flow regime outcomes. SSP2-4.5 shows continued modest high flow increases (+16.3%) with near-baseline mid-range flows (Q40: +1.4% to 36.74 m³/s, Q50: -0.3% to 21.14 m³/s) and persistent low flow deficits (Q90: -7.0% to 7.33 m³/s). This stabilization pattern suggests that moderate emission pathways produce relatively constrained hydrological impacts, with flow regimes adjusting to new equilibrium conditions similar to historical baselines.

In stark contrast, SSP5-8.5 produces massive increases across the entire flow spectrum, representing fundamental transformation of basin hydrology. Q10 increases by 41.9% (to 273.88 m³/s), Q25 by 39.9% (to 139.45 m³/s), Q40 by 41.6% (to 51.30 m³/s), Q50 by 39.9% (to 29.65 m³/s), and even Q90 rises by 14.8% (to 9.05 m³/s). This near-uniform 40% amplification across all exceedance probabilities indicates wholesale intensification of the hydrological cycle under extreme forcing, with profound implications for both water availability and infrastructure design.

The 40-percentage-point difference in Q40 response between SSP2-4.5 (+1.4%) and SSP5-8.5 (+41.6%) by far-future quantifies the "mitigation dividend" in hydrological terms. Emission reductions prevent massive flow regime transformation, maintaining conditions within historical variability ranges and avoiding infrastructure obsolescence or capacity exceedance issues.

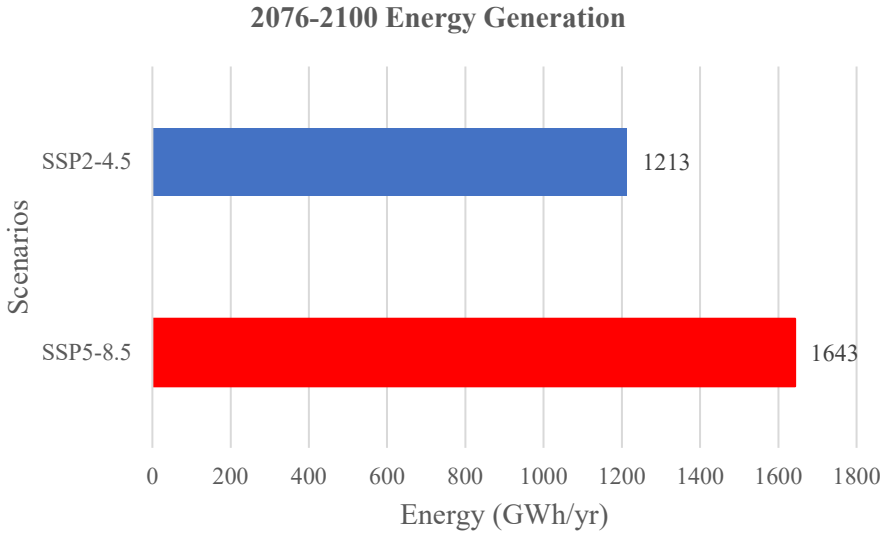

Figure 4-12 The mitigation dividend: Far-future (2076-2100) basin-wide generation under alternative emission scenarios

4.2.5 Implications for Water Resources and Hydropower

The projected streamflow changes have significant implications for water resources management and hydropower operations in the MRB. The non-monotonic Q40 trajectory – declining 7-17% in near-term, recovering to ±5% by mid-century, then diverging dramatically (+1.4% vs. +41.6%) by far-future – determines run-of-river generation potential across the basin's 193 MW installed capacity.

Detailed analysis of climate change impacts on hydropower energy generation for the basin's five run-of-river projects is presented in Section 4.3, which translates these hydrological changes into specific generation outcomes (GWh/yr) accounting for project-specific design constraints and capacity limitations. This analysis employs industry-standard Q40-based methodologies, incorporates SWAT-DPR calibration adjustments, and evaluates capacity saturation effects under high-flow scenarios.

4.3 Climate Change Impacts on Hydropower Energy Generation

Annual energy generation from the basin's five run-of-river hydropower projects (193 MW combined installed capacity) exhibits a three-phase temporal trajectory mirroring the Q40 flow patterns described in Section 4.2.4. Baseline generation totals 1,120 GWh/yr across all projects. The Q40-based methodology employed matches industry-standard Detailed Project Report (DPR) practices, enabling direct comparison with original design projections and translation of flow changes into generation impacts.

4.3.1 Methodological Note: SWAT-DPR Calibration

SWAT baseline Q40 estimates were systematically 5-31% lower than DPR design assumptions across all five projects, a common discrepancy arising from model-observation differences in flow regime representation. To reconcile this while preserving climate change signals, efficiency calibration factors (0.57-0.81) were derived by matching SWAT baseline Q40-calculated generation to DPR-reported baseline values for each project. These factors were then consistently applied across all climate scenarios, ensuring that relative changes (percentages) accurately reflect climate impacts while absolute generation values align with industry design standards.

4.3.2 Near-term Decline (2026–2050)

Basin-wide energy generation decreases by 8.5% under SSP2-4.5 (to 1,026 GWh/yr) and 9.8% under SSP5-8.5 (to 1,010 GWh/yr) during the near-term period. This decline directly reflects the Q40 flow reductions documented in Section 4.2.4, with generation changes tracking flow

changes nearly one-to-one for projects operating below installed capacity. The minimal scenario differentiation (<2% difference) indicates that near-term impacts derive primarily from committed climate change rather than emission pathway differences.

Individual project impacts range from -7.7% to -10.3%, with the most downstream project (Darbang Myagdi HP) experiencing the largest percentage decline (-10.3% under SSP5-8.5). This near-term generation deficit represents approximately 95-110 GWh/yr of foregone energy production relative to baseline expectations, translating to substantial revenue losses for project operators assuming current power purchase agreement rates.

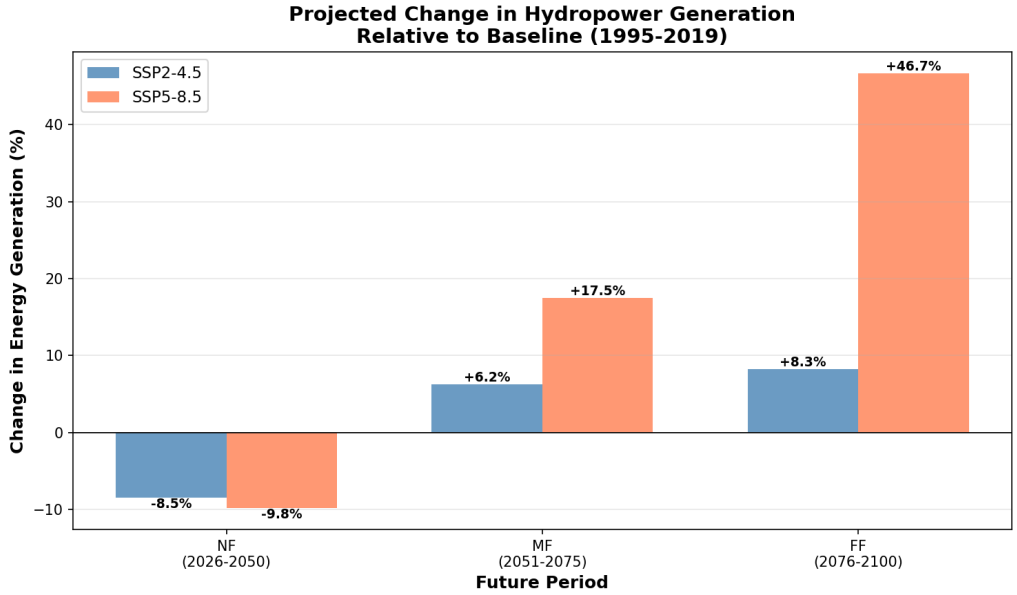

Figure 4-13 Percentage change in hydropower generation relative to baseline

4.3.3 Mid-century Recovery (2051–2075)

Energy generation recovers by mid-century, with basin-wide totals reaching 1,190 GWh/yr (+6.25%) under SSP2-4.5 and 1,316 GWh/yr (+17.5%) under SSP5-8.5. This 11-percentage-point scenario difference reflects emerging divergence in hydrological response, with higher emission forcing producing proportionally greater flow and generation increases. The SSP5-8.5 mid-century generation (+196 GWh/yr above baseline) more than compensates for near-term deficits, suggesting that projects surviving the transition period would experience net positive outcomes over project lifetimes extending beyond 2050.

Individual project responses vary from near-baseline recovery (Darbang Myagdi HP: -0.2% under SSP2-4.5) to substantial gains (Myagdi Khola HP: +24.9% under SSP5-8.5). This spread reflects spatial variability in climate forcing across the basin and differences in project

elevation, suggesting that upper-elevation projects may benefit more from enhanced snowmelt contributions while lower-elevation projects depend primarily on monsoon rainfall changes.

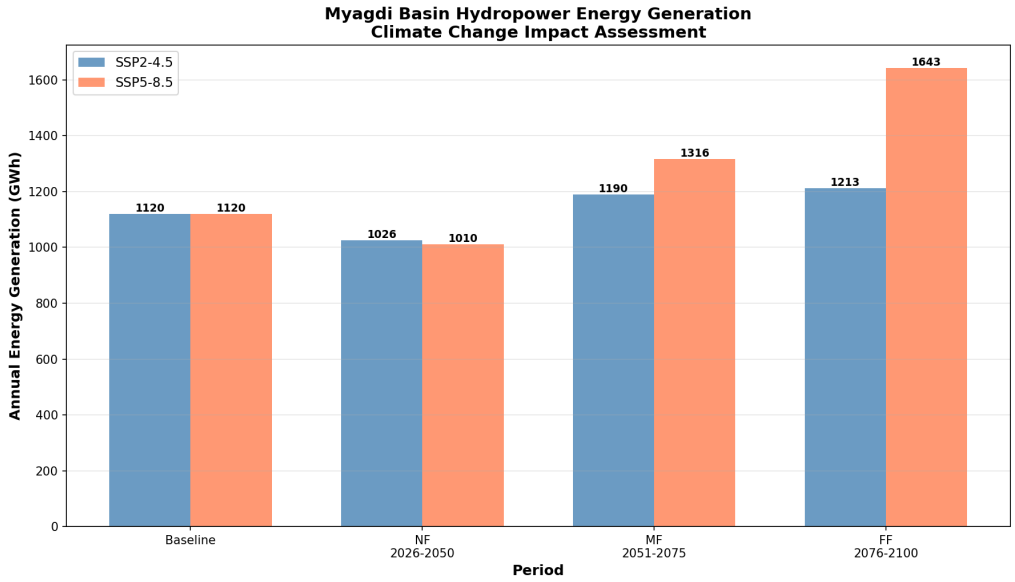

Figure 4-14 Changes in hydropower energy generation in Myagdi River Basin under different projected scenarios

4.3.4 Far-future Divergence (2076–2100)

Far-future projections exhibit dramatic scenario-dependent outcomes. SSP2-4.5 shows moderate continued increase to 1,213 GWh/yr (+8.26%), representing near-stabilization at levels modestly above baseline. SSP5-8.5 demonstrates transformative change, with generation reaching 1,643 GWh/yr (+46.67%), equivalent to adding 523 GWh/yr of new generation capacity – approximately 47% of current total output.

The 430 GWh/yr difference between scenarios (1,643 vs. 1,213 GWh/yr) quantifies the "mitigation dividend" in energy terms. Emission reductions under SSP2-4.5 avoid the massive flow increases projected under SSP5-8.5, maintaining generation within ranges manageable by existing infrastructure while avoiding capacity exceedance and associated spillage losses.

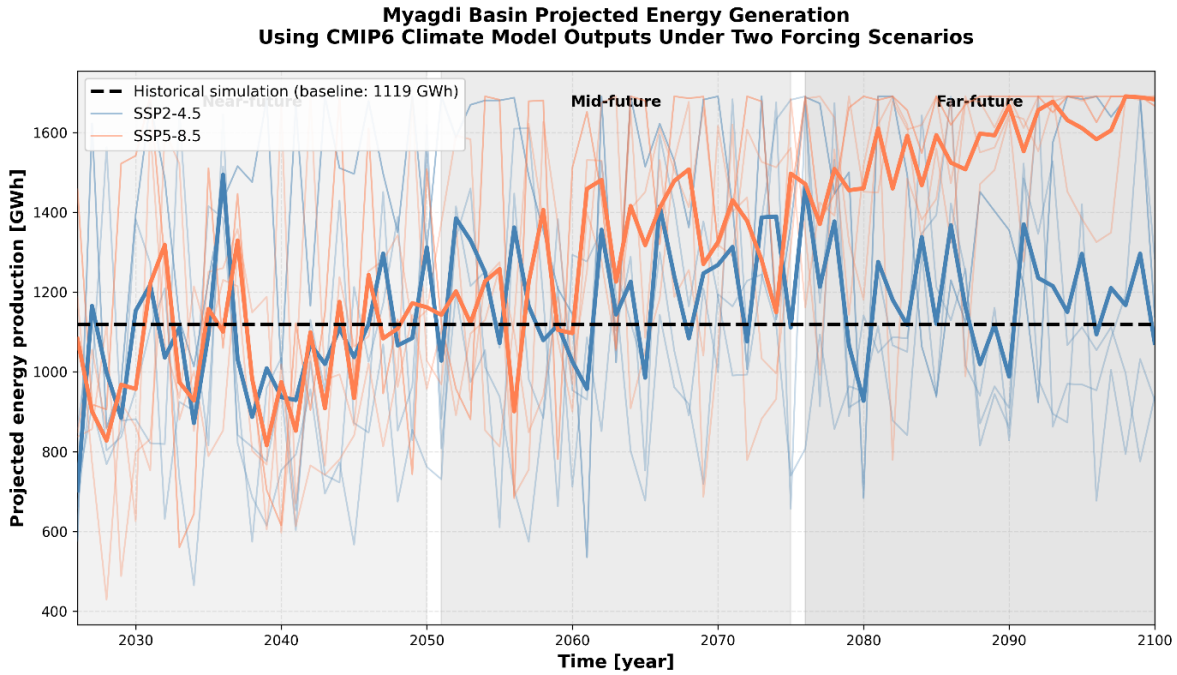

Figure 4-15 Projected energy generation in the Myagdi River Basin under two forcing scenarios

4.3.5 Capacity Saturation Effects Under High-Emission Scenarios

Far-future SSP5-8.5 projections reveal a critical infrastructure constraint: capacity saturation effects suppress theoretical generation gains when flow increases exceed design limits. While Q40 increases by 41.6%, basin-wide generation increases only 46.67% – a ratio suggesting near-linear response. However, project-level analysis reveals substantial capacity bottlenecks that mask the true hydrological potential.

4.3.5.1 Project-Specific Capacity Analysis

Two of the five basin projects, Myagdi Khola HP (65 MW) and Upper Myagdi HP (37 MW), reach 100% capacity factor under SSP5-8.5 far-future conditions, operating at installed capacity limits for extended periods. These projects exhibit "capped" generation increases of +49.0% and +51.0% respectively, values that would be substantially higher (estimated +65-75%) without infrastructure constraints.

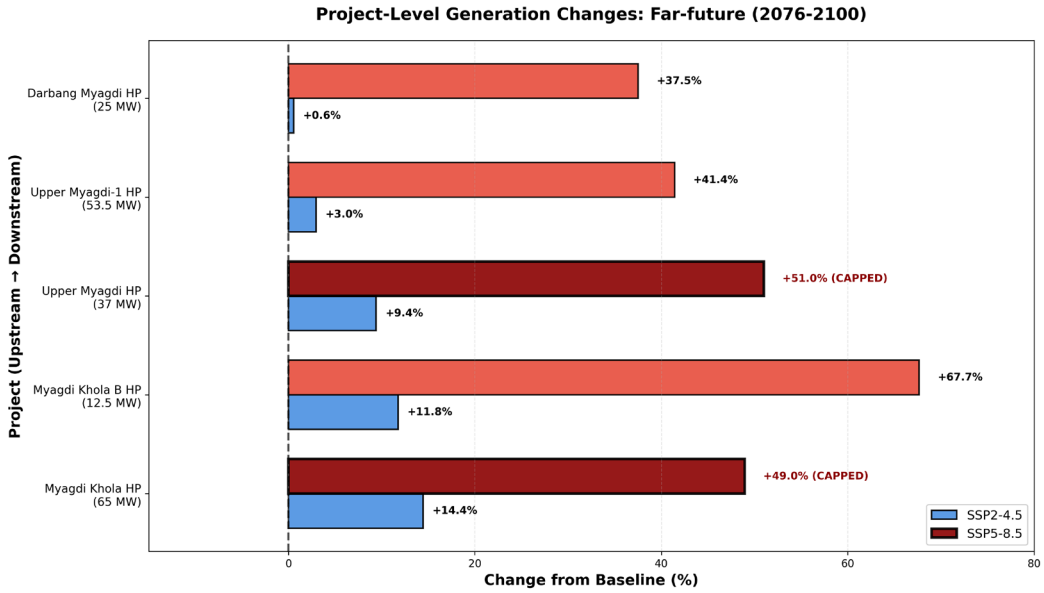

Figure 4-16 Project-specific generation changes in far-future period (2076-2100) relative to baseline

The three remaining projects approach critical capacity thresholds, with capacity factors exceeding 89-95%. Upper Myagdi-1 HP (53.5 MW) operates at 95% capacity factor, suggesting imminent saturation with only modest additional flow increases. This project's +41.4% generation increase understates available hydrological resources.

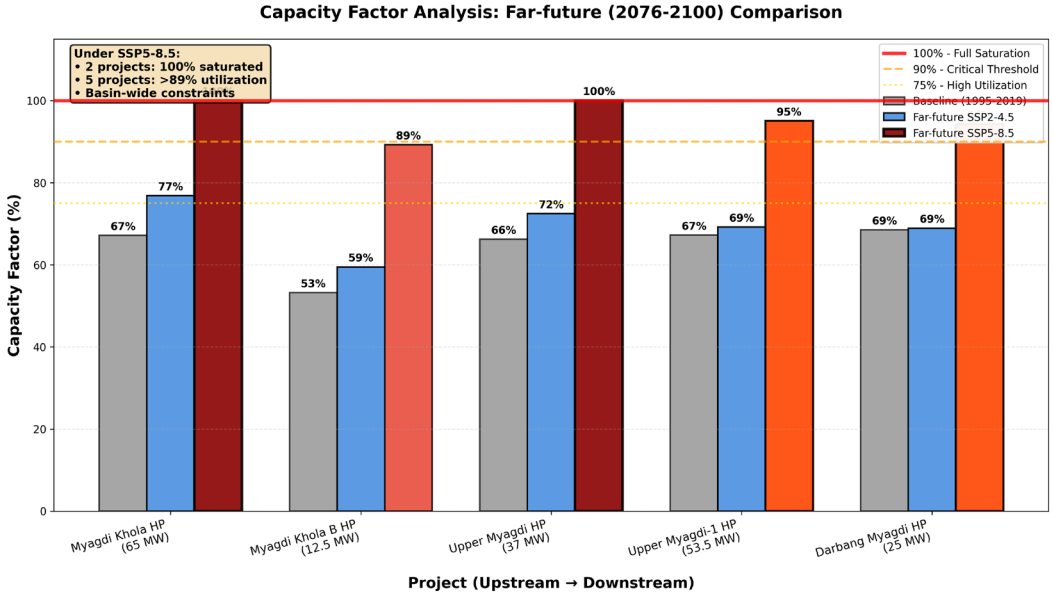

Figure 4-17 Project-level capacity factor analysis for far-future period

In contrast, SSP2-4.5 maintains all projects well below capacity limits (capacity factors 53-77%), enabling full utilization of climate-driven flow increases without infrastructure upgrades. The moderate emission pathway produces generation increases (+8.26%) that existing infrastructure can accommodate without costly expansion.

5 CONCLUSION AND RECOMMENDATION

5.1 Conclusion

This study assessed the impacts of climate change on streamflow and hydropower energy generation in the MRB using SWAT hydrological model and an ensemble of CMIP6 climate projections. By integrating historical climate analysis, model calibration, and scenario-based simulations, three core objectives were addressed: (1) evaluating the performance of the SWAT model, (2) projecting streamflow changes under climate scenarios, and (3) forecasting climate change impacts on hydropower generation in the MRB.

5.1.1 Model Performance and Reliability

The SWAT model demonstrated satisfactory to very good performance during calibration (1995-2010: NSE 0.59, R^2 0.60, PBIAS -8.20%) and validation (2011-2019: NSE 0.73, R^2 0.73, PBIAS -4.80%). The model successfully captured seasonal flow patterns including monsoon peaks and pre-monsoon snowmelt-sustained baseflow, as evidenced by strong visual and statistical agreement between observed and simulated hydrographs. These performance metrics confirm the model's suitability for climate change impact assessment and provide confidence in future streamflow projections.

5.1.2 Non-Monotonic Three-Phase Hydrological Response

The projected streamflow results indicate that climate change will significantly alter the hydrological regime of the MRB. The projected streamflow results reveal a critical non-monotonic trajectory. This three-phase response pattern – near-term decline, mid-century recovery, and far-future scenario-dependent divergence – represents the study's most significant finding for adaptation planning.

Phase 1 - Near-term Vulnerability (2026-2050): Despite annual discharge increases (+8.5% under SSP2-4.5, +9.8% under SSP5-8.5 relative to baseline), mid-range flows (Q40) experience substantial reductions of 7.0-17.4% despite 10-11% increases in monsoon peak flows. This bifurcated response, with both enhanced extreme flows and depleted sustained flows, creates immediate operational challenges for run-of-river hydropower. Basin-wide energy generation declines to 1,026 GWh/yr (SSP2-4.5, -8.45%) and 1,010 GWh/yr (SSP5-8.5, -9.81%) from the 1,120 GWh/yr baseline. Individual project impacts range from -7.7% to -10.3%, translating to 95-110 GWh/yr of foregone generation. The minimal scenario differentiation (<2% difference) indicates near-term impacts derive primarily from committed climate change rather than emission pathway divergence.

Phase 2 - Mid-century Recovery (2051-2075): Hydrological conditions recover as intensified monsoon compensates for early-period deficits. Q40 reaches 34.91 m³/s (-3.6%) under SSP2-4.5 and 37.95 m³/s (+4.7%) under SSP5-8.5. Annual generation reaches 1,190 GWh/yr (+6.25%, moderate emissions) and 1,316 GWh/yr (+17.50%, high emissions), with the 11-percentage-point scenario difference reflecting emerging hydrological divergence as cumulative forcing differences manifest.

Phase 3 - Far-future Scenario Divergence (2076-2100): Emission pathways produce fundamentally different outcomes by century-end. SSP2-4.5 stabilizes near baseline conditions (Q40: +1.4%, annual generation: +8.26% at 1,213 GWh/yr), suggesting that moderate mitigation constrains long-term hydrological impacts within historically manageable ranges. In stark contrast, SSP5-8.5 produces transformative change with Q40 increasing 41.6% (to 51.30 m³/s) and annual generation rising 46.67% (to 1,643 GWh/yr). This represents an additional 523 GWh/yr – equivalent to nearly half of current basin-wide capacity – demonstrating wholesale intensification of the hydrological cycle under extreme forcing.

The mitigation dividend – the difference between emission scenarios – totals 430 GWh/yr (1,643 - 1,213 GWh/yr), a 38.4-percentage-point gap (46.67% vs. 8.26%) that illustrates how emission reductions prevent massive flow regime transformation and associated infrastructure adaptation requirements.

5.1.3 Implications for Climate-Resilient Hydropower Development

The three-phase trajectory challenges infrastructure planning paradigms based on linear extrapolation or end-century projections. Near-term deficits require immediate operational adaptation and financial hedging, while long-term abundance necessitates flexible designs capable of future expansion. Projects commissioned in 2026-2040 will initially underperform before recovering and potentially exceeding design generation by mid-century.

Capacity saturation findings reveal that increased flows under SSP5-8.5 become infrastructure inadequacy problems when existing designs cannot utilize available water, highlighting the necessity of climate-informed design anticipating future regimes rather than optimizing for historical averages. The 430 GWh/yr mitigation dividend (38.4-percentage-point generation gap) directly connects global emission trajectories to basin-scale outcomes: SSP2-4.5 constrains impacts to manageable levels (+8.26%) compatible with existing infrastructure, while SSP5-8.5 necessitates fundamental reconfiguration to capture +46.67% potential.

Key implications for infrastructure planning and policy include: (1) near-term vulnerability (2026-2050) requires proactive adaptation measures despite projected long-term increases, demanding operational flexibility and financial hedging strategies; (2) infrastructure design should target mid-century recovery conditions rather than historical baselines or speculative far-future extremes, with built-in expansion flexibility to accommodate scenario-dependent outcomes; (3) capacity saturation under high-emission scenarios necessitates modular, expandable designs rather than fixed-capacity infrastructure optimized for historical flow regimes; and (4) the quantified mitigation dividend (430 GWh/yr, 38.4-percentage-point gap) strengthens economic arguments for emission reductions by demonstrating tangible energy security benefits of climate policy.

5.2 Recommendations for Future Research

This study establishes the three-phase non-monotonic response framework for climate impacts on Himalayan hydropower but identifies critical research gaps requiring attention:

1. Economic quantification of hydropower potential: Translate physical generation changes to economic value through tariff analysis and net present value calculations. Monetize the 430 GWh/yr mitigation dividend and 150-180 GWh/yr capacity saturation losses to inform investment decisions.
2. Seasonal generation patterns and PPA penalty assessment: Decompose projected generation by season (dry: Dec-May vs. wet: Jun-Nov) to assess Power Purchase Agreement compliance and penalty exposure. Enable operators to anticipate financial implications beyond annual generation averages.
3. Cost-reflective tariff setting: Link projected generation profiles to levelized costs of electricity (LCOE) for evidence-based PPA tariff negotiations. Support climate-informed tariff adjustments for projects facing near-term deficits (-8-10%) followed by long-term recovery (+6-47%).
4. Climate-resilient infrastructure investment analysis: Conduct cost-benefit analysis comparing "design-for-climate-change" versus "design-for-baseline" approaches under deep uncertainty. Evaluate modular expansion designs, real options for phased capacity additions, and portfolio optimization.
5. Turbine degradation under altered flow regimes: Incorporate turbine degradation curves, cavitation risks, and maintenance schedules into coupled hydrological-mechanical analysis. Account for accelerated equipment wear from higher sediment loads (+10-42% peak flows) and flow variability.

6. Basin-wide Q_{design} optimization: Determine optimal design flows (Q30, Q40, Q50) for each project under future flow regimes to maximize total basin revenue. Reassess design discharge assumptions given +41.6% Q40 increases under SSP5-8.5 far-future conditions.
7. Structural impacts of monsoon peak intensification: Assess structural adequacy and factor-of-safety margins of hydraulic structures (spillways, intake works, weirs) under intensified monsoon conditions. Evaluate flood damage risks, sediment management capacity, and structural reinforcement needs for enhanced peak flows (+10-42%).

REFERENCES

Abbaspour, K. (n.d.). *Calibration and Uncertainty Analysis*.

Abbaspour, K. C., Rouholahnejad, E., Vaghefi, S., Srinivasan, R., Yang, H., & Kløve, B. (2015). A continental-scale hydrology and water quality model for Europe: Calibration and uncertainty of a high-resolution large-scale SWAT model. *Journal of Hydrology*, *524*, 733–752. https://doi.org/10.1016/j.jhydrol.2015.03.027

Abbaspour, K., Vaghefi, S., & Srinivasan, R. (2017). A Guideline for Successful Calibration and Uncertainty Analysis for Soil and Water Assessment: A Review of Papers from the 2016 International SWAT Conference. *Water*, *10*(1), 6. https://doi.org/10.3390/w10010006

Aryal, A., Tran, T.-N.-D., Kumar, B., & Lakshmi, V. (2023). Evaluation of Satellite-Derived Precipitation Products for Streamflow Simulation of a Mountainous Himalayan Watershed: A Study of Myagdi Khola in Kali Gandaki Basin, Nepal. *Remote Sensing*, *15*(19), 4762. https://doi.org/10.3390/rs15194762

Bajracharya, A. R., Bajracharya, S. R., Shrestha, A. B., & Maharjan, S. B. (2018). Climate change impact assessment on the hydrological regime of the Kaligandaki Basin, Nepal. *Science of The Total Environment*, *625*, 837–848. https://doi.org/10.1016/j.scitotenv.2017.12.332

Bharati, L., Gurung, P., Maharjan, L., & Bhattarai, U. (2016). Past and future variability in the hydrological regime of the Koshi Basin, Nepal. *Hydrological Sciences Journal*, *61*(1), 79–93. https://doi.org/10.1080/02626667.2014.952639

Cannon, A. J., Sobie, S. R., & Murdock, T. Q. (2015). Bias Correction of GCM Precipitation by Quantile Mapping: How Well Do Methods Preserve Changes in Quantiles and Extremes? *Journal of Climate*, *28*(17), 6938–6959. https://doi.org/10.1175/JCLI-D-14-00754.1

CMIP6 Frequently Asked Questions – ClimateData.ca. (n.d.). Retrieved January 4, 2026, from https://climatedata.ca/resource/cmip6-faq/

CMIP6: The next generation of climate models explained—Carbon Brief. (n.d.). Retrieved January 4, 2026, from https://www.carbonbrief.org/cmip6-the-next-generation-of-climate-models-explained/

D. N. Moriasi, J. G. Arnold, M. W. Van Liew, R. L. Bingner, R. D. Harmel, & T. L. Veith. (2007). Model Evaluation Guidelines for Systematic Quantification of Accuracy in Watershed Simulations. *Transactions of the ASABE*, *50*(3), 885–900. https://doi.org/10.13031/2013.23153

Eyring, V., Bony, S., Meehl, G. A., Senior, C. A., Stevens, B., Stouffer, R. J., & Taylor, K. E. (2016). Overview of the Coupled Model Intercomparison Project Phase 6 (CMIP6) experimental design and organization. *Geoscientific Model Development*, *9*(5), 1937–1958. https://doi.org/10.5194/gmd-9-1937-2016

Hasson, S. U. (2016). Future Water Availability from Hindukush-Karakoram-Himalaya upper Indus Basin under Conflicting Climate Change Scenarios. *Climate*, *4*(3), 40. https://doi.org/10.3390/cli4030040

Hawkins, E., & Sutton, R. (2009). The Potential to Narrow Uncertainty in Regional Climate Predictions. *Bulletin of the American Meteorological Society*, *90*(8), 1095–1108. https://doi.org/10.1175/2009BAMS2607.1

Immerzeel, W. W., Pellicciotti, F., & Bierkens, M. F. P. (2013). Rising river flows throughout the twenty-first century in two Himalayan glacierized watersheds. *Nature Geoscience*, *6*(9), 742–745. https://doi.org/10.1038/ngeo1896

Immerzeel, W. W., van Beek, L. P. H., & Bierkens, M. F. P. (2010). Climate Change Will Affect the Asian Water Towers. *Science*, *328*(5984), 1382–1385. https://doi.org/10.1126/science.1183188

J. G. Arnold, D. N. Moriasi, P. W. Gassman, K. C. Abbaspour, M. J. White, R. Srinivasan, C. Santhi, R. D. Harmel, A. Van Griensven, M. W. Van Liew, N. Kannan, & M. K. Jha. (2012). SWAT: Model Use, Calibration, and Validation. *Transactions of the ASABE*, *55*(4), 1491–1508. https://doi.org/10.13031/2013.42256

Khatri, D., Pandey, V. P., Lamsal, G. R., & Baniya, R. (2024). Climate change impact on hydropower generation and adaptation through reservoir operation in a Himalayan river, Tamor. *Journal of Water and Climate Change*, *15*(9), 4631–4646. https://doi.org/10.2166/wcc.2024.246

Large area hydrologic modeling and assessment part 1.pdf. (n.d.). Retrieved January 5, 2026, from https://ssl.tamu.edu/media/11951/large%20area%20dyrologic%20modeling%20and%20assessment%20part%201.pdf

Lutz, A. F., Immerzeel, W. W., Shrestha, A. B., & Bierkens, M. F. P. (2014). Consistent increase in High Asia's runoff due to increasing glacier melt and precipitation. *Nature Climate Change*, *4*(7), 587–592. https://doi.org/10.1038/nclimate2237

Ma, D., Bai, Z., Xu, Y.-P., Gu, H., & Gao, C. (2024). Assessing streamflow and sediment responses to future climate change over the Upper Mekong River Basin: A comparison between CMIP5 and CMIP6 models. *Journal of Hydrology: Regional Studies*, *52*, 101685. https://doi.org/10.1016/j.ejrh.2024.101685

Marahatta, S., Devkota, L. P., & Aryal, D. (n.d.). *Application of SWAT in Hydrological Simulation of Complex Mountainous River Basin (Part I: Model Development)*.

Maraun, D., Wetterhall, F., Ireson, A. M., Chandler, R. E., Kendon, E. J., Widmann, M., Brienen, S., Rust, H. W., Sauter, T., Themeßl, M., Venema, V. K. C., Chun, K. P., Goodess, C. M., Jones, R. G., Onof, C., Vrac, M., & Thiele-Eich, I. (2010). Precipitation downscaling under climate change: Recent developments to bridge the gap between dynamical models and the end user. *Reviews of Geophysics*, *48*(3). https://doi.org/10.1029/2009RG000314

Maurer, J. M., Schaefer, J. M., Rupper, S., & Corley, A. (2019). Acceleration of ice loss across the Himalayas over the past 40 years. *Science Advances*, *5*(6), eaav7266. https://doi.org/10.1126/sciadv.aav7266

Meinshausen, M., Nicholls, Z. R. J., Lewis, J., Gidden, M. J., Vogel, E., Freund, M., Beyerle, U., Gessner, C., Nauels, A., Bauer, N., Canadell, J. G., Daniel, J. S., John, A., Krummel, P. B., Luderer, G., Meinshausen, N., Montzka, S. A., Rayner, P. J., Reimann, S., … Wang, R. H. J. (2020). The shared socio-economic pathway (SSP) greenhouse gas concentrations and their extensions to 2500. *Geoscientific Model Development*, *13*(8), 3571–3605. https://doi.org/10.5194/gmd-13-3571-2020

Moriasi, D.N., Gitau, M.W., Pai, N., & Daggupati, P. (2015). *Hydrologic and Water Quality Models: Performance Measures and Evaluation Criteria*. https://doi.org/10.13031/trans.58.10715

NASA Earth Exchange Global Daily Downscaled Projections (NEX-GDDP-CMIP6) | NASA Center for Climate Simulation. (n.d.). Retrieved January 4, 2026, from https://www.nccs.nasa.gov/services/data-collections/land-based-products/nex-gddp-cmip6

NEA-Annual-Report-2024-2025. (n.d.).

Neitsch, S. L., Arnold, J. G., Kiniry, J. R., & Williams, J. R. (2011). *Soil and Water Assessment Tool Theoretical Documentation Version 2009*. Texas Water Resources Institute. https://hdl.handle.net/1969.1/128050

Nepal, S. (2016). Impacts of climate change on the hydrological regime of the Koshi river basin in the Himalayan region. *Journal of Hydro-Environment Research*, *10*, 76–89. https://doi.org/10.1016/j.jher.2015.12.001

Nepal, S., Flügel, W., Krause, P., Fink, M., & Fischer, C. (2017). Assessment of spatial transferability of process-based hydrological model parameters in two neighbouring catchments in the Himalayan Region. *Hydrological Processes*, *31*(16), 2812–2826. https://doi.org/10.1002/hyp.11199

O'Neill, B. C., Tebaldi, C., Van Vuuren, D. P., Eyring, V., Friedlingstein, P., Hurtt, G., Knutti, R., Kriegler, E., Lamarque, J.-F., Lowe, J., Meehl, G. A., Moss, R., Riahi, K., & Sanderson, B. M. (2016). The Scenario Model Intercomparison Project (ScenarioMIP) for CMIP6. *Geoscientific Model Development*, *9*(9), 3461–3482. https://doi.org/10.5194/gmd-9-3461-2016

Ragettli, S., Pellicciotti, F., Immerzeel, W. W., Miles, E. S., Petersen, L., Heynen, M., Shea, J. M., Stumm, D., Joshi, S., & Shrestha, A. (2015). Unraveling the hydrology of a Himalayan catchment through integration of high resolution in situ data and remote sensing with an advanced simulation model. *Advances in Water Resources*, *78*, 94–111. https://doi.org/10.1016/j.advwatres.2015.01.013

Shrestha, A. B., & Aryal, R. (2011). Climate change in Nepal and its impact on Himalayan glaciers. *Regional Environmental Change*, *11*(1), 65–77. https://doi.org/10.1007/s10113-010-0174-9

Shrestha, M., Acharya, S. C., & Shrestha, P. K. (2017). Bias correction of climate models for hydrological modelling – are simple methods still useful? *Meteorological Applications*, *24*(3), 531–539. https://doi.org/10.1002/met.1655

Shrestha, S., Bajracharya, A. R., & Babel, M. S. (2016). Assessment of risks due to climate change for the Upper Tamakoshi Hydropower Project in Nepal. *Climate Risk Management*, *14*, 27–41. https://doi.org/10.1016/j.crm.2016.08.002

Shrestha, S., Maskey, G., & Kayastha, R. B. (2023). Assessment of Climate Change Effects on the Hydrological Regime of Bagmati River Basin using SWAT Model. *Journal of Hydrology and Meteorology*, *11*(1), 28–41. https://doi.org/10.3126/jhm.v11i1.59663

Shrestha, U. B., Gautam, S., & Bawa, K. S. (2012). Widespread Climate Change in the Himalayas and Associated Changes in Local Ecosystems. *PLOS ONE*, *7*(5), e36741. https://doi.org/10.1371/journal.pone.0036741

Singh, P., & Bengtsson, L. (2005). Impact of warmer climate on melt and evaporation for the rainfed, snowfed and glacierfed basins in the Himalayan region. *Journal of Hydrology*, *300*(1), 140–154. https://doi.org/10.1016/j.jhydrol.2004.06.005

Subedi, S. R., Lamichhane, M., Dhungana, S., Chalise, B., Bhattarai, S., Chaulagain, U., & Khatiwada, R. (2024). Assessing the impact of climate change on streamflow in the Tamor River Basin, Nepal: An analysis using SWAT and CMIP6 scenarios. *Discover Civil Engineering*, *1*(1), 135. https://doi.org/10.1007/s44290-024-00143-2

Tan, M. L., Gassman, P. W., Yang, X., & Haywood, J. (2020). A review of SWAT applications, performance and future needs for simulation of hydro-climatic extremes. *Advances in Water Resources*, *143*, 103662. https://doi.org/10.1016/j.advwatres.2020.103662

Taylor, K. E., Stouffer, R. J., & Meehl, G. A. (2012). An Overview of CMIP5 and the Experiment Design. *Bulletin of the American Meteorological Society*, *93*(4), 485–498. https://doi.org/10.1175/BAMS-D-11-00094.1

Tebaldi, C., Debeire, K., Eyring, V., Fischer, E., Fyfe, J., Friedlingstein, P., Knutti, R., Lowe, J., O'Neill, B., Sanderson, B., van Vuuren, D., Riahi, K., Meinshausen, M., Nicholls, Z., Tokarska, K. B., Hurtt, G., Kriegler, E., Lamarque, J.-F., Meehl, G., … Ziehn, T. (2021). Climate model projections from the Scenario Model Intercomparison Project (ScenarioMIP) of CMIP6. *Earth System Dynamics*, *12*(1), 253–293. https://doi.org/10.5194/esd-12-253-2021

Teutschbein, C., & Seibert, J. (2012). Bias correction of regional climate model simulations for hydrological climate-change impact studies: Review and evaluation of different methods. *Journal of Hydrology*, *456–457*, 12–29. https://doi.org/10.1016/j.jhydrol.2012.05.052

The Soil and Water Assessment Tool: Historical Development, Applications, and Future Research Directions. (n.d.). Retrieved January 5, 2026, from https://doi.org/10.13031/2013.23637

Thrasher, B., Wang, W., Michaelis, A., Melton, F., Lee, T., & Nemani, R. (2022). NASA Global Daily Downscaled Projections, CMIP6. *Scientific Data*, *9*(1), 262. https://doi.org/10.1038/s41597-022-01393-4

Viviroli, D., Dürr, H. H., Messerli, B., Meybeck, M., & Weingartner, R. (2007). Mountains of the world, water towers for humanity: Typology, mapping, and global significance. *Water Resources Research*, *43*(7). https://doi.org/10.1029/2006WR005653

Wood, A. W., Leung, L. R., Sridhar, V., & Lettenmaier, D. P. (2004). Hydrologic Implications of Dynamical and Statistical Approaches to Downscaling Climate Model Outputs. *Climatic Change*, *62*(1–3), 189–216. https://doi.org/10.1023/B:CLIM.0000013685.99609.9e

Wood, A. W., Maurer, E. P., Kumar, A., & Lettenmaier, D. P. (2002). Long-range experimental hydrologic forecasting for the eastern United States. *Journal of Geophysical Research: Atmospheres*, *107*(D20). https://doi.org/10.1029/2001JD000659

राष्ट्रिय निर्धारित योगदान (Nationally Determined Contribution-NDC 3.0) नेपाल सरकार (मन्त्रिपरिषद्) को मिति २०८२/१/३१ गतेको बैठकबाट स्वीकृत भएकोले सम्बन्धित सबैको जानकारीको लागि यो सूचना प्रकाशित गरिएको छ । | *Ministry of Forests and Environment, Government of Nepal*. (n.d.). Retrieved January 6, 2026, from https://mofe.gov.np/content/251/national-scheduled-contribution--ndionally-detrimined-contribution-ndc-3-0-/

विद्युत विकास विभाग | *Department of Electricity Development, Kathmandu*. (n.d.). Retrieved January 13, 2026, from https://doed.gov.np/

APPENDIX I

Table A1 1 List of meteorological stations

Precipitation Stations

ID	NAME	LAT	LONG	ELEVATION
1	PCP601	28.78	83.73	2741
2	PCP606	28.48	83.64	1161
3	PCP607	28.63	83.61	2490
4	PCP616	28.59	83.24	2627
5	PCP621	28.41	83.39	1160
6	PCP626	28.44	83.58	1682
7	PCP628	28.5	83.32	1970
8	PCP629	28.57	83.38	1884

Temperature Stations

ID	NAME	LAT	LONG	ELEVATION
1	TMP601	28.78	83.73	2741
2	TMP607	28.63	83.61	2490
3	TMP616	28.59	83.24	2627

Relative Humidity Station

ID	NAME	LAT	LONG	ELEVATION
1	RH616	28.59	83.24	2627

Table A1 2 Hydrological station details

Station Code	Station Location	Outlet ID	Latitude	Longitude	Elevation
404.7	Mangalghat	35	28° 21′ 10″ N	83° 31′ 16″ E	914

APPENDIX II

Table A2 1 Calibrated SWAT parameters with best-fit value

SN	Parameter_Name	Fitted_Value	Min_value	Max_value	Change Type
1	V__PLAPS.sub	43.800003	0	60	Replace
2	V__SMFMX.bsn	3.175	0	5	Replace
3	V__TIMP.bsn	0.635	0	1	Replace
4	V__SMTMP.bsn	-1.925	-2	3	Replace
5	V__SMFMN.bsn	0.3225	-0.5	3	Replace
6	V__TLAPS.sub	-7.805	-8	-5	Replace
7	V__SFTMP.bsn	0.71	-1	1	Replace
8	R__OV_N.hru	0.21825	0.15	0.3	Multiply
9	V__ALPHA_BNK.rte	0.461	0.45	0.65	Replace
10	V__GWQMN.gw	462.75	300	650	Replace
11	R__GW_REVAP.gw	-0.04475	-0.05	-0.02	Multiply
12	V__REVAPMN.gw	26.700001	15	35	Replace
13	V__ALPHA_BF.gw	0.85875	0.65	0.9	Replace
14	R__SOL_BD(..).sol	-0.04755	-0.05	0.02	Multiply
15	V__ESCO.hru	0.75375	0.75	0.9	Replace
16	V__EPCO.hru	0.763	0.65	0.85	Replace
17	V__CANMX.hru	97.900002	80	100	Replace
18	R__CN2.mgt	-0.0509	-0.06	0.08	Multiply
19	V__LAT_TTIME.hru	114.199997	80	120	Replace
20	V__GW_DELAY.gw	21.799999	20	60	Replace
21	V__CH_N2.rte	0.11125	0.07	0.12	Replace
22	V__CH_K2.rte	61.5	60	120	Replace
23	R__SOL_K(..).sol	-0.13625	-0.2	-0.05	Multiply
24	R__SOL_AWC(..).sol	0.22825	0.1	0.25	Multiply
25	V__SLSUBBSN.hru	50.200001	40	80	Replace

Table A2 2 Description of SWAT calibration parameters

SN	Parameter	Full Name	Definition	Units
1	PLAPS	Precipitation Lapse Rate	Rate of change of precipitation with elevation	mm/km
2	SMFMX	Maximum Snowmelt Factor	Maximum snowmelt rate occurring on June 21	mm H_2O / °C-day
3	TIMP	Snowpack Temperature Lag Factor	Factor controlling the influence of the previous day's temperature on snowpack temperature	–
4	SMTMP	Snowmelt Base Temperature	Threshold air temperature above which snowmelt begins	°C
5	SMFMN	Minimum Snowmelt Factor	Minimum snowmelt rate occurring on December 21	mm H_2O / °C-day
6	TLAPS	Temperature Lapse Rate	Rate of decrease of air temperature with elevation	°C/km
7	SFTMP	Snowfall Temperature	Threshold temperature below which precipitation falls as snow	°C
8	OV_N	Overland Flow Manning's *n*	Surface roughness coefficient controlling overland flow velocity	–
9	ALPHA_BNK	Baseflow Alpha Factor for Bank Storage	Recession constant governing bank storage return flow	days
10	GWQMN	Threshold Depth of Water in Shallow Aquifer	Minimum water depth in the shallow aquifer required for baseflow to occur	mm
11	GW_REVAP	Groundwater Revap Coefficient	Coefficient controlling upward movement of water from the shallow aquifer to the unsaturated zone	–
12	REVAPMN	Threshold Depth for Revap	Minimum water depth in the shallow aquifer required for revaporization	mm
13	ALPHA_BF	Baseflow Alpha Factor	Recession constant describing the rate of baseflow decline	days
14	SOL_BD	Moist Bulk Density	Moist bulk density of the soil layer	g/cm³
15	ESCO	Soil Evaporation Compensation Factor	Factor controlling the depth distribution of soil evaporation demand	–
16	EPCO	Plant Uptake Compensation Factor	Factor controlling the depth distribution of plant water uptake	–
17	CANMX	Maximum Canopy Storage	Maximum amount of water that can be intercepted and stored in the canopy	mm
18	CN2	Initial SCS Curve Number (AMC II)	Runoff curve number for average antecedent moisture condition	–
19	LAT_TTIME	Lateral Flow Travel Time	Time required for lateral subsurface flow to reach the channel	days
20	GW_DELAY	Groundwater Delay Time	Time lag for water percolating from the root zone to reach the shallow aquifer	days
21	CH_N2	Manning's *n* for Main Channel	Roughness coefficient for main channel flow routing	–
22	CH_K2	Effective Hydraulic Conductivity in Main Channel	Hydraulic conductivity of the channel bed material	mm/hr
23	SOL_K	Saturated Hydraulic Conductivity	Rate of water movement through saturated soil	mm/hr
24	SOL_AWC	Available Water Capacity	Amount of water available for plant uptake per unit soil depth	mm H_2O / mm soil
25	SLSUBBSN	Average Slope Length	Average overland flow length within a sub-basin	m

APPENDIX III STREAMFLOW STATISTICS AT MYAGDI RIVER BASIN OUTLET (REACH 49)

Table A3 1 Baseline annual streamflow statistics

Particulars	Flow (m^3/s)
mean	62.45
std	6.86
min	51.47
max	74.96
p10	53.93
p25	57.47
p50	61.77
p75	66.81
p90	71.50

Table A3 2 Baseline monthly streamflow statistics

Month	Flow (m^3/s)
1	11.83
2	10.85
3	9.58
4	9.96
5	14.75
6	66.89
7	169.82
8	194.65
9	148.16
10	63.74
11	28.27
12	16.44

Table A3 3 Baseline seasonal streamflow statistics

Season Code	Season	Flow (m^3/s)
DJF	Winter	13.08
MAM	Pre-Monsoon	11.45
JJA	Monsoon	144.62
SON	Post-Monsoon	79.88

Table A3 4 Comparison of monthly streamflow statistics: Baseline v NF

Month	Flow (m^3/s)						
	Baseline	**SSP2-4.5_mean**	**SSP2-4.5_p10**	**SSP2-4.5_p90**	**SSP5-8.5_mean**	**SSP5-8.5_p10**	**SSP5-8.5_p90**
1	11.83	12.38	11.27	14.33	11.90	11.51	12.46
2	10.85	10.18	9.22	11.56	9.78	9.42	10.06
3	9.58	8.71	7.78	10.18	8.33	7.68	8.90
4	9.96	9.75	7.77	13.02	8.23	7.51	9.00
5	14.75	24.08	12.94	37.82	21.53	13.69	28.70
6	66.89	83.36	60.74	106.87	82.17	66.35	100.11
7	169.82	178.40	168.87	187.87	189.06	172.20	215.12
8	194.65	213.06	185.55	238.64	215.88	197.03	242.66
9	148.16	157.12	144.13	173.20	147.22	141.41	152.89
10	63.74	75.01	59.94	93.56	68.96	63.85	74.41
11	28.27	29.25	25.76	33.23	28.14	26.46	29.47
12	16.44	17.47	15.36	20.66	16.40	15.86	17.12

Table A3 5 Comparison of monthly streamflow statistics: Baseline v MF

Month	Flow (m^3/s)						
	Baseline	**SSP2-4.5_mean**	**SSP2-4.5_p10**	**SSP2-4.5_p90**	**SSP5-8.5_mean**	**SSP5-8.5_p10**	**SSP5-8.5_p90**
1	11.83	12.32	11.80	13.05	12.90	12.41	13.53
2	10.85	10.34	9.78	11.04	10.79	9.92	11.52
3	9.58	9.05	8.47	9.77	9.07	8.06	9.99
4	9.96	9.99	7.95	13.22	9.09	7.81	10.67
5	14.75	30.56	13.84	51.60	25.99	15.94	37.82
6	66.89	92.25	67.72	114.21	95.69	82.52	110.70
7	169.82	196.11	182.73	211.24	200.37	189.04	220.18
8	194.65	231.16	206.57	259.53	256.04	213.50	306.85
9	148.16	165.19	155.62	176.39	182.25	167.47	200.88
10	63.74	79.17	68.84	89.57	84.57	75.93	95.81
11	28.27	31.20	28.71	33.97	32.33	29.97	34.79
12	16.44	17.98	16.77	19.12	18.90	17.63	20.00

Table A3 6 Comparison of monthly streamflow statistics: Baseline v FF

Month	Flow (m^3/s)						
	Baseline	**SSP2-4.5_mean**	**SSP2-4.5_p10**	**SSP2-4.5_p90**	**SSP5-8.5_mean**	**SSP5-8.5_p10**	**SSP5-8.5_p90**
1	11.83	12.34	11.72	13.14	14.98	14.24	15.88
2	10.85	10.16	9.54	10.78	12.45	11.97	12.91
3	9.58	8.42	7.96	8.97	11.00	10.05	12.24
4	9.96	9.52	7.67	12.31	12.05	10.19	13.86
5	14.75	22.54	13.20	30.94	36.84	20.24	55.67
6	66.89	97.56	62.93	127.79	131.63	89.34	175.18
7	169.82	196.29	181.22	210.12	263.84	238.15	293.46
8	194.65	239.79	211.10	270.84	289.64	247.28	338.46
9	148.16	173.77	159.00	184.71	229.60	203.84	248.80
10	63.74	72.73	67.60	80.43	103.87	84.41	122.27
11	28.27	29.27	28.92	29.52	39.67	38.20	41.86
12	16.44	17.04	16.75	17.39	21.79	20.46	23.04

Table A3 7 Comparison of seasonal streamflow statistics: Baseline v NF

Season Code	Flow (m^3/s)						
	Baseline	**SSP2-4.5_mean**	**SSP2-4.5_p10**	**SSP2-4.5_p90**	**SSP5-8.5_mean**	**SSP5-8.5_p10**	**SSP5-8.5_p90**
DJF	13.08	13.53	12.13	15.71	12.93	12.42	13.47
MAM	11.45	14.23	9.68	20.31	12.75	10.08	15.27
JJA	144.62	159.09	144.62	173.62	163.24	154.11	176.79
SON	79.88	86.99	78.51	95.87	81.30	78.98	83.87

Table A3 8 Comparison of seasonal streamflow statistics: Baseline v MF

Season Code	Flow (m^3/s)						
	Baseline	**SSP2-4.5_mean**	**SSP2-4.5_p10**	**SSP2-4.5_p90**	**SSP5-8.5_mean**	**SSP5-8.5_p10**	**SSP5-8.5_p90**
DJF	13.08	13.70	13.06	14.47	14.40	13.64	14.95
MAM	11.45	16.60	10.19	24.99	14.78	11.30	19.39
JJA	144.62	174.05	161.20	186.13	184.99	167.45	205.64
SON	79.88	91.72	90.10	93.36	99.55	92.40	106.31

Table A3 9 Comparison of seasonal streamflow statistics: Baseline v FF

Season Code	Flow (m^3/s)						
	Baseline	**SSP2-4.5_mean**	**SSP2-4.5_p10**	**SSP2-4.5_p90**	**SSP5-8.5_mean**	**SSP5-8.5_p10**	**SSP5-8.5_p90**
DJF	13.08	13.27	12.86	13.66	16.77	15.83	17.60
MAM	11.45	13.54	9.79	17.34	20.05	13.85	27.29
JJA	144.62	178.75	168.30	186.55	229.42	201.52	255.10
SON	79.88	91.72	85.22	96.97	124.16	109.10	136.45

Table A3 10 Comparison of Flow Duration Curve quantiles: Baseline v NF

Exceedance_%	Flow (m^3/s)		
	Baseline	**SSP2-4.5_median**	**SSP5-8.5_median**
10	193.00	214.54	212.73
25	99.68	87.31	90.56
40	36.23	29.92	33.70
50	21.20	18.21	20.75
90	7.88	6.66	6.47
95	6.72	5.72	5.56

Table A3 11 Comparison of Flow Duration Curve quantiles: Baseline v MF

Exceedance_%	Flow (m^3/s)		
	Baseline	**SSP2-4.5_median**	**SSP5-8.5_median**
10	193.00	224.84	233.60
25	99.68	103.55	101.82
40	36.23	34.91	37.95
50	21.20	21.27	22.54
90	7.88	7.49	7.37
95	6.72	6.39	6.22

Table A3 12 Comparison of Flow Duration Curve quantiles: Baseline v FF

Exceedance_%	Flow (m^3/s)		
	Baseline	**SSP2-4.5_median**	**SSP5-8.5_median**
10	193.00	224.48	273.88
25	99.68	98.00	139.45
40	36.23	36.74	51.30
50	21.20	21.14	29.65
90	7.88	7.33	9.05
95	6.72	6.22	7.83

Table A3 13 Comparison of monthly baseline and monthly ensemble flow for S2-NF

Month	Flow (m^3/s)		
	baseline_mean	**future_ensemble_mean**	**percent_change**
1	11.83	12.38	4.62
2	10.85	10.18	-6.17
3	9.58	8.71	-9.11
4	9.96	9.75	-2.10
5	14.75	24.08	63.25
6	66.89	83.36	24.64
7	169.82	178.40	5.05
8	194.65	213.06	9.46
9	148.16	157.12	6.05
10	63.74	75.01	17.69
11	28.27	29.25	3.47
12	16.44	17.47	6.28

Table A3 14 Comparison of monthly baseline and monthly ensemble flow for S2-MF

Month	Flow (m^3/s)		
	baseline_mean	**future_ensemble_mean**	**percent_change**
1	11.83	12.32	4.10
2	10.85	10.34	-4.77
3	9.58	9.05	-5.57
4	9.96	9.99	0.33
5	14.75	30.56	107.14
6	66.89	92.25	37.92
7	169.82	196.11	15.48
8	194.65	231.16	18.76
9	148.16	165.19	11.49
10	63.74	79.17	24.22
11	28.27	31.20	10.36
12	16.44	17.98	9.38

Table A3 15 Comparison of monthly baseline and monthly ensemble flow for S2-FF

Month	Flow (m^3/s)		
	baseline_mean	**future_ensemble_mean**	**percent_change**
1	11.83	12.34	4.30
2	10.85	10.16	-6.42
3	9.58	8.42	-12.08
4	9.96	9.52	-4.40
5	14.75	22.54	52.77
6	66.89	97.56	45.86
7	169.82	196.29	15.58
8	194.65	239.79	23.19
9	148.16	173.77	17.28
10	63.74	72.73	14.12
11	28.27	29.27	3.56
12	16.44	17.04	3.65

Table A3 16 Comparison of monthly baseline and monthly ensemble flow for S5-NF

Month	Flow (m^3/s)		
	baseline_mean	**future_ensemble_mean**	**percent_change**
1	11.83	11.90	0.58
2	10.85	9.78	-9.92
3	9.58	8.33	-13.05
4	9.96	8.23	-17.31
5	14.75	21.53	45.96
6	66.89	82.17	22.84
7	169.82	189.06	11.33
8	194.65	215.88	10.91
9	148.16	147.22	-0.64
10	63.74	68.96	8.19
11	28.27	28.14	-0.45
12	16.44	16.40	-0.24

Table A3 17 Comparison of monthly baseline and monthly ensemble flow for S5-MF

Month	Flow (m^3/s)		
	baseline_mean	**future_ensemble_mean**	**percent_change**
1	11.83	12.90	8.99
2	10.85	10.79	-0.62
3	9.58	9.07	-5.30
4	9.96	9.09	-8.67
5	14.75	25.99	76.21
6	66.89	95.69	43.06
7	169.82	200.37	17.99
8	194.65	256.04	31.54
9	148.16	182.25	23.00
10	63.74	84.57	32.69
11	28.27	32.33	14.37
12	16.44	18.90	14.99

Table A3 18 Comparison of monthly baseline and monthly ensemble flow for S5-FF

Month	Flow (m^3/s)		
	baseline_mean	**future_ensemble_mean**	**percent_change**
1	11.83	14.98	26.55
2	10.85	12.45	14.68
3	9.58	11.00	14.76
4	9.96	12.05	21.07
5	14.75	36.84	149.77
6	66.89	131.63	96.79
7	169.82	263.84	55.36
8	194.65	289.64	48.80
9	148.16	229.60	54.97
10	63.74	103.87	62.98
11	28.27	39.67	40.34
12	16.44	21.79	32.59

APPENDIX IV POWER GENERATION STATISTICS IN THE MYAGDI RIVER BASIN

Table A4 1 Baseline contribution from hydropower projects in the Myagdi River Basin in annual energy generation (GWh)

Project	Reach_ID	Capacity_MW	Baseline_GWh	Baseline_%
Myagdi Khola HP	10	65	382.28	34.12
Myagdi Khola B HP	18	12.5	58.28	5.20
Upper Myagdi HP	23	37	214.65	19.16
Upper Myagdi -1 HP	27	53.5	315.01	28.12
Darbang Myagdi HP	37	25	150.08	13.40
Total		**193**	**1120.30**	

Table A4 2 Total basin annual energy generation capacity: Baseline v future scenarios

Scenario	Period	Energy_GWh	Delta_GWh	Change_%
Baseline	1995-2019	1120.30	0.00	0.00
S2	2026-2050	1025.60	-94.70	-8.45
S2	2051-2075	1190.30	70.00	6.25
S2	2076-2100	1212.78	92.49	8.26
S5	2026-2050	1010.43	-109.87	-9.81
S5	2051-2075	1316.32	196.02	17.50
S5	2076-2100	1643.14	522.84	46.67

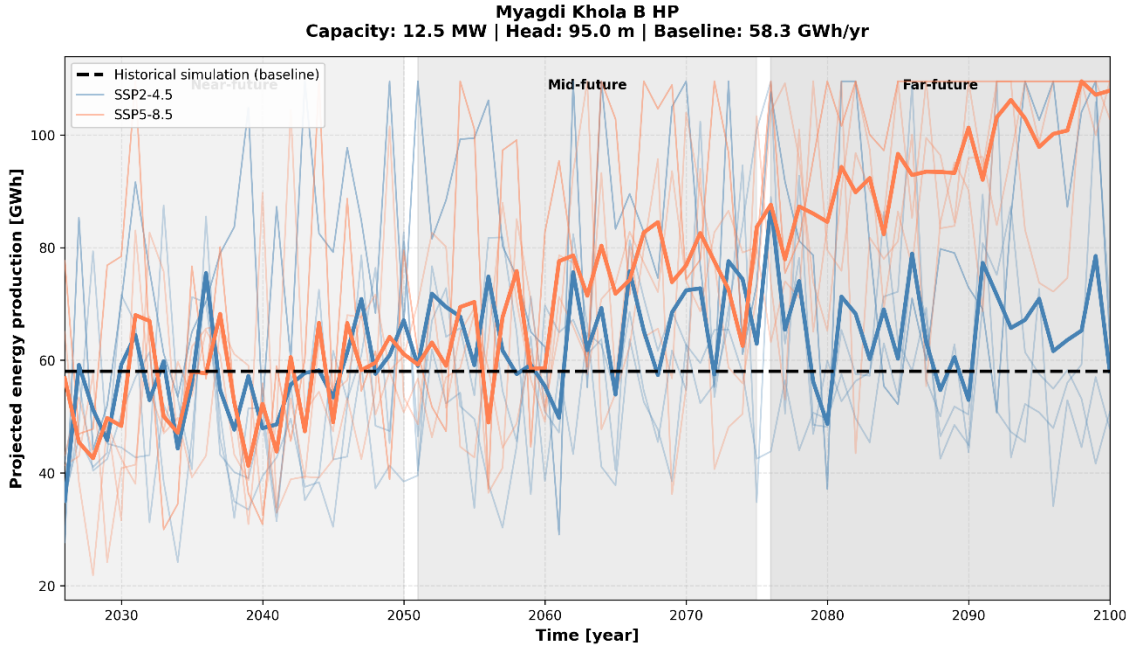

Figure A4 1 Projected energy generation from Myagdi Khola B HP under two forcing scenarios

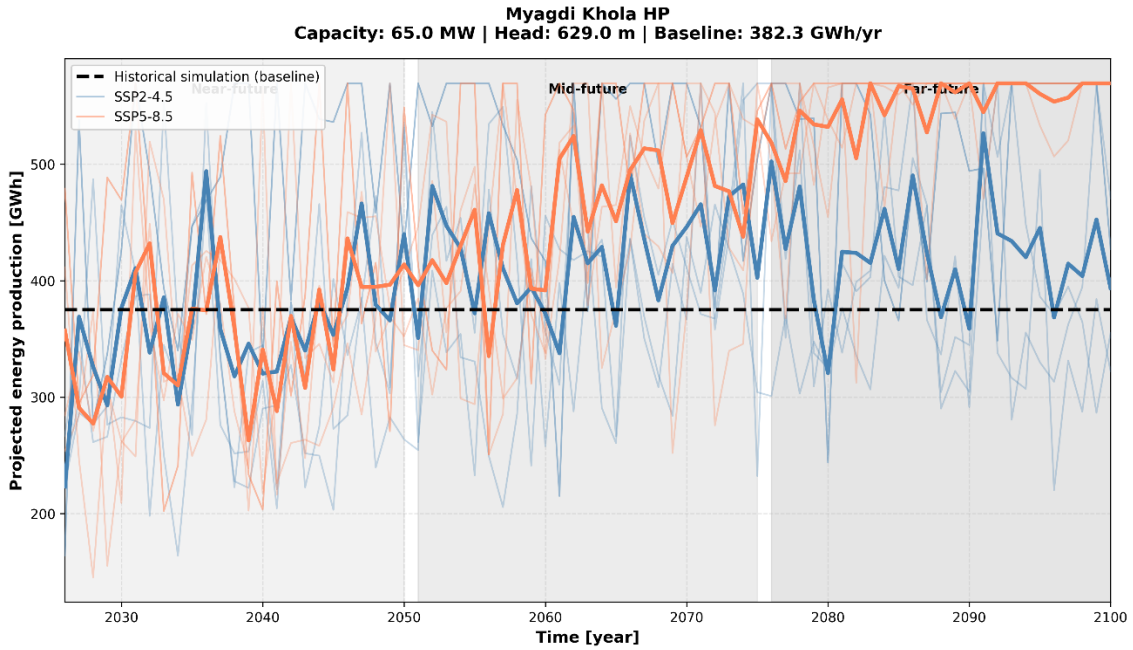

Figure A4 2 Projected energy generation from Myagdi Khola HP under two forcing scenarios

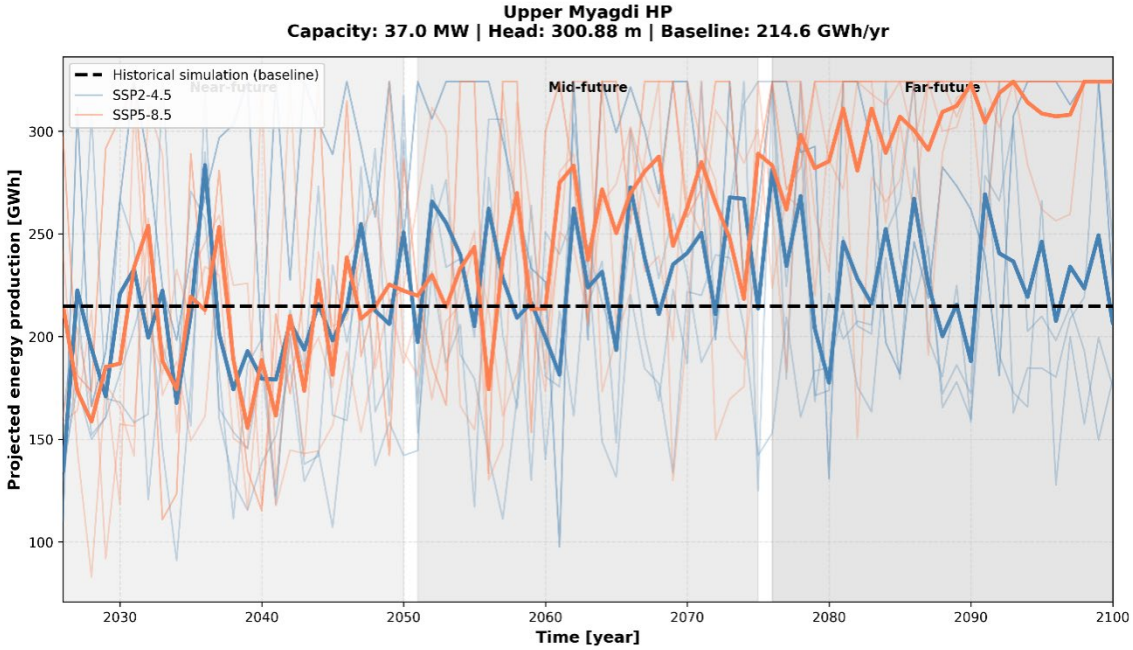

Figure A4 3 Projected energy generation from Upper Myagdi HP under two forcing scenarios

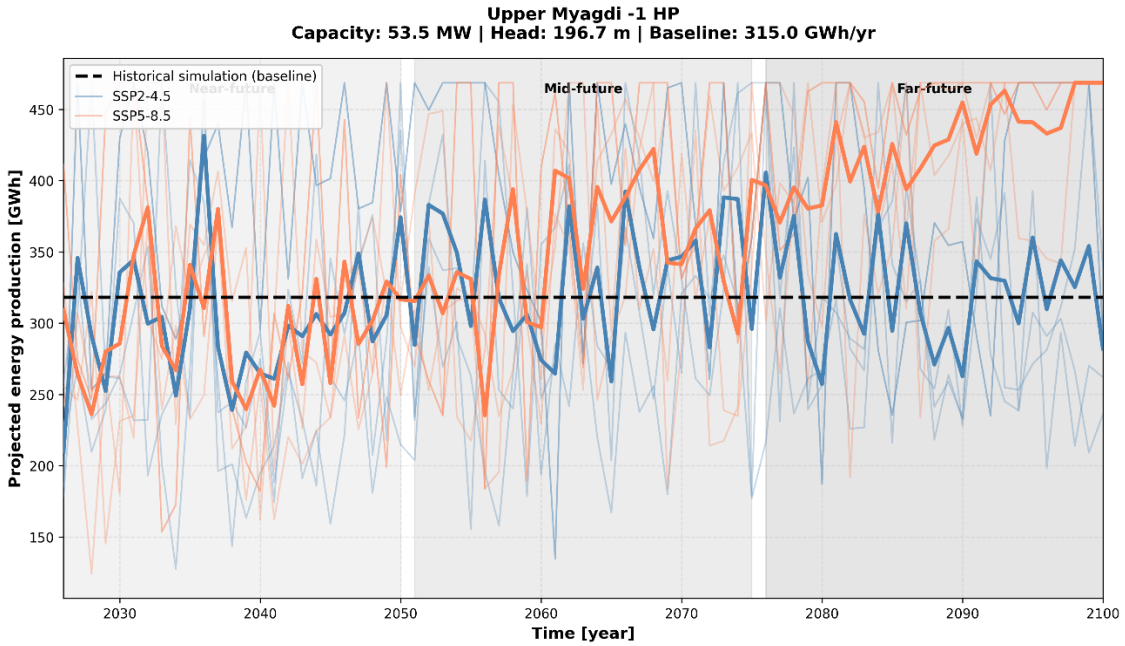

Figure A4 4 Projected energy generation from Upper Myagdi-1 HP under two forcing scenarios

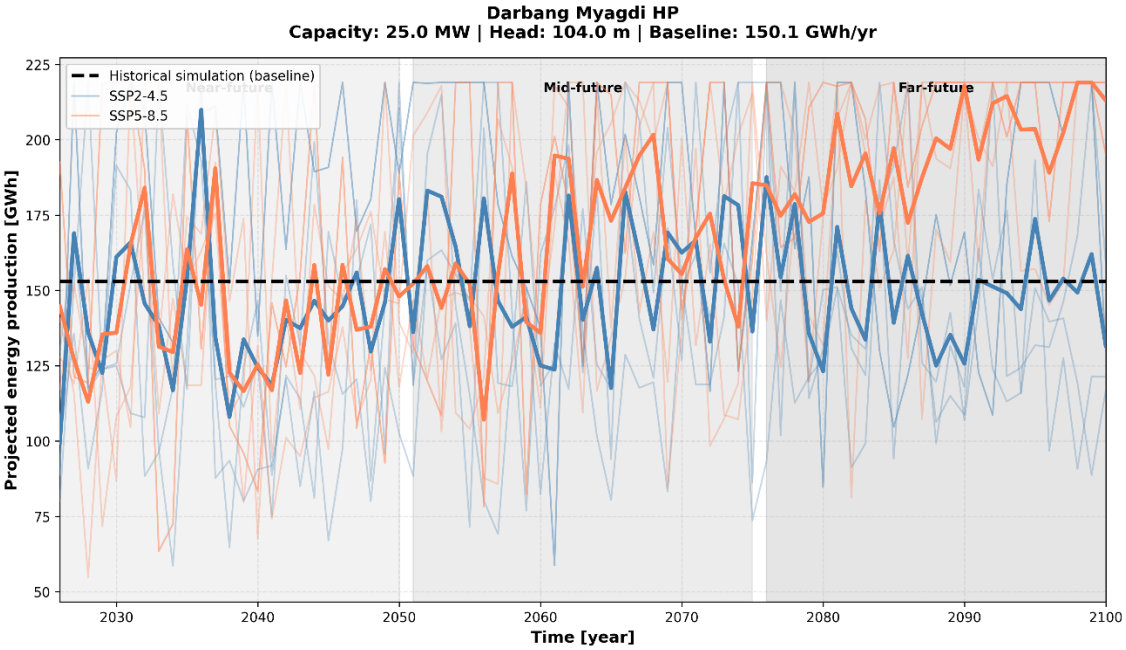

Figure A4 5 Projected energy generation from Darbang Myagdi HP under two forcing scenarios

Table A4 3 Comparison of flow and energy generation of hydropower projects in the Myagdi River Basin: Baseline v future periods

Hydro Project		Myagdi Khola B HP				Myagdi Khola HP				Upper Myagdi HP				Upper Myagdi-1 HP				Darbang Myagdi HP			
Scenario	**Period**	**Q40_cms**	**Energy_GWh**	**Delta_GWh**	**Change_%**	**Q40_cms**	**Energy_GWh**	**Delta_GWh**	**Change_%**	**Q40_cms**	**Energy_GWh**	**Delta_GWh**	**Change_%**	**Q40_cms**	**Energy_GWh**	**Delta_GWh**	**Change_%**	**Q40_cms**	**Energy_GWh**	**Delta_GWh**	**Change_%**
Baseline	1995-2019	11.60	58.28	0.00	0.00	9.68	382.28	0.00	0.00	13.65	214.65	0.00	0.00	23.04	315.01	0.00	0.00	29.58	150.08	0.00	0.00
S2	NF	10.65	53.50	-4.78	-8.19	8.93	352.90	-29.38	-7.68	12.56	197.46	-17.18	-8.01	20.93	286.08	-28.93	-9.18	26.74	135.64	-14.44	-9.62
	MF	12.64	63.53	5.25	9.00	10.75	424.50	42.22	11.04	14.68	230.75	16.11	7.50	23.53	321.73	6.72	2.13	29.52	149.79	-0.29	-0.19
	FF	12.96	65.13	6.85	11.76	11.07	437.52	55.24	14.45	14.94	234.83	20.18	9.40	23.73	324.37	9.36	2.97	29.75	150.93	0.85	0.57
S5	NF	10.48	52.63	-5.65	-9.70	8.69	343.47	-38.81	-10.15	12.39	194.73	-19.91	-9.28	20.85	284.99	-30.02	-9.53	26.53	134.61	-15.47	-10.31
	MF	14.07	70.68	12.40	21.28	12.09	477.48	95.20	24.90	16.15	253.95	39.31	18.31	25.67	350.89	35.88	11.39	32.19	163.31	13.23	8.81
	FF	20.65	97.71	39.43	67.66	18.34	569.40	187.12	48.95	23.08	324.12	109.47	51.00	34.16	445.52	130.51	41.43	41.94	206.38	56.30	37.51

Sneha Shakya

Assessing Climate Change Impacts on Streamflow and Power Generation in the Myagdi River Basin Using SWAT and CMIP6 ...

Tribhuvan University

Document Details

Submission ID
trn:oid:::3117:549160873

Submission Date
Jan 25, 2026, 12:50 PM GMT+5:45

Download Date
Jan 25, 2026, 12:52 PM GMT+5:45

File Name
Final-Thesis-Report_vFinal.pdf

File Size
6.7 MB

97 Pages

22,249 Words

136,058 Characters

8% Overall Similarity

The combined total of all matches, including overlapping sources, for each database.

Filtered from the Report

- Bibliography
- Quoted Text
- Cited Text
- Small Matches (less than 10 words)

Custom Section Exclusions

{titlesCount} Section Titles, {keywordsCount} Keywords

Section title	No. of Section Starters	Section Starters
"Acknowledgements"	4	Acknowledgements Acknowledgement Acknowledgment Acknowledgments

Match Groups

- **106** Not Cited or Quoted 8%
  Matches with neither in-text citation nor quotation marks
- **0** Missing Quotations 0%
  Matches that are still very similar to source material
- **0** Missing Citation 0%
  Matches that have quotation marks, but no in-text citation
- **0** Cited and Quoted 0%
  Matches with in-text citation present, but no quotation marks

Top Sources

7% Internet sources
5% Publications
0% Submitted works (Student Papers)

Integrity Flags

0 Integrity Flags for Review

No suspicious text manipulations found.

Our system's algorithms look deeply at a document for any inconsistencies that would set it apart from a normal submission. If we notice something strange, we flag it for you to review.

A Flag is not necessarily an indicator of a problem. However, we'd recommend you focus your attention there for further review.

Match Groups

- **106** Not Cited or Quoted 8%
  Matches with neither in-text citation nor quotation marks
- **0** Missing Quotations 0%
  Matches that are still very similar to source material
- **0** Missing Citation 0%
  Matches that have quotation marks, but no in-text citation
- **0** Cited and Quoted 0%
  Matches with in-text citation present, but no quotation marks

Top Sources

7% Internet sources
5% Publications
0% Submitted works (Student Papers)

Top Sources

The sources with the highest number of matches within the submission. Overlapping sources will not be displayed.

1	Internet	elibrary.tucl.edu.np 2%
2	Internet	www.mdpi.com <1%
3	Publication	Deepak Chaulagain, Ram Lakhan Ray, Abdulfatai Olatunji Yakub, Noel Ngando Sa... <1%
4	Internet	link.springer.com <1%
5	Publication	"Harmonized World Soil Database version 2.0", Food and Agriculture Organizatio... <1%
6	Internet	iwaponline.com <1%
7	Internet	www.udsspace.uds.edu.gh <1%
8	Internet	etd.astu.edu.et <1%
9	Internet	worldwidescience.org <1%
10	Publication	Jürgen Schuol. "Modeling blue and green water availability in Africa", Water Reso... <1%

11	Publication	Sangam Shrestha, Binod Bhatta, Manish Shrestha, Pallav K. Shrestha. "Integrated... <1%
12	Internet	download.bibis.ir <1%
13	Internet	www.adcoesao.pt <1%
14	Publication	Xin Xiang, Tianqi Ao, Qintai Xiao, Xiaodong Li, Li Zhou, Yao Chen, Yao Bi, Jingyu G... <1%
15	Publication	Laurent, F.. "Assessing impacts of alternative land use and agricultural practices ... <1%
16	Publication	Min Cui, Duoying Ji, John C. Moore, He Zhang et al. "CAS-ESM2.0 Dataset for the G... <1%
17	Publication	Yuqing Zhang, Qinglong You, Safi Ullah, Changchun Chen, Liucheng Shen, Zhu Liu... <1%
18	Internet	www.weap21.org <1%
19	Publication	Dipak Mudbhari, Mitthan Lal Kansal, Praveen Kalura. "Impact of climate change o... <1%
20	Publication	Fitsum T. Teshome, Haimanote K. Bayabil, L. N. Thakural, Fikadu G. Welidehanna. ... <1%
21	Internet	api.mountainscholar.org <1%
22	Internet	etj.uotechnology.edu.iq <1%
23	Internet	www.db-thueringen.de <1%
24	Publication	Debjani Deb, Jonathan Butcher, Raghavan Srinivasan. "Projected Hydrologic Chan... <1%

25 Publication

Pouya Khalili, Saman Razavi, Evan G.R. Davies, Daniel S. Alessi, Monireh Faramarzi... <1%

26 Publication

Xue Fang, Weijun He, FaGuang Wen, Min An, Bei Wang, Boxuan Cheng. "SWAT mo... <1%

27 Publication

Sai Kumar Dasari, Pooja Preetha, Hari Manikanta Ghantasala. "Predictive Analysis... <1%

28 Internet

scholarspace.manoa.hawaii.edu <1%

29 Internet

www.diva-portal.org <1%

30 Internet

www.scribd.com <1%

31 Internet

zone.biblio.laurentian.ca <1%

32 Publication

Eyasu Tafese Mekuria, Fekadu Fufa Feyessa, Tamene Adugna Demissie. "Investig... <1%

33 Publication

Fetene Muluken Chanie. "Evaluation of CMIP6 model performance and future cli... <1%

34 Publication

Sukanya S, Sabu Joseph. "Climate change impacts on water resources: An overvie... <1%

35 Publication

Tarik El Orfi, Mohamed El Ghachi, Sébastien Lebaut, Ionel Haidu. "Projected clima... <1%

36 Internet

csdms.colorado.edu <1%

37 Internet

ruor.uottawa.ca <1%

38 Internet

thesesups.ups-tlse.fr <1%

39 Internet

uu.diva-portal.org <1%

40 Publication

Listowel Abugri Anaba, Noble Banadda, Nicholas Kiggundu, Joshua Wanyama, Be... <1%

41 Publication

Lyuliu Liu, Chan Xiao, Yihua Liu. "Projected Water Scarcity and Hydrological Extre... <1%

42 Publication

Misigo W. S. Angalika, Seiji Suzuki, Wataru Tanaka, Huynh V. Vu, Tomoaki Itayam... <1%

43 Publication

Utsav Poudel, Sanskar Adhikari, Saroj Karki, Ram Krishna Regmi. "Climate change... <1%

44 Publication

Yog Aryal, Darren L. Ficklin, Daniel T. Myers. "Projected changes in rain-on-snow e... <1%

45 Internet

hdl.handle.net <1%

46 Internet

ir.jkuat.ac.ke <1%

47 Internet

library.wur.nl <1%

48 Internet

open.uct.ac.za <1%

49 Internet

openjicareport.jica.go.jp <1%

50 Internet

progearthplanetsci.springeropen.com <1%

51 Internet

www.waza.org <1%

52 Publication

Changbin Li, Jiaguo Qi, Zhaodong Feng, Runsheng Yin, Songbing Zou, Feng Zhang... <1%

53 Publication

Changjian Zou, Rui Ma, Jing Xiong, Zhao Pan, Ziyong Sun. "Seasonal variation of g... <1%

54 Publication

Darren L. Ficklin, Sarah E. Null, John T. Abatzoglou, Kimberly A. Novick, Daniel T. ... <1%

55 Publication

Dickembs Khatri, Vishnu Prasad Pandey, Girish Raj Lamsal, Rupesh Baniya. "Clim... <1%

56 Publication

Jiaying Huang, Qingxiang Li, Zhaoyang Song. "Historical global land surface air ap... <1%

57 Publication

Pornampai Narenpitak, Saifhon Tomkratoke, Sirod Sirisup, Siriwat Kongkulsiri. "P... <1%

58 Publication

Taylor, Sam D., Yi He, and Kevin M. Hiscock. "Modelling the impacts of agricultura... <1%

59 Publication

Valentina Krysanova, Mike White. "Advances in water resources assessment with ... <1%

60 Publication

Vilaysane, Bounhieng, Kaoru Takara, Pingping Luo, Inthavy Akkharath, and Weili ... <1%

61 Publication

Viviane de Souza Dias, Marta Pereira da Luz, Gabriela M. Medero, Diego Tarley Fe... <1%

62 Publication

Yiyan Gao, Minpei Zhou, Zhongbo Yu, Qin Ju, Lei Wen, Junliang Jin, Dawei Zhang. "... <1%

63 Publication

Ziyan Chen, Buda Su, Mengxia Zhao, Yimling Siu, Jinlong Huang, Mingjin Zhan, To... <1%

64 Internet

comptes-rendus.academie-sciences.fr <1%

65 Internet

etd.aau.edu.et <1%

66 Internet

files.core.ac.uk <1%

67 Internet

ir.kiu.ac.ug <1%

68 Internet

ousar.lib.okayama-u.ac.jp <1%

69 Internet

pastureproject.org <1%

70 Internet

rdrr.io <1%

71 Internet

www.iwmi.cgiar.org <1%

72 Internet

www.researchgate.net <1%

73 Internet

www.taccire.sua.ac.tz <1%

74 Internet

www.wem.ctw.utwente.nl <1%

Gmail Sneha Shakya <snehashakya977@gmail.com>

Manuscript Submission - CLIMATE IMPACTS ON HIMALAYAN HYDROPOWER: CMIP6-SWAT ANALYSIS OF NEPAL'S MYAGDI RIVER BASIN

3 messages

Sneha Shakya <snehashakya977@gmail.com> Tue, Jan 13, 2026 at 6:39 PM
To: editor@jsce.com.np
Cc: "076msesp017.sneha@pcampus.edu.np" <076msesp017.sneha@pcampus.edu.np>

Dear Editor,

I am pleased to submit the manuscript entitled "CLIMATE IMPACTS ON HIMALAYAN HYDROPOWER: CMIP6-SWAT ANALYSIS OF NEPAL'S MYAGDI RIVER BASIN" for your consideration for publication in the Journal of Science and Engineering.

The manuscript has not been published previously and is not under consideration elsewhere. All authors have approved the submission and agree with its content.

Thank you for your time and consideration. I look forward to your response.

Sincerely,
Sneha Shakya

Sneha-Shakya-JScE-January-2026.doc
2725K

JsCE Editor <editor@jsce.com.np> Wed, Jan 14, 2026 at 8:27 AM
To: Sneha Shakya <snehashakya977@gmail.com>

Dear Corresponding Author,

Your manuscript has been received. We will correspond with you in future with the status of the manuscript.

regards
[Quoted text hidden]

JsCE Editor <editor@jsce.com.np> Wed, Jan 14, 2026 at 12:57 PM
To: Sneha Shakya <snehashakya977@gmail.com>

Dear Corresponding Author,

Your manuscript with title "CLIMATE IMPACTS ON HIMALAYAN HYDROPOWER: CMIP6-SWAT ANALYSIS OF NEPAL'S MYAGDI RIVER BASIN" has been received. After an initial editorial screening, the manuscript has now been forwarded to expert reviewers for the peer review process.

We will contact you again once the review reports are received and a decision has been made. Thank you for considering our journal for the publication of your work.

With best regards

--

Assoc. Prof. Phanindra Prasad Bhandari, PhD (Optimization)

Chief Editor

Journal of Science and Engineering (JScE)